

STUDY ON INFLUENCE OF DIRECT X-RAY IRRADIATED
ON DIODE



E076475



เลขหมู่.....
เลขทะเบียน..... 76475
วัน,เดือน,ปี..... 25 ส.ค. 2557

.b.....
.i.....

A THESIS SUBMITTED IN PARTIAL FULFILLMENT
OF THE REQUIREMENT FOR THE DEGREE OF
DOCTOR OF ENGINEERING IN ELECTRICAL ENGINEERING
FACULTY OF ENGINEERING
KING MONGKUT'S INSTITUTE OF TECHNOLOGY LADKRABANG
2012
KMITL 2012 -EN-D-018-196



COPYRIGHT 2012

FACULTY OF ENGINEERING

KING MONGKUT'S INSTITUTE OF TECHNOLOGY LADKRABANG

This material is reserved for educational use only, not allowed for commercial use.

Forbidden to modify the content, and cite the document when use.

Thesis title	Study on Influence of Direct X-ray Irradiated on Diode
Student	Mr. Itsara Srithanachai
Student ID	53610129
Degree	Doctor of Engineering
Program	Electrical Engineering
Year	2012
Thesis Advisor	Asst. Prof. Dr. Surasak Niemcharoen
Thesis Co-Advisor	Dr. Amporn Poyai

Abstract

This thesis study and analyze the effect of X-ray irradiation on the electrical properties of P-N diode. The X-rays are use in this thesis various energies and times. The energy of X-rays are various from 40 to 70 keV, times 5, 55 and 205 sec. The P-N diode are fabrication by using CMOS technology at TMEC on n-type silicon, resistivity 120-135 ohm-cm. The device are measurement I - V and C - V characteristics by using a HP4156B. The I - V characteristic results were measured on the wafer with a bias step of 25 mV from the reverse (V_R) to forward (V_F) voltage, in the range of -10 to +1 V. The reverse and forward current before and after irradiation can be explained relative to the following parameters: carrier generation lifetime (τ_g), Carrier recombination lifetime (τ_r), activation energy (E_a), ideality factor (n), series resistance (R_s), carrier concentration (N), and depletion width (W). After irradiation at 40 and 55 keV, a small increase in the diode leakage current was seen, while at 70 keV of exposure, the leakage current was slightly decreased. On the other hand, the forward current was dramatically increase by about three orders of magnitude. I - V characteristics of the diodes with different doses, where the leakage current versus voltage before and after X-ray irradiation at 40 keV and 55 keV slightly increases with the increasing dose. This result clearly shows the impact of the X-ray irradiation at a higher reverse bias in the case of the 70 keV exposed energy, where the leakage current after exposure is slightly decrease. The change in the leakage current depends on carrier generation lifetime and diffusion current. The carrier generation lifetime and diffusion current is changed after irradiated by X-ray. In out former work, a longer operation lifetime was achieved for lower

This material is reserved for educational use only, not allowed for commercial use.

Forbidden to modify the content, and cite the document when use.

dose operation. This can also be due to defects annealed by the X-ray . For the prolonging diode lifetime, the longer exposure after a typical sensing operation may be a concern.

The forward bias characteristics of the P-N junction diode after irradiation is increased about three orders of magnitude. The change in the forward current seems to be caused by a series resistance reduction that affects the ideality factor of the diode. The series resistance of diodes after irradiation are decreased from $k\Omega$ to Ω . Soft X-ray annealing method can use for improve the performance of device base on silicon for laboratory and semiconductor industry.



Acknowledgment

This doctor thesis has been done to kindness Asst.Prof.Dr. Surasak Niemchroen and Dr. Amporn Poyai is director of Thai Microelectronics Center (TMEC) to support and suggestion for device fabrication at TMEC.

Thank you Assoc.Prof.Dr. Wisut Titiroongruang, Assoc.Prof.Dr. Toempong Pechakul, Assoc.Prof.Dr. Preecha Yupapin, Dr. Narin Atiwongsaengthong, Dr. Yotin Wongprosert at King Mongkut's Institute of Technology Ladkrabang.

The thesis support by Thailand Graduate Institute of Science and Technology (TGIST) of National Electronics and Computer Technology Center (NECTEC), Thailand under scholarship number TG-44-22-53-014D.

Thank you Dr. ekalak chaowicharat, Dr. Putapon Pengpat and Dr. Nipapan Klunngien from TMEC for support *I-V* and *C-V* measurement.

Thank you Mr. Prasong Thusaranon for support X-ray radiation generator at King Mongkut's University Technology North Bangkok (KMUTNB).

Thank you Mr. Porpol Rujanapich and Mr. Jirawat Prabket for support and suggestion to study and analyze the electrical properties of P-N junction diode and Miss. Surada Ueamanapong, Miss. Yuwadee Sundarasaradula to help measure and analyze the results.

Finally, I very thank you my father, mother and relatives for kindness, instruct, encouragement and support for learning of the doctor degree at KMITL.

For the benefits of this thesis, I would like respect to teacher at electronics engineering, Faculty of engineering, King Mongkut's Institute of Technology Ladkrabang, Thailand. Which is the place to knowledge and experience in conducting research until graduate.

Itsara Srithanachai

Contents

	Page
Abstract.....	i
Acknowledge.....	iii
Content.....	iv
Content of table.....	vii
Content of picture.....	viii
Abbreviation.....	xi
List of symbol.....	xiii
Chapter 1 Introduction.....	1
1.1 Background and Motivation.....	1
1.1.1 Proton radiation.....	3
1.1.2 Electron radiation.....	5
1.1.3 Neutron radiation.....	8
1.1.4 X-ray radiation.....	12
1.2 Aim of thesis.....	14
1.3 Hypothesis.....	14
1.4 Objective.....	14
1.5 Summary and layout of thesis.....	14
Chapter 2 Background and Theory.....	16
2.1 X-ray radiation.....	16
2.1.1 X-ray properties.....	16
2.1.2 Applications of X-ray radiation.....	18
2.1.2.1 Medical work.....	19
2.1.2.2 Agriculture work.....	19
2.1.2.3 Industrial work.....	19
2.2 P-N junction diode.....	20
2.2.1 Ideal P-N junction diode.....	20

Contents (Cont.)

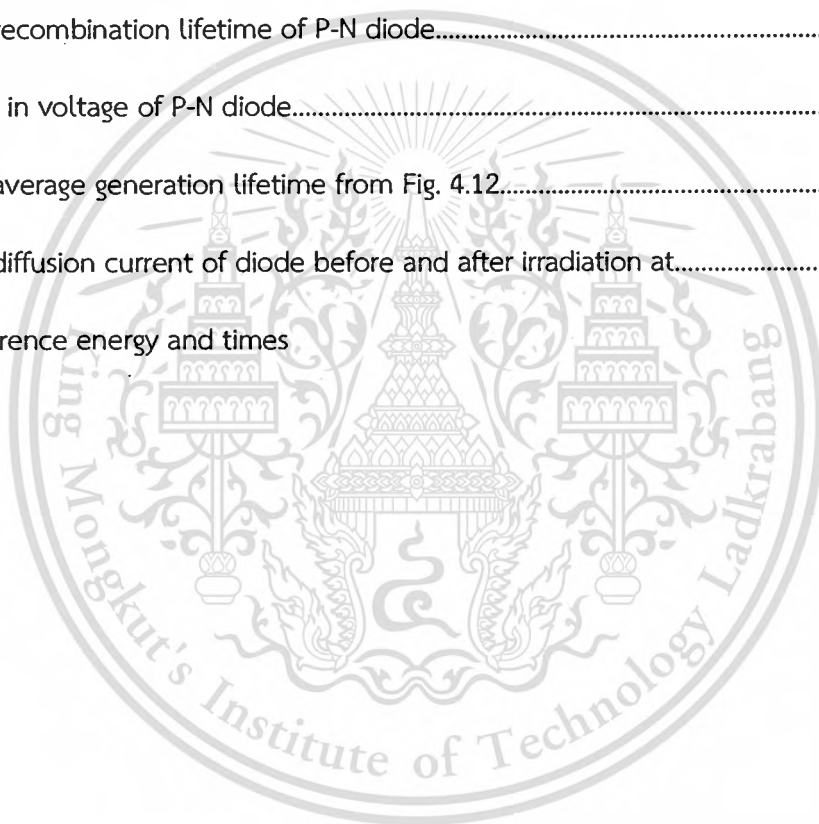
	Page
2.2.2 P-N junction diode in equilibrium.....	20
2.3 Electrical characteristics.....	22
2.3.1 Current-voltage characteristics (I - V).....	22
2.3.1.1 Activation energy (E_g).....	24
2.3.1.2 Carrier lifetime (τ).....	26
2.3.1.3 Series resistance (R_s).....	28
2.3.2 Capacitance-voltage characteristics (C - V).....	32
2.3.2.1 Depletion width (W).....	33
2.3.3.2 Carrier concentration (N).....	34
Chapter 3 Device fabrication and design of experiment.....	35
3.1 Device fabrication.....	35
3.2 Experiment.....	39
Chapter 4 Results and Discussions.....	43
4.1 Current-voltage characteristics (I - V).....	43
4.1.1 Forward bias.....	44
4.1.1.1 Series resistance (R_s).....	46
4.1.1.2 Ideality factor (n).....	49
4.1.1.3 Carrier Recombination lifetime (τ_r).....	50
4.1.1.4 Build in voltage (V_{bi}).....	51
4.1.2 Reverse bias.....	52
4.1.2.1 Activation energy (E_g).....	54
4.1.2.2 Diffusion current (I_d).....	56
4.1.2.3 Carrier generation lifetime (τ_g).....	58
4.2 Capacitance-voltage characteristics (C - V).....	60

Contents (Cont.)

	Page
4.2.1 Carrier concentration (N).....	62
4.2.2 Built in voltage (V_{bi}).....	64
4.3.4 Depletion width (W).....	64
Chapter 5 Conclusion.....	67
Reference.....	69
Appendix.....	76
Appendix A. X-ray Radiation Generator.....	77
Appendix B. CMOS Technology for Device Fabrication at TMEC.....	91
Appendix C. Paper publications.....	95
Author profile.....	112

Content of table

	Page
Table 3.1 X-ray radiation various energy and times.....	41
Table. 4.1. Series resistance of P-N junction diodes various energy and times.....	47
Table. 4.2. Sheet resistance of P-N junction diodes before and after exposure by X-ray.....	47
Table 4.3 shows the ideality factor of P-N diode before and after irradiation.....	50
by X-ray various energy and times	
Table. 4.4 The recombination lifetime of P-N diode.....	51
Table. 4.5 build in voltage of P-N diode.....	52
Table 4.6. The average generation lifetime from Fig. 4.12.....	57
Table 4.7. The diffusion current of diode before and after irradiation at.....	60
difference energy and times	



Content of picture

	Page
Fig. 1.1 An evolution of cell phone.....	1
Fig.1.2 The invention of a computer.....	2
Fig. 1.3 The I-V characteristics of $n^+ - p$ diode before and after irradiation by proton.....	3
Fig. 1.4 The forward bias I-V characteristics of Schottky diode for representative.....	4
203 MeV proton irradiation various fluence	
Fig. 1.5 Reverse bias I-V characteristics for representative 203 MeV proton irradiation.....	5
Fig. 1.6 The C-DLTS spectra of the silicon diode irradiated with 600 keV electrons.....	6
Fig. 1.7 The reverse current-voltage characteristics of Si photo-detector at various.....	7
temperature (a) unirradiated (b) irradiated with electron of dose 350 kGy	
Fig. 1.8 The variation of capacitance with temperature of Si photo-detector.....	8
(a) unirradiated, (b) electron irradiated	
Fig. 1.9 Schematic of photodiode.....	9
Fig. 1.10 The forward current of photodiode before and after neutron exposure.....	9
Fig. 1.11 Forward I-V characteristics of photodiode showing series resistance.....	10
calculation and change in the diode ideality factor	
Fig. 1.12 $I_F - V_F$ characteristics of Si detector, irradiated by neutron at various fluences.....	11
Fig. 1.13 Reverse branch of the current-voltage characteristics of silicon diode.....	12
1) before irradiation, 2) X-ray radiation for 15 min, 3) 50 min, 4) 100 min, 5) 140 min	
Fig. 1.14 Dependence of IR for silicon diode on the irradiation time 1) diode held.....	13
at reverse voltage, 2) V_r applied only for measurement (irradiation by X-ray)	
Fig. 2.1 The electromagnetic spectrum.....	16
Fig. 2.2 The penetrate of electromagnetic spectrum.....	17
Fig. 2.3 Diagram of the X-ray production by Bremsstrahlung.....	18
Fig. 2.4 Ideal I-V characteristics (a) Linear plot (b) Semi-log plot.....	20
Fig. 2.5 Figure Forming a p-n junction (a) The p-and n-type regions before junction.....	21
formation. (b) A schematic of the junction and the band profile showing the vacuum level and the semiconductor bands	

Content of picture (Cont.)

	Page
Fig. 2.6 Comparison of forward current between ideal and real diode.....	22
Fig. 2.7 The reverse current of ideal and reverse cases.....	23
Fig. 2.8 Arrhenius plot of J_A verse $1/kT$	25
Fig. 2.9 Recombination mechanisms of diode.....	27
Fig. 2.10 Generation mechanism in the term of reverse-biased.....	28
Fig. 2.11 Series resistance in P-N junction.....	29
Fig. 2.12 Forward bias characteristics of P-N diode showing the effect of series resistance.....	29
Fig. 2.13 Current versus voltage for P-N diode with the effect of series resistance.....	30
Fig. 2.14 The relation between semi-log current and voltage (a) shows the part of I-V curve where R_s is negligible (b) shows the part of the R_s -dominated curve	31
Fig. 2.15 Series resistance of P-N diode.....	32
Fig. 2.16 (a) A reverse-biased Schottky diode, and 16(b) the doping density and majority carrier density profiles in the depletion approximation	34
Fig. 3.1 The plan for this thesis.....	34
Fig. 3.2 The process flow of P-N diode fabrication using CMOS technology at TMEC.....	35
Fig. 3.3 P-N diode after fabrication.....	35
Fig. 3.4 Experiment diagram for the study of the effect of X-ray radiation on electrical characteristics of P-N diode	39
Fig. 3.5 Probe station at TMEC (a), (b) the Cascade Microtech Model M150..... (c) I-V probe station and (d). chunk of probe station	40
Fig. 3.6 X-ray radiation machine (C-arm Siemens Siremobil Compact 650 135)..... (a) control systems, (b) monitor and (c) point of X-ray irradiate	41
Fig. 4.1 The forward and reverse bias current vs voltage characteristics of the P-N junction diodes	43
Fig. 4.2. Forward I-V characteristics of the P-N junction diodes for different energy and dose	44

Content of picture (Cont.)

	Page
Fig 4.3. A plot V/I vs. $[\ln((I-I_0)/I_0)]/I$ obtained from forward bias current-voltage.....	45
characteristic of P-N diode	
Fig. 4.4 Capacitance-voltage characteristics of P-N diode.....	47
Fig. 4.5 A plot J_A vs. V obtained from forward bias current-voltage characteristics of.....	48
P-N diode	
Fig. 4.6 The relation between I vs. V for found V_{bi}	50
Fig. 4.7. Leakage current of diode before and after irradiated with various energy.....	51
and exposure dose	
Fig. 4.8 Arrhenius plot of generation current vs. temperature of the difference bias.....	53
Fig. 4.9 The value of the activation energy versus bias voltage.....	54
Fig 4.10 The leakage current versus the depletion width of the silicon p-n junction.....	57
Diode	
Fig. 4.11 The generation lifetime of P-N diode before and after X-ray irradiation.....	58
Fig. 4.12 Capacitance-voltage characteristics of P-N diode.....	60
Fig. 4.13 Carrier concentration of p-n junction diode at (a) 40 kV, (b) 55 kV and (c) 70 kV.....	62
Fig. 4.14 Graph relation between $1/C^2$ vs. V	64
Fig. 4.15 The depletion width of diode compare before and after irradiation.....	65

Abbreviation

Abbreviation word	Full word
Al	Aluminum
B	Boron
FESEM	Field Emission Scanning Electron Microscope
FFR	Floating Field Ring
GaAs	Gallium Arsenide
Ge	Germanium
IC	Integrated Circuit
KeV	Kilo-Electron Volt
LPCVD	Low-Pressure Chemical Vapor Deposition
MeV	Mega-Electron Volt
P	Phosphorus
PECVD	Plasma-Enhanced Chemical Vapor Deposition
RF	Radio Frequency
R-G	Generation-Recombination
Si	Silicon
SiGe	Silicon-Germanium
Si ₃ N ₄	Silicon-Nitride

Abbreviation (Cont.)

Abbreviation word	Full word
SiO ₂	Silicon Dioxide
SOI	Silicon-on-Insulator
STI	Shallow Trench Insulator
TCAD	Technology Computer-Aided Design
TMEC	Thai Microelectronics Center
UV	Ultraviolet



List of Symbol

A	is	Area of P-N diode
B	is	Radiation recombination coefficient
C_j	is	Junction capacitance
C_n	is	Auger recombination
C_p	is	Auger recombination
D	is	Dimension between point of X-rays and device
D_{TxR}	is	Average of radiation absorb in tissue
D_p	is	Diffusion coefficient of hole
D_n	is	Diffusion coefficient of electron
E_a	is	Activation energy
E_C	is	Conduction band
E_F	is	Fermi level
E_{Fi}	is	Fermi level intrinsic
E_V	is	Valence band
E_t	is	Trapping energy level
H_T	is	dose equivalent
k	is	Boltzmann constant
I_0	is	Saturation current
I_d	is	Diffusion current
I_g	is	Generation current
J_{0p}	is	Saturation current density
J_{gen}	is	Generation current density
J_{rec}	is	Recombination current density
$J_{n(diff)}$	is	Diffusion current density of electron
$J_{n(drift)}$	is	Drift current density of electron
$J_{p(diff)}$	is	Diffusion current density of hole
$J_{p(drift)}$	is	Drift current density of hole
J_R	is	Reverse current density

List of symbol (Cont.)

kV_p	is	X-ray energy
L_p	is	Diffusion range of hole
L_n	is	Diffusion range of electron
n	is	Electron density
p	is	Hole density
N_A	is	Acceptor density
N_C	is	Electron concentration in valence band
N_D	is	Donor density
N_T	is	Deep carrier concentration
n_i	is	Intrinsic carrier concentration
n_0	is	Equilibrium density of electron
n_{p0}	is	Electron concentration in p-type semiconductor
n_{n0}	is	Electron concentration in n-type semiconductor
Δn	is	Change of electron concentration
p_0	is	Equilibrium density of hole
p_{p0}	is	Hole concentration in p-type semiconductor
p_{n0}	is	Hole concentration in n-type semiconductor
Δp	is	Change of hole concentration
R	is	Recombination rate of electron and hole
R_S	is	Series resistance
S	is	Time of X-ray exposure
T	is	Temperature
V_A	is	Bias voltage
V_{bi}	is	Built in voltage
V_R	is	Reverse bias
V_T	is	Temperature on voltage
V_{th}	is	Temperature velocity

List of symbol (Cont.)

W_R	is	radiation weighting factor
W	is	Depletion region
μ_p	is	Hole mobility
μ_n	is	Electron mobility
\mathcal{E}	is	Junction electric field
\mathcal{E}_0	is	Vacuum permittivity
\mathcal{E}_s	is	Semiconductor permittivity
\mathcal{E}_{si}	is	Silicon permittivity
ϕ_{Fn}	is	Work function of n-type semiconductor
ϕ_{Fp}	is	Work function of p-type semiconductor
τ_0	is	Carrier lifetime
τ_g	is	Carrier generation lifetime
τ_r	is	Carrier recombination lifetime
τ_{SRH}	is	Carrier lifetime of SRH
τ_{rad}	is	Carrier lifetime by electromagnetic wave
τ_{Auger}	is	Carrier lifetime of Auger
τ_p	is	Hole lifetime
τ_n	is	Electron lifetime
η	is	Idea factor
σ_n	is	capture cross section of electron
σ_p	is	capture cross section of hole

CHAPTER 1

INTRODUCTION

1.1 Background and Motivation

The evolution of electronic devices has changed considerably compared with the previous time. In the past, people do not have the electronic devices, which can use in many applications and the size is so small like today. You can see the old cell phone in the early 1990s, it was like a huge brick, not handheld, and it could not fit in ones pocket. Besides, most people never had a cell phone because it was very expensive. This is completely different from the present cell phone as shown in Fig.1. The old cell phone has replaced by a smart cell phone that built on a mobile operating system, with advance computing capability and connectivity.



Fig.1.1 An evolution of cell phone (a) big telephone, and (b) small telephone.

Another obviously example of evolved electronic devices is a computer. The development of computer from vacuum tube to solid-state devices such as the transistor and later the integrated circuit. By 1959, discrete transistors were considered sufficiently reliable and economical that they made further vacuum tube computers uncompetitive. Computer main memory slowly moved away from magnetic core memory devices to solid-state static and dynamic semiconductor memory, which greatly reduced the cost, size and power consumption of computer devices. Eventually the cost of integrated circuit devices became low enough that home computers and personal computers became widespread.

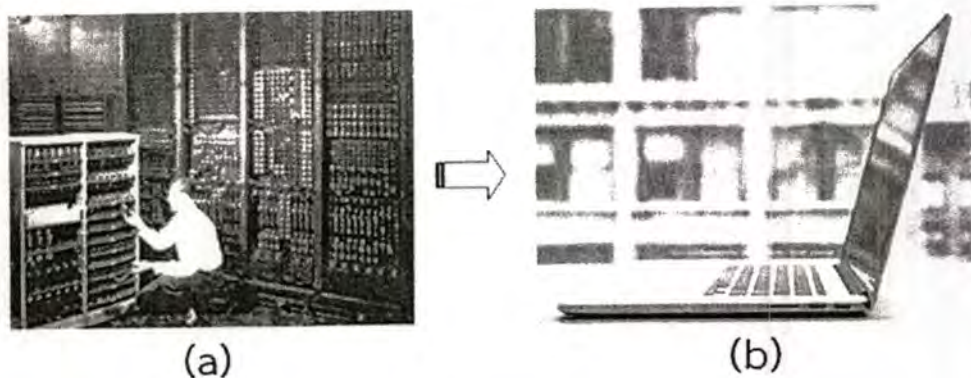


Fig.1.2 The invention of a computer

(a) very big computer, and (b) small computer.

All devices consist of the electronic components, which are important parts to make each device connect each other. Although many researchers want to down size of electronics device but enhancement of the device will come with more parts, therefore, high performance devices will also have a big size. During the researcher found the way to improve the device and decrease size, another group was found a new material that can improve the electronics device. It is not only the cell phone and computer, but also almost all of the electric equipments were built from semiconductor. A semiconductor is a incredible solid material because it has electrical conductivity in between a conductor and an insulator, and it can vary over that wide range either permanently or dynamically. The big size electronic circuit can down scale by using the semiconductor technology. Semiconductor devices are manufactured both as single discrete devices and as integrated circuits (ICs), which consist of a number from a few to millions of devices manufactured and interconnected on a single semiconductor substrate, for example, CMOS (Complementary Metal Oxide Semiconductor), capacitor, resistor, and transistor etc. Semiconductors that were used in the present such as silicon (Si) [1,2], germanium (Ge) [3,4], gallium-arsenic (GaAs) [5,6] and gallium nitride [7,8]. Silicon is a popular material for electronic devices because there is plenty of it on the earth, so its price is cheap. Moreover, silicon is not toxic as germanium and gallium-arsenic.

All the devices mentioned above were used in side of the world. Factors that cause equipment degradation that are temperature, humidity and deterioration of the material. In the present, many groups of research found a new area and more is a journey from the earth to another planet. The journey to the planets have been

implemented a long time, it has a limited such as period of journey and radiation damage to the device. The period times of the satellite are study of the energy and the speed of machine, while the other hand, the radiation damage is an important case because the satellite cannot to arrive in planet when the devices have damage. Moreover, the radiations are used in many works such as agriculture [9], medical [10], automobile [11], and construction [12] etc. Many kinds of rays are used, for example, proton [13-15], neutron [16-19], electron [20-23], and X-ray [24, 25]. The effect of radiation are difference effect on the electrical properties because the difference of energy.

1.1.1 Proton radiation

Proton radiation have high energy about more 1 MeV, many papers present the effect of proton to the electrical properties of the device base on silicon substrate. The examples papers are study the effects of proton radiation as shown

- 2011, Amporn Poyai – [IMEC, Belgium] this paper study the effect of high energy proton about 20 MeV compare the shape of device between square and meander.

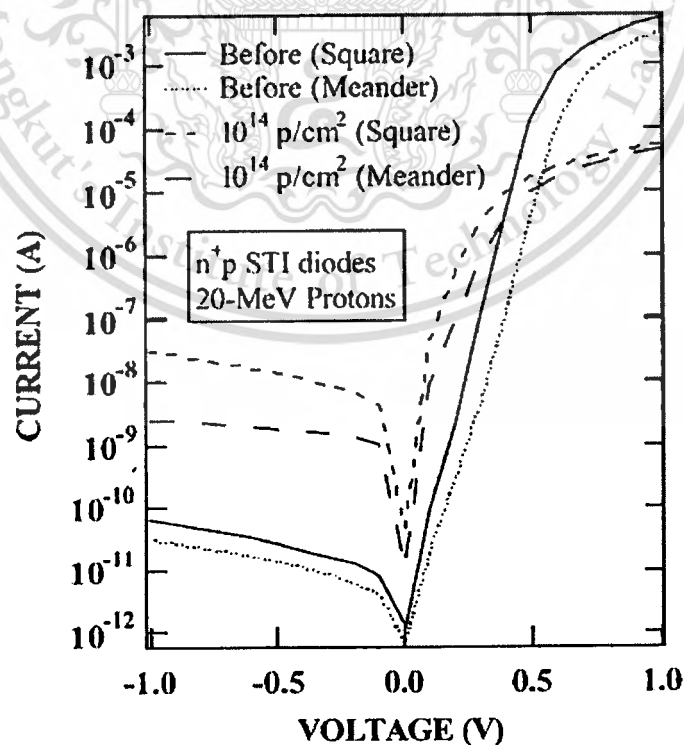


Fig. 1.3 The I-V characteristics of n^+p diode before and after irradiation by proton.

The current-voltage characteristics (I - V) are shown in Fig. 1.3 From this figure the leakage current after irradiation are increase about 2 to 3 orders and the forward current are decrease about 1 order. From the result shows that the proton radiations are damage in the device mechanism, therefore, the device performances are degradation. The leakage current are increase after high energy proton irradiation have many problems such as the radiation are induced trapping center in silicon bulk while the carrier are recombination before move to contact, the defects are decrease generation lifetime of carrier. The forward current term decrease about 1 order is cause from the proton radiation, the recombination lifetime and series resistance are important parameters to change the forward bias characteristics. In this paper are not to study the parameter of the device [26].

- 2006, Richard D. - [Analex Coporation, USA] the paper present effects of proton irradiation on Schottky diode. The I - V characteristics are shown in Fig. 1.4 and 1.5.

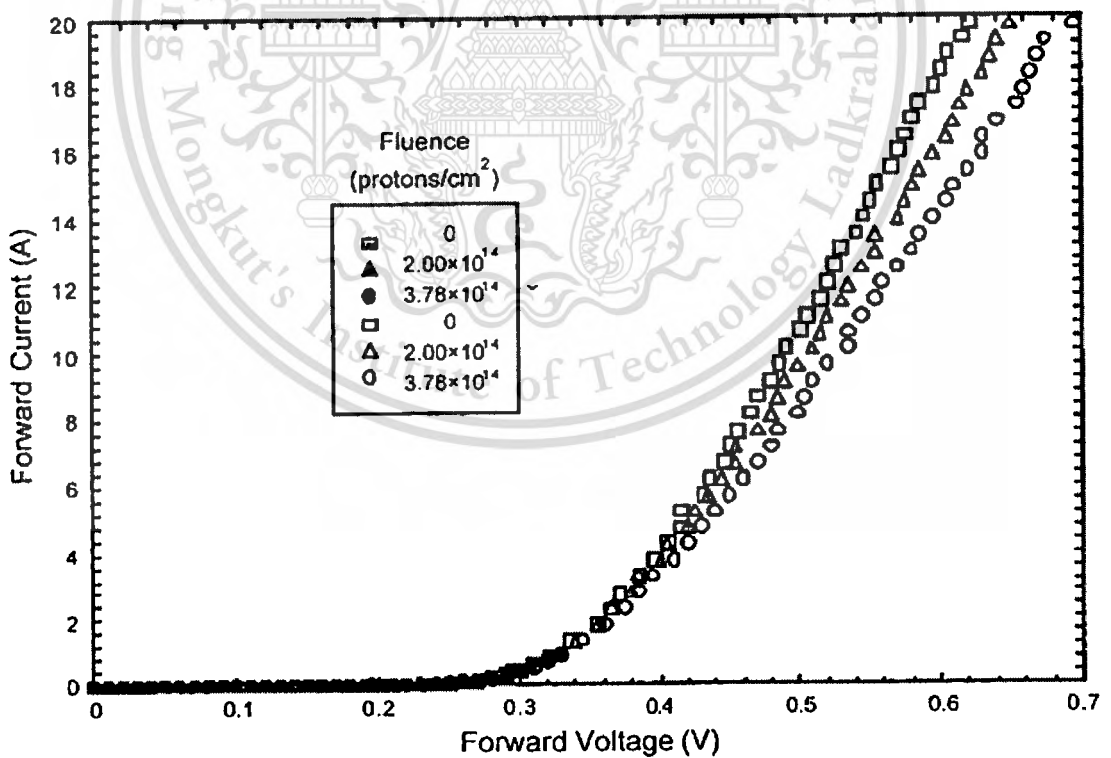


Fig. 1.4 The forward bias I - V characteristics of Schottky diode for representative 203 MeV proton irradiation various fluence.

This material is reserved for educational use only, not allowed for commercial use.

Forbidden to modify the content, and cite the document when use.

From Fig. 1.4 the shows the forward bias of Schottky irradiation by high energy proton at 203 MeV various proton fluence, the forward current decrease when increase the proton fluence. The reverse current is shown in Fig. 1.5, the leakage current are decrease at 2×10^{13} photon/cm², on the other hand, the leakage current are increase at 3.78×10^{14} photon/cm². From the results show that the proton radiation are effect to the forward and reverse current, the forward current are decrease after irradiation every fluence while the leakage current decrease at 2×10^{13} photon/cm². Therefore, the radiation not only decrease the device performance, on the other hand, it can use for improve the device characteristics at the optimize fluence [27].

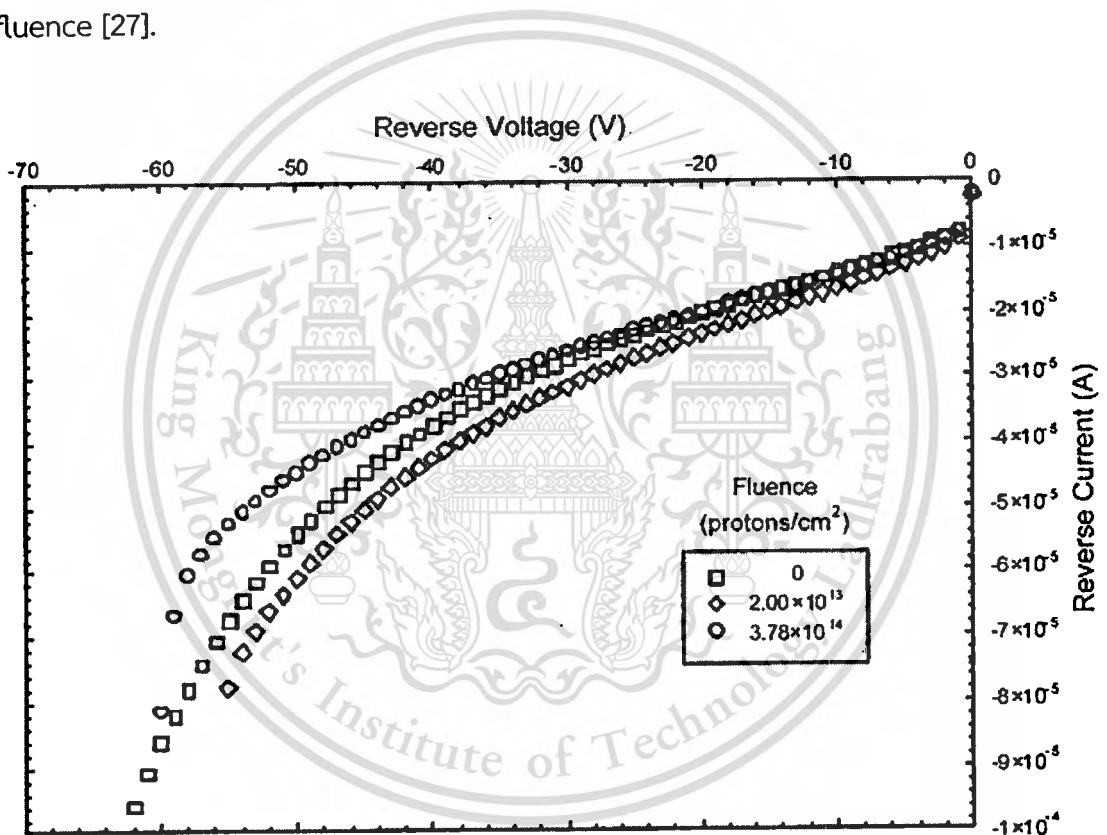


Fig. 1.5 Reverse bias I-V characteristics for representative 203 MeV proton irradiation.

1.1.2 Electron radiation

Electron radiation are high energy but less than proton radiation, the electron energy are research in the present use in range about 400 keV to 5 MeV. Many papers are study the effect of electron radiation on the properties of device because the radiation come to human life.

This material is reserved for educational use only, not allowed for commercial use.

Forbidden to modify the content, and cite the document when use.

- 2006, P. Hazdra – [Department of microelectronics, Czech republic] the paper of the electron defect in silicon device. The silicon device was irradiated with 600 keV electrons to fluences from 2×10^{13} to $1 \times 10^{15} \text{ cm}^{-2}$. The results of this paper shows in the vicinity of the anode junction, the profile of vacancy-related defect centers in strongly influenced by electric field and an excessive generation of vacancies. In the bulk, the slope of the profile can be derived from the distribution of absorbed dose taking into the account the threshold energy necessary for Frenkel pair formation and the dependency of the defect introduction rate on the electron energy. The C-DLTS spectra in Fig. 1.6 shows a typical series of deep levels in the n-silicon base of diode irradiated with 600 keV electrons [28].

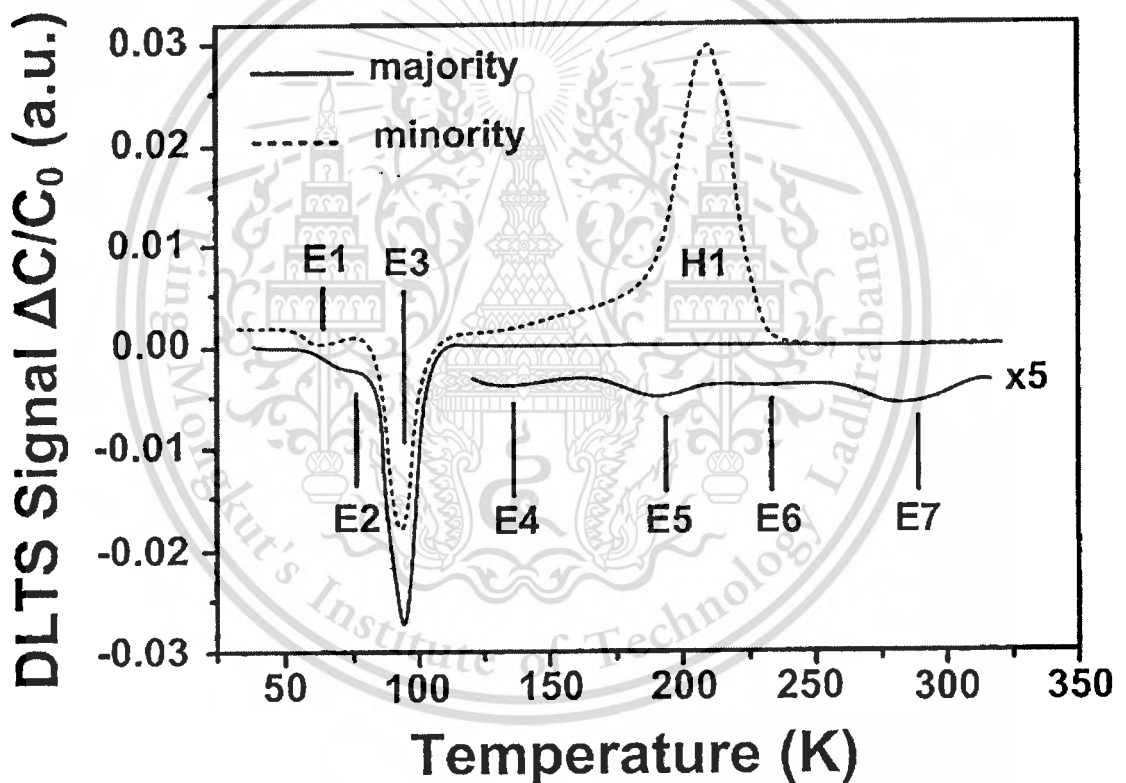


Fig. 1.6 The C-DLTS spectra of the silicon diode irradiated with 600 keV electrons.

- 2007, Manjunatha Pattabi – [Mangalore University, India] The paper present, the current transport mechanisms of $n^+ - p$ silicon (Si) photo-detectors in different and bias regions before and after irradiation with a dose of 350 kilo-gray (kGy).

The reverse current after irradiation are increase every temperature shown in Fig. 1.7. From Fig. 1.7 the reverse current are increase about $20 \mu\text{A}$ at 370 K. Fig. 1.8

shows C-T variations at 1 MHz of the devices before and after irradiation. there is a slight deviation from linearity.

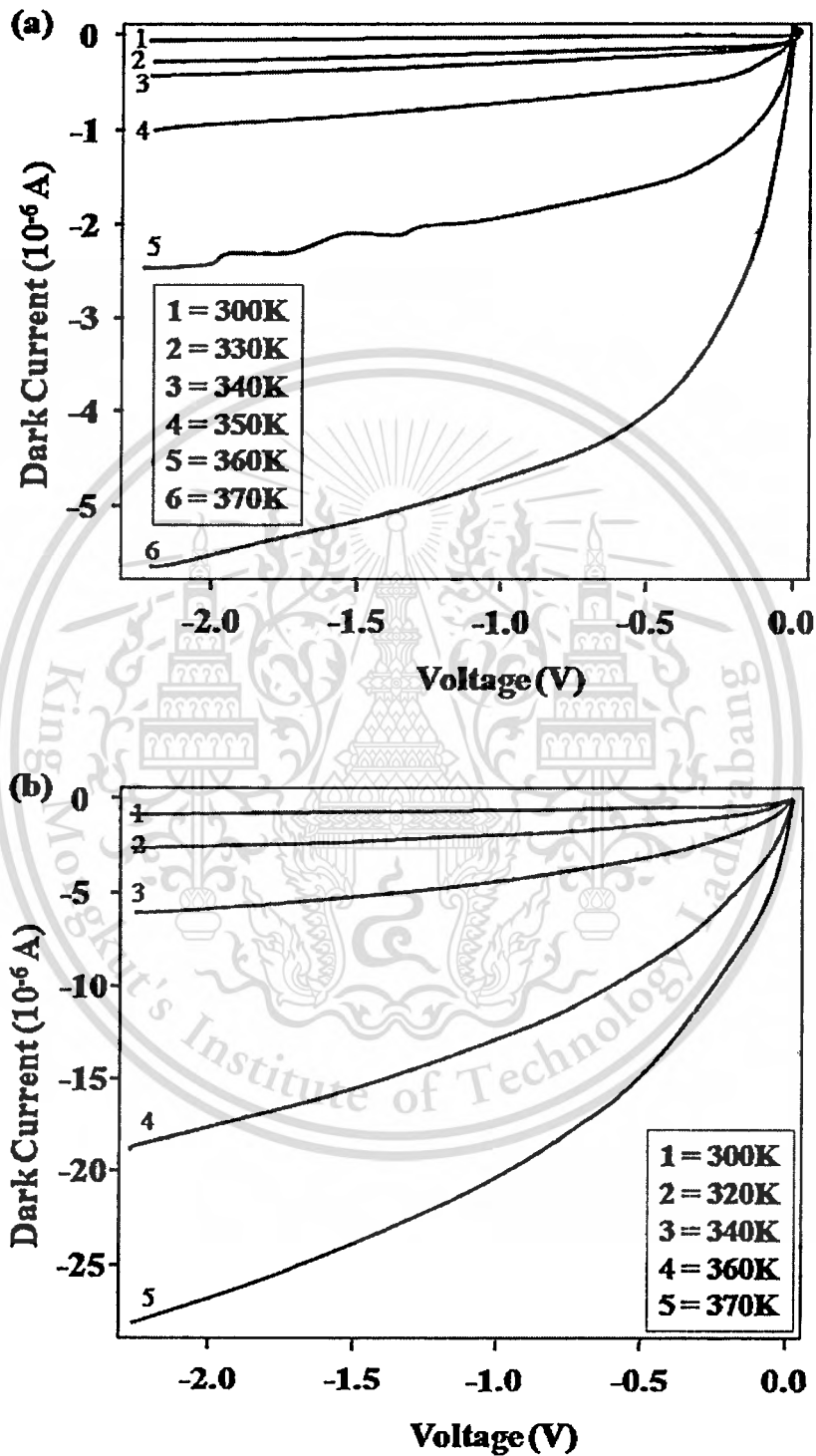


Fig. 1.7 The reverse current-voltage characteristics of Si photodetector at various temperature (a) unirradiated (b) irradiated with electron of dose 350 kGy.

This material is reserved for educational use only, not allowed for commercial use.

Forbidden to modify the content, and cite the document when use.

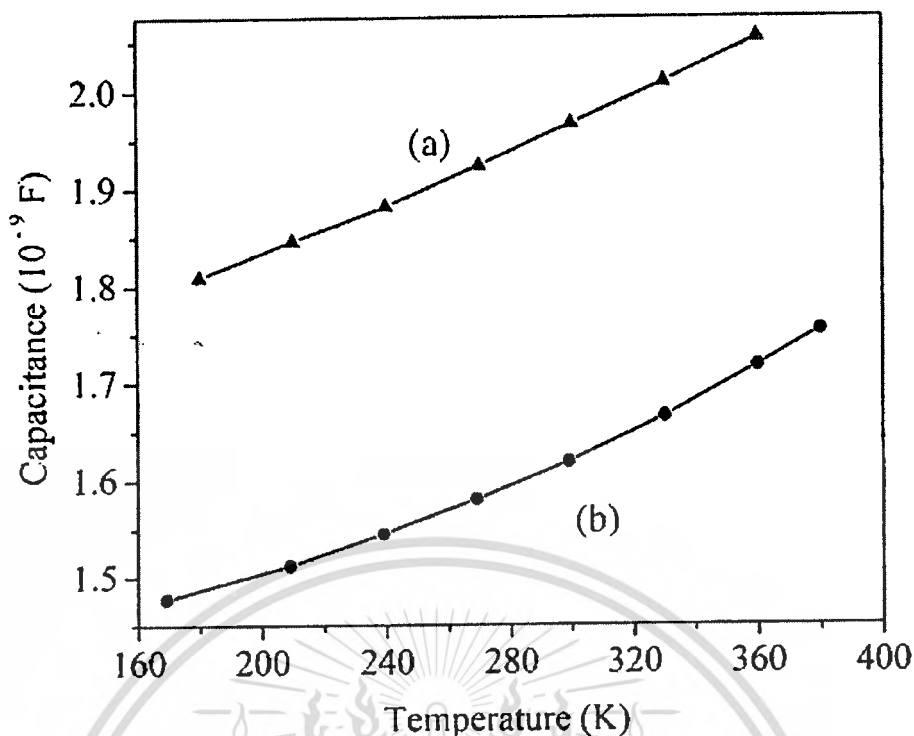


Fig. 1.8 The variation of capacitance with temperature of Si photodetector (a) unirradiated, (b) electron irradiated.

The results of this paper show (i) electron irradiation might not have caused any major change in the depletion region of the device as generation recombination part of the dark current is not change due to irradiation and (ii) capacitance-voltage measurements indicate that considerable numbers of deep levels were not introduced by irradiation [29].

1.1.3 neutron radiation

- 1989, R. Korde - [United Detector Technology, California] The effect of neutron irradiation on the silicon photodiode are present in the paper. The silicon photodiode are being used routinely in military systems in ring laser gyros, fiber optics, laser range finders, and ocean communication systems. The system of photodiode are shown in Fig. 1.9.

From Fig. 1.10 shows the forward I-V characteristics of photodiode before and after neutron irradiation. As seen from this figure, neutron exposure increase the static and dynamic resistance of the diode. The resistance of the diode before and after irradiated are shown in Fig. 1.11.

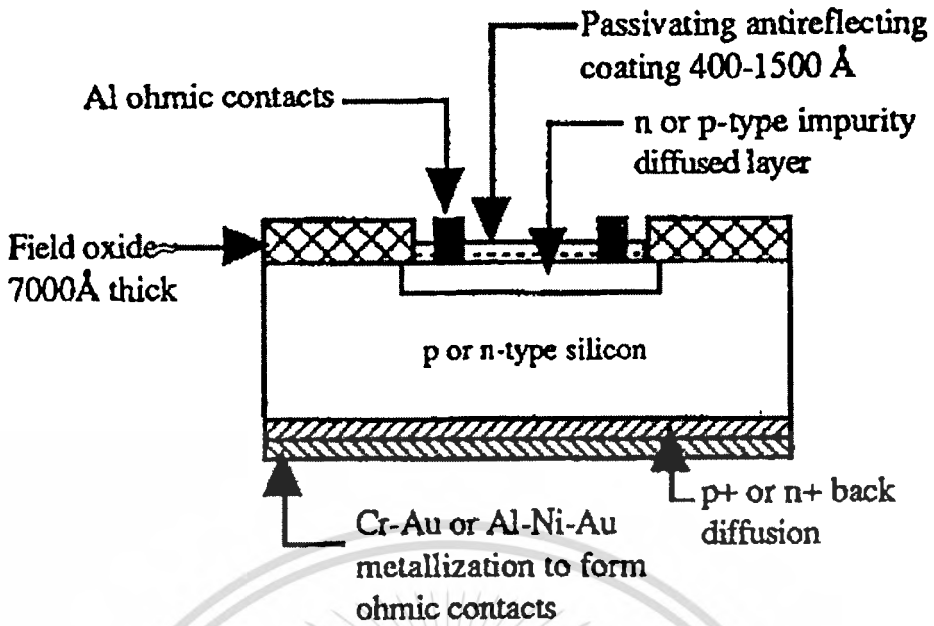


Fig. 1.9 Schematic of photodiode.

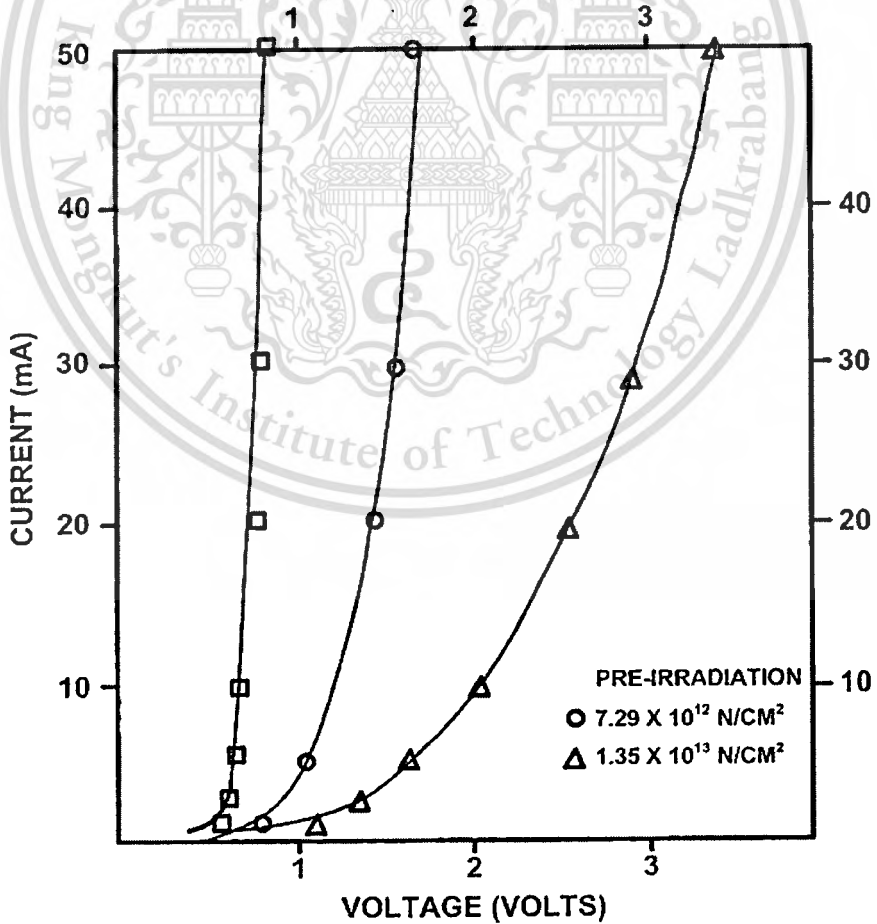


Fig. 1.10 The forward current of photodiode before and after neutron exposure.

The P-N junction theory as the diode ideality factor (η) values observed are 1 and 2 for moderate and high currents respectively. The series resistance are increase from 0.75 to 0.95 ohm after irradiation [30].

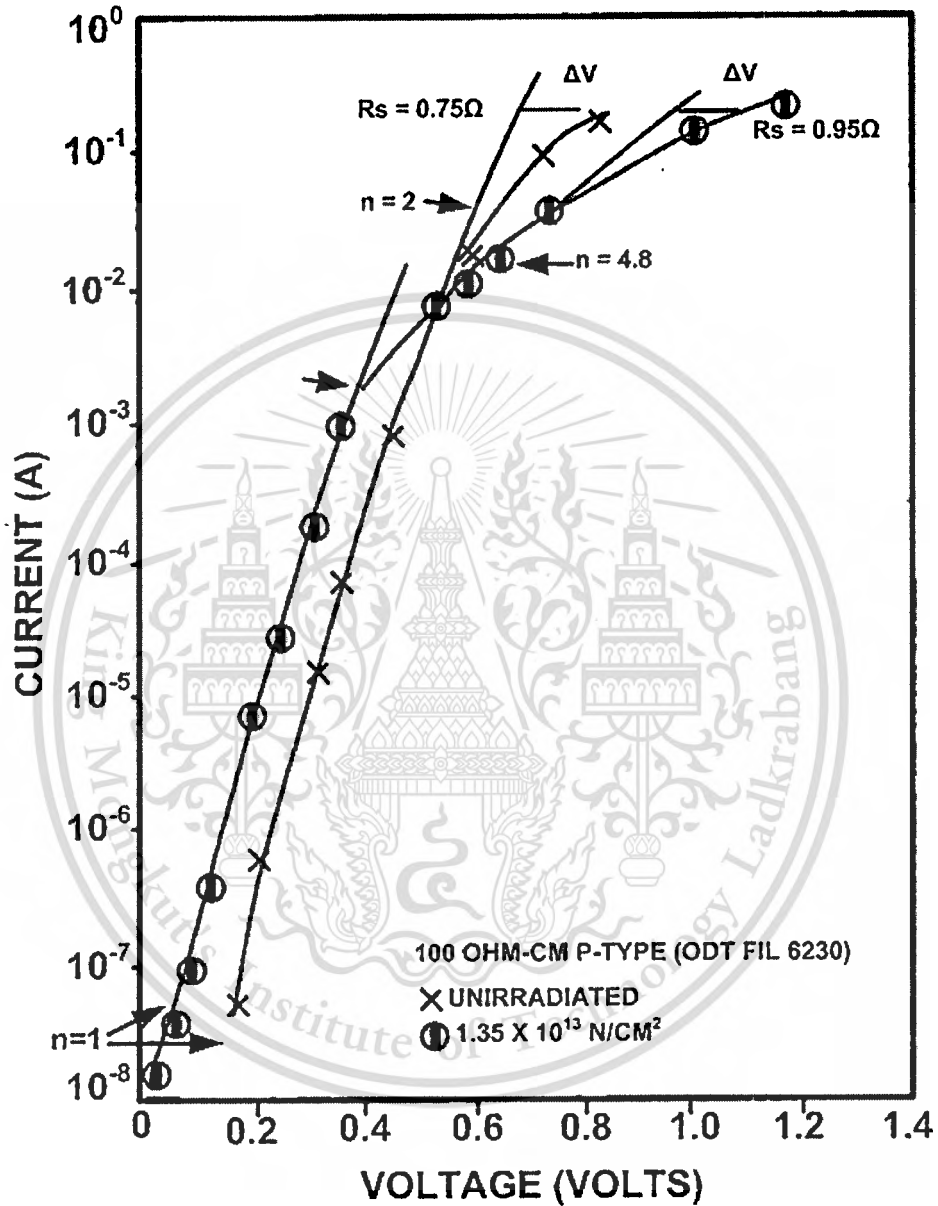


Fig. 1.11 Forward I-V characteristics of photodiode showing series resistance calculation and change in the diode ideality factor.

- 1996, N. Croitoru - [United Detector Technology, California] Current-voltage characteristics of neutron irradiated silicon detector are present in this paper. The devices irradiated by neutron at 10 MeV and flux 6.475×10^{11} n/cm²s. On Fig. 1.12 This material is reserved for educational use only, not allowed for commercial use.

Forbidden to modify the content, and cite the document when use.

shows the forward I-V characteristics of diode are irradiated by neutron various flux of radiation, the forward current are decrease when the electron flux increase. This seems to indicate that, after a strong reduction of ratification of the detector, a new type of damage is being induced, which does not continue too much to decrease the rectification [31].

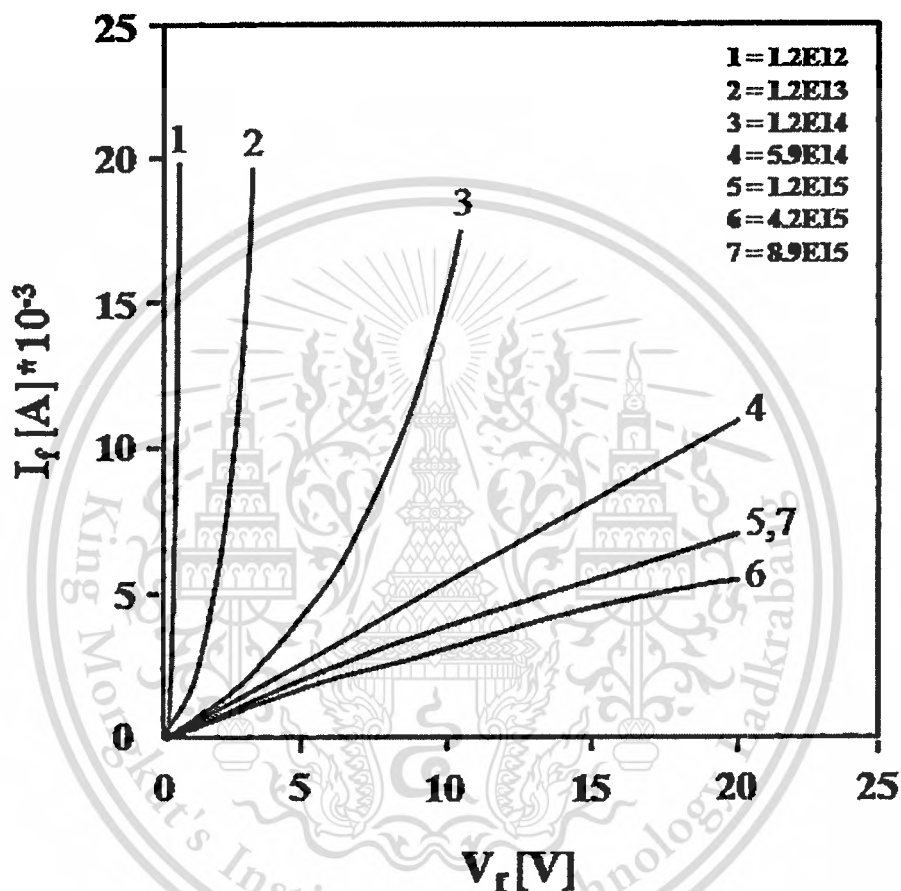


Fig. 1.12 I_F - V_F characteristics of Si detector, irradiated by neutron at various fluences.

From the papers of proton, electron and neutron present that high energy radiation are damage in the mechanism of devices such as carrier lifetime and induced defects, etc. The current after irradiation change in the trend of degradation performance. Although high energy radiation are impact to the device performance, on the other hand, the research important because the radiation come in people life and we have to found way to defend it. X-ray radiation are popular to use in many work but have a little to research and explain the effect to semiconductor device.

This material is reserved for educational use only, not allowed for commercial use.

Forbidden to modify the content, and cite the document when use.

1.1.4 X-ray radiation

- 1967 and 1969, M. A. Krivov - [Siberian Physic technical Institute, Tomsk State University] The effect of X-ray studied in the old time shown in Fig. 1.13.

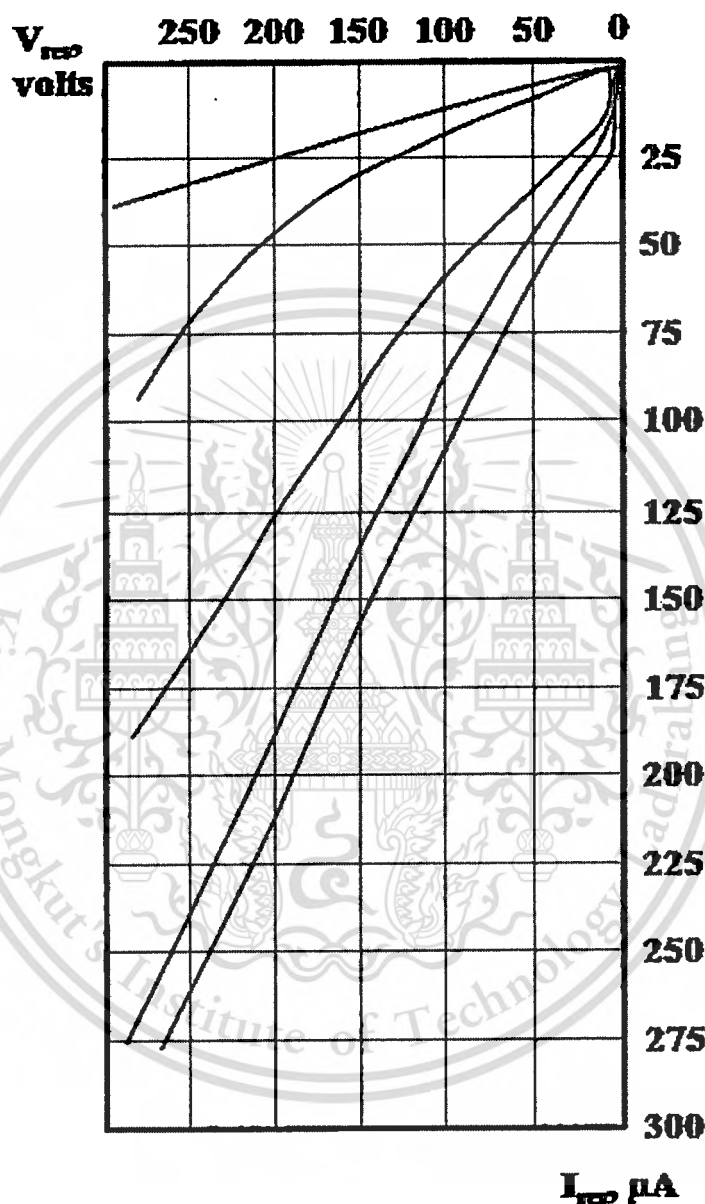


Fig. 1.13 Reverse branch of the current-voltage characteristics of silicon diode 1) before irradiation, 2) X-ray radiation for 15 min, 3) 50 min, 4) 100 min, 5) 140 min.

From Fig. 1.13 shows the leakage current after irradiation by X-ray various times are increase, the leakage current increase when time of exposure increase. Fig. 1.14 shows that the line number 1 is before and 2 is after irradiation, the leakage

current decrease when the exposure time about 100 min. In this case is very interesting because the X-ray can reduce the leakage current at the optimize exposure time. Although, this paper have an interesting point but the research are not to study continue and do not explain the effect of X-ray to device parameters.

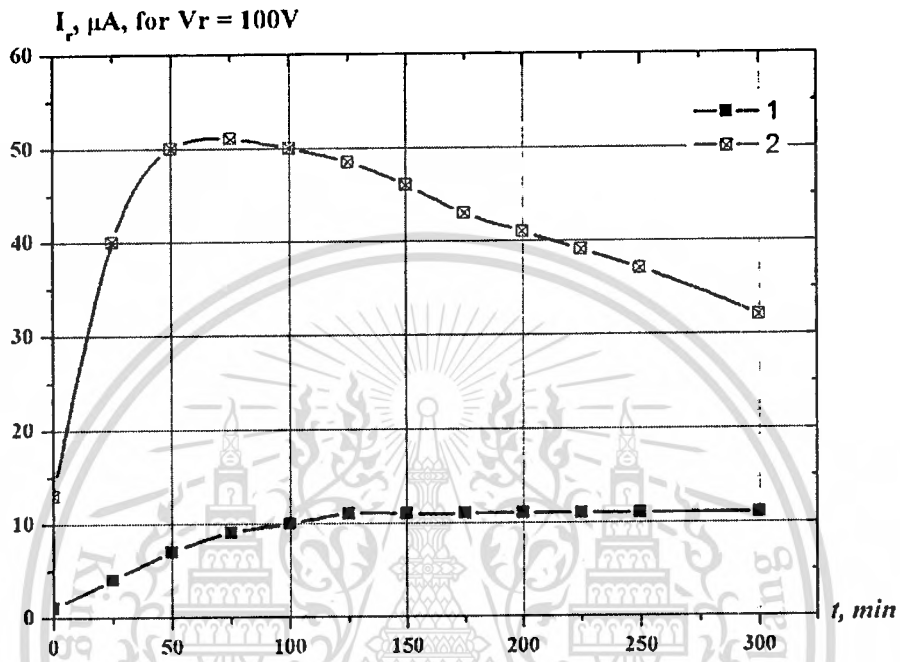


Fig. 1.14 Dependence of IR for silicon diode on the irradiation time 1) diode held at reverse voltage, 2) V_r applied only for measurement (irradiation by X-ray).

Many papers are present relate the effect of proton, neutron and electron radiation to semiconductor device. On the other hand, X-ray radiation can improve the device performance with optimize dose but have a little papers. Therefore, this thesis study the effects of X-ray radiation to the device properties and find optimize time and energy to use for improve the device performance [24,32].

1.2 Aim of thesis

One of the primary objective of this work was the study and analysis the effect of X-ray irradiation on the electrical properties of P-N diode. The radiation are use in many application, therefore, radiation device require to improve lifetime and performance. With this goal of mind, the effect of X-ray to P-N diode parameters are

first studied. The next stage of the study involve the use of X-ray irradiation to improve performance of the semiconductor device.

1.3 Hypothesis

From the literature papers present that many researcher were studied the characteristics of device after irradiation because human life are involved with the radiation. Therefore, the researcher should understand the behavior of the radiation of semiconductor device to use with human. The goal of this thesis study and analyze of the characteristics of P-N diode after X-ray irradiation and find the optimize of X-ray time and energy to use in semiconductor technology in the present and future.

1.4 Objective

This thesis use the X-ray radiation to study on the characteristics of semiconductor devices. the objective of this thesis consist of

- Study and analysis the effect of X-ray to P-N diode properties.
- Find the way to develop the device to use with X-ray radiation.
- Study the X-ray radiation for improve the P-N diode performance.

1.5 Summary and Layout of thesis

Chapter 1 This chapter relevant literature survey old research to study the effect of radiation on electrical properties of the semiconductor device and motivation to study the effect of X-ray radiation on the characteristics of P-N junction diode.

Chapter 2 This chapter present background and theory of the P-N diode and research literature of the radiation device such as proton, electron, neutron and X-ray devices. The technique to analyze of the electrical characteristics of P-N diode are present in this chapter. The I-V and C-V characteristics are important to study the X-ray effect on P-N diode properties.

Chapter 3 This chapter description of all the processing steps involved in the fabrication of the device, the device fabrication in the thesis use CMOS technology at Thai Microelectronics Center (TMEC). The experiment step of the X-ray irradiation on the device at various energy and times present in the chapter.

This material is reserved for educational use only, not allowed for commercial use.

Forbidden to modify the content, and cite the document when use.

Chapter 4 This chapter present of experiment results and discussion of this research. The results show the characteristics of P-N diode before and after irradiation by X-ray. The I-V and C-V characteristics consist of many parameters to analyze the device properties such as carrier concentration (N), carrier lifetime (τ), activation energy (E_a), series resistance (R_s), etc.

Chapter 5 The conclusion of the work and a list of suggestions for further work are presented in this chapter.



Chapter 2

Background and Theory

In this thesis studies the effect of X-ray radiation on the electrical properties of P-N junction diode. This chapter presents the background and theory of X-ray radiation, P-N junction diode and measurement analysis. The measurement technique are use in the thesis such as I - V , C - V characteristics, and including analysis important parameter to influence of diode properties such as activation energy (E_a), series resistance (R_s) and carrier lifetime (τ).

2.1 X-ray radiation

X-rays are a high-energy type of electromagnetic (EM) radiation. X-ray radiation has a shorter wavelength than visible light, so X-ray have much higher energies than photons of light.

2.1.1 X-ray properties

X-rays lie between ultraviolet and gamma rays on the electromagnetic spectrum. X-rays have wavelengths between about 10 nanometers and 10 picometers. X-ray radiation oscillates at rates between about 30 petahertz (PHz or 10^{15} hertz) and 30 exahertz (EHZ or 10^{18} hertz) shows in Fig. 2.1. [33]

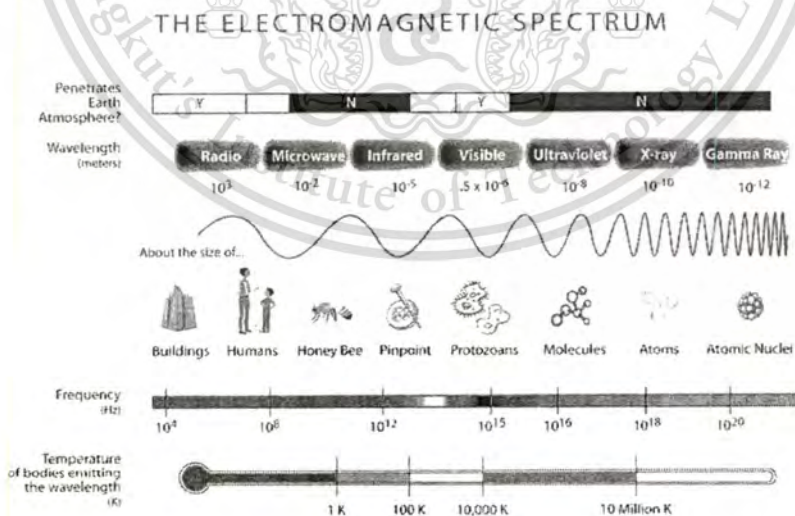


Fig. 2.1 The electromagnetic spectrum.

X-rays are subdivided into hard X-rays and soft X-rays. The lower energy soft X-rays have longer wavelengths, while the higher energy hard X-rays have shorter wavelengths. The cutoff between the two types of X-rays is around a wavelength of 100 picometers. X-rays with energies between 10 to 100 keV are considered soft X-rays.

There is no sharp distinction between the highest energy X-rays and the lowest energy gamma rays. The distinction between X-rays and gamma rays is actually based on the origin of the radiation, not on the frequency or wavelength of the electromagnetic waves. Gamma rays are produced by nuclear transitions, while X-rays are the result of accelerating electrons. [34]

X-rays are absorbed by high dense materials such as lead and uranium, such that they can penetrate only a short distance into the material. This is why lead shielding is used to protect people from excessive exposure to x-rays.

The thickness of the shielding is determined by the voltages used to generate the X-rays, which in turn determines the amplitude and wavelength of the radiation. For X-rays generated by peak voltages of 75 kilovolts (kV), a thickness of only 1 millimeter (mm) or 0.039 inches of lead shielding is sufficient to stop the X-rays. But for X-rays generated with 900 kV, a thickness of 51 mm or 2 inches of lead shielding is required. The examples of X-ray penetrate on difference material shows in Fig. 2.2.

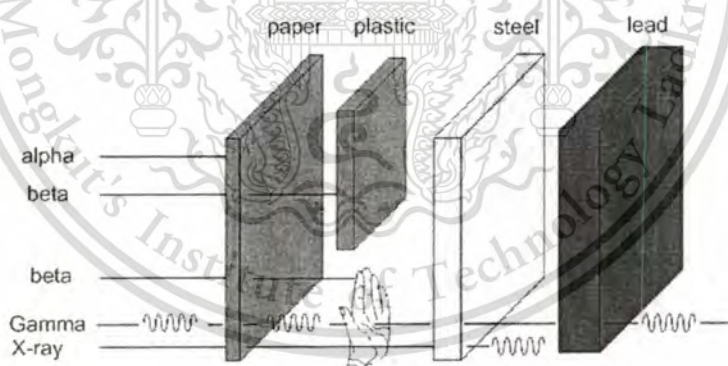


Fig. 2.2 The penetrate of electromagnetic spectrum.

There are three major ways that x-rays are produced or generated. The most common is the Bremsstrahlung process, where a high speed electron traveling in a material is slowed or stopped by the forces of an atom it encounters, thus emitting an X-ray show in Fig. 2.3. [35]

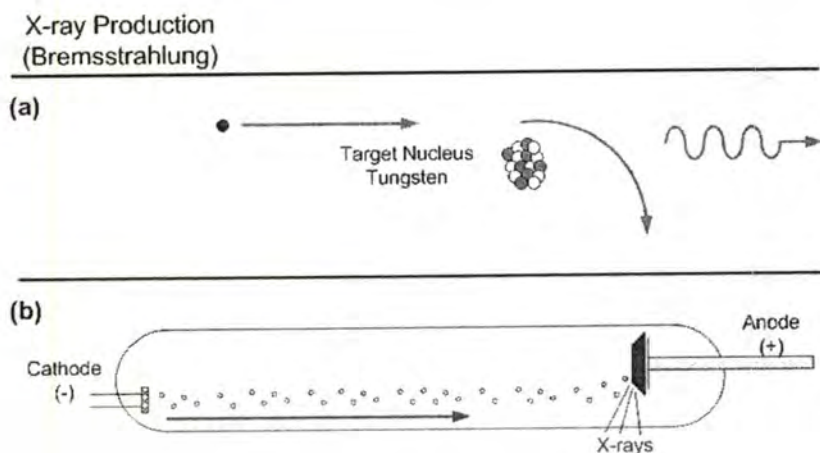


Fig. 2.3 Diagram of the X-ray production by Bremsstrahlung (a) mechanism of particle collision (b) particle bombard in tube.

X-rays are produced when swiftly moving electrons strike a solid target. According to classical electrodynamics, a moving charged particle emits electromagnetic radiation when it is accelerated; the sudden stopping of an electron gives rise to a pulse of radiation which takes the form of X-rays. In practice, X-rays are sometimes produced in a low pressure, gas filled cathode-ray tube in which a metal anticathode is situated opposite the cathode. The anticathode serves as target for the electron emitted from the cathode and as the source of X-rays. In the more frequently used Coolidge tube, the cathode is a wire which is heated to such a temperature that it emits thermoelectrons. The tube is evacuated until there is no appreciable amount of gas remaining, so that all of the current through the tube is carried by the thermoelectrons. The anticathode is usually a metal of high atomic weight such as tungsten, because the energy carried by the X-rays from heavy metals has been found to be greater than the energy of the X-rays from light metal. One of the most important properties of X-rays is the strong penetrate power. [36]

2.1.2 Applications of X-ray radiation

X-rays are important in many work such as medical, industrial and agriculture. Although, X-rays is important but it have high energy and high damage to X-ray detector. Therefore, the device lifetime is very short. [37]

2.1.2.1 Medical work

X-rays refer to radiation, waves or particles that travel through the air like light or radio signals. X-ray energy is high enough that some radiation penetrate objects (such as internal organs, body tissues, and clothing) and onto X-ray detectors (such as film or a detector linked to a computer monitor). In general, objects that are more dense (such as bones and calcium deposits) absorb more of the radiation from the x-rays and don't allow as much to pass through them. These objects leave a different image on the detector than less dense objects. Specially trained or experienced physicians can read these images to diagnose medical conditions or injuries.

The most common use of x-rays is in medicine and dentistry. X-rays are used to examine inside the body to try to see if there is anything abnormal. Broken bones, cancerous growths, and tooth decay are some of the problems that can be detected by an X-ray of a person. [38]

2.1.1.2 Agriculture work

As the volume of imported foods increases and food product safety has become a major concern, the application of X-ray imaging for agricultural inspection is growing rapidly. Products such as baby foods are scanned for foreign objects and nuts, grains, and seeds are screened for size, density, and pest control. Most organic materials do not require high energy X-ray photons for penetration (<30kV), however, volumes of material often pass through inspection at a rapid rate. Rad-ikon's standard (non-EV) camera products can be used at higher frame rates to accommodate volume inspection. [39]

2.1.1.3 Industrial work

Another use of x-rays is in industry. They can be used to detect structural problems and cracks in metals that cannot be seen from the outside. X-rays are used on commercial airplanes and bridges to make sure there are no stress fractures or other dangerous cracks in the material.

That can be seen from the examples of X-ray radiation. Although, X-rays are widely use in many fields but found that the research and develop of a device are quite a few. Therefore, this thesis is recognize the important of the study and analysis of X-rays effect on detector for improve device performance and long lifetime in use. [40]

2.2 P-N junction diode

P-N junction diode is one of most important junctions in solid-state electronics. The junction is used as a device in applications such as rectifiers, waveform shapers, variable capacitors, lasers, detectors, etc. In this thesis studies the effect of X-ray irradiation on the characterization of P-N junction diode. Before investigate this experiment, we have to study the general characteristics of P-N diode.

2.2.1 Ideal P-N junction diode

P-N junction diodes have three regions (p region, n region and depletion region). The Fig. 2.4 (a) shows the reverse and forward current density of P-N diode and semi-log shown in Fig. 2.4(b).

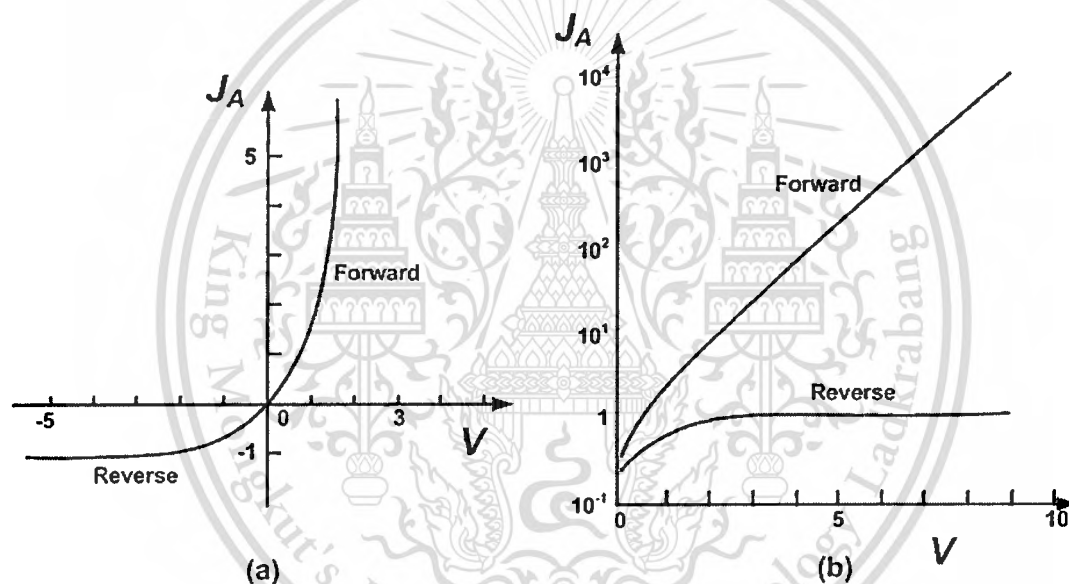


Fig. 2.4 Ideal I-V characteristics (a) Linear plot (b) Semi-log plot.

2.2.2 P-N junction diode in equilibrium

P-N junctions have 2 types of semiconductors, p- and n-type semiconductor without forming a junction as shown in Fig. 2.5. The electron affinity $e\chi$, defined as the energy difference between the conduction band and vacuum level, is shown along with the work function ($e\phi_{sp}$ or $e\phi_{sn}$). The work function represents the energy required to remove an electron from the semiconductor to the "free" vacuum level and is the difference between the vacuum level and the Fermi level. [41]

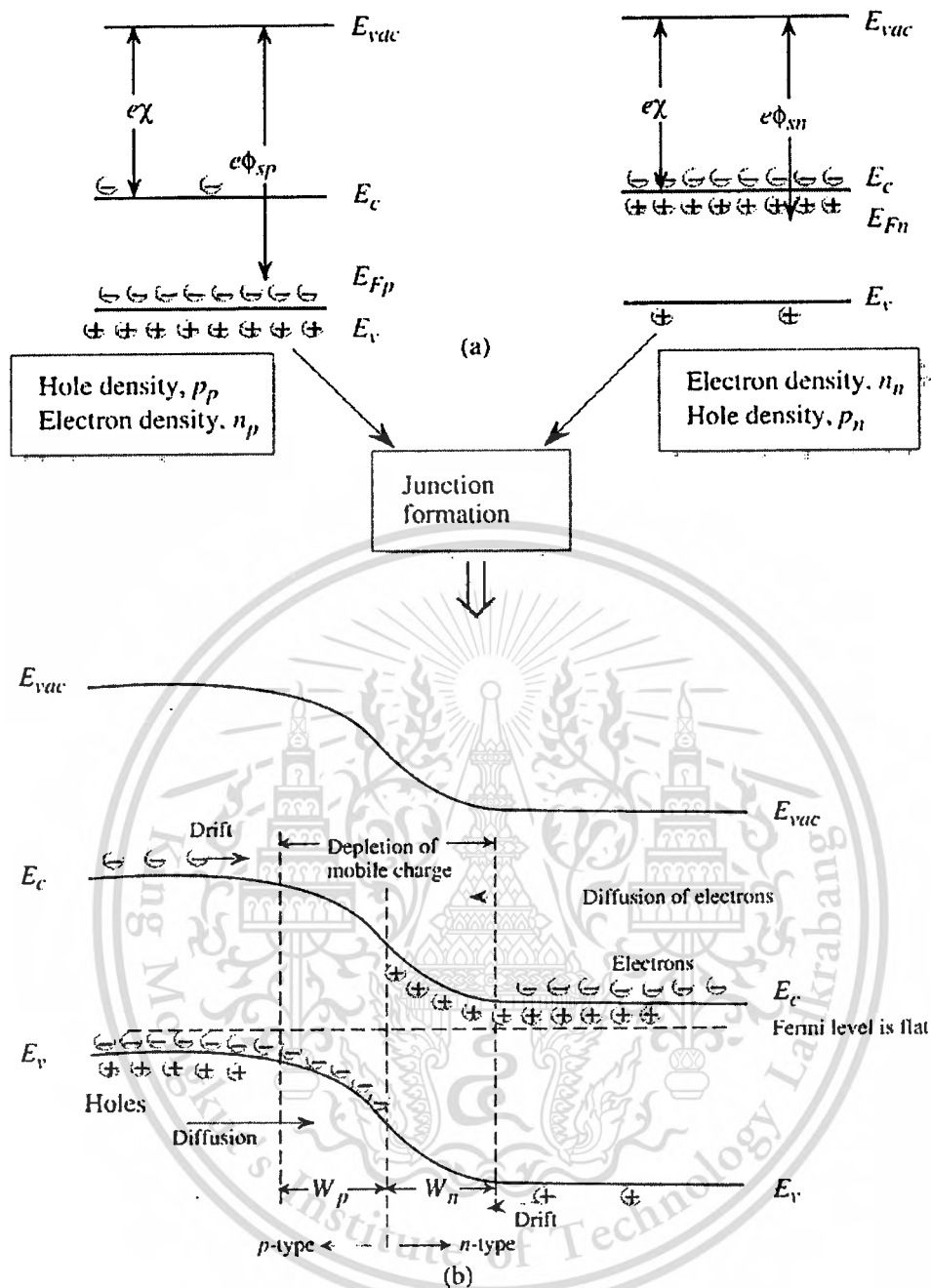


Fig. 2.5 Figure Forming a P-N junction (a) The P-and N-type regions before junction formation. (b) A schematic of the junction and the band profile showing the vacuum level and the semiconductor bands.

We have to examine what happens when the P- and N-type materials are made to form a junction. In the unapplied bias, there is no current in the system and the Fermi level is uniform throughout the structure. In figure 2.5 (b) we show a schematic of the band diagram of a P-N junction.

Majority carriers near the interface on P- and N-side diffuse across the junction, as a result of the difference in electron and hole densities across the junction. The electrons with n-type diffuse to the p-side recombine with hole, and holes with p-side which diffuse to the n-side recombine with electrons. As a result, a region is formed near the junction that has been depleted of mobile carriers. The electric field exists in depletion region that sweeps out any electrons and holes that enter the region.

Three regions can be identified as seen in Fig. 2.5 (b):

- 1) P-type region is neutral and the bands are flat material. The density of acceptors exactly balances the density of hole.
- 2) N-type region where again the material is neutral and the density of immobile donors exactly balances the free electron density.
- 3) Around the junction there is depletion region where the bands are bent and a field exists that sweeps the mobile carriers, leaving behind negatively charged acceptors in the p-region and positively charged donors in the n-region.

2.3 Electrical characteristics

The properties of P-N diode are studied by the electrical characteristics, the electrical can explain many effects in the device such as silicon growth damage, fabrication damage and every damage from user. The electrical properties of diode have 2 characteristics (or techniques) which are current-voltage (I-V) and capacitance-voltage (C-V) characteristics.

2.3.1 Current-voltage characteristics (I-V)

The current of P-N junction is often written as a function of the diode voltage as

$$I = I_0 \left(e^{qV_d/nkT} - 1 \right) \quad (2.1)$$

Where η is the diode ideality factor, V_d is the voltage across the space-charge region and excludes any voltage drops across the p and n quasi-neutral regions. If both I_0 and n are constant, then a plot of $\log(I)$ versus V_d yields a straight line for $V_c > nkT/q$.

Fig. 2.7 shows the reverse current of diode in the case of ideal and real. The reverse bias in real case has the leakage current more ideal case. The leakage current in real case occurs some defects in the device such as bulk defects and crystal defects.

Fig. 2.6 and 2.7 show a plot of the absolute value of the ideal forward and reverse current compared with a real. Three effects can cause a deviation in the forward current. At low forward bias [42], B1 is due to the recombination current in the bulk, [43] B2 caused by high carrier injection, while the small current at B3 relates to the series resistance [44].

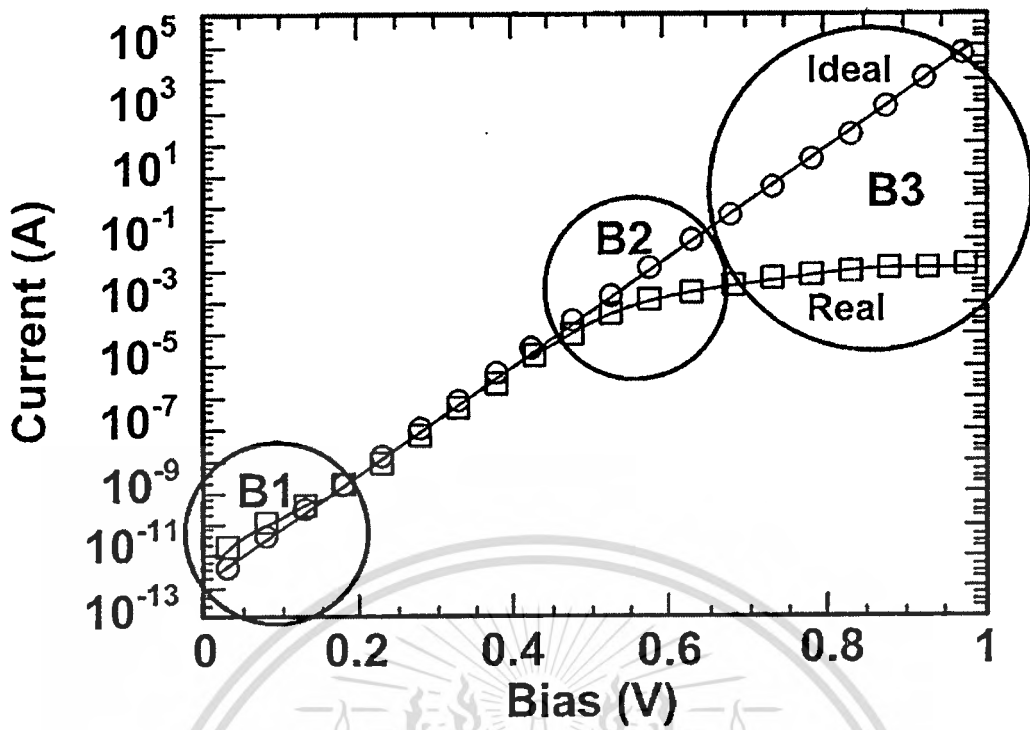


Fig. 2.6 Comparison of forward current between ideal and real diode.

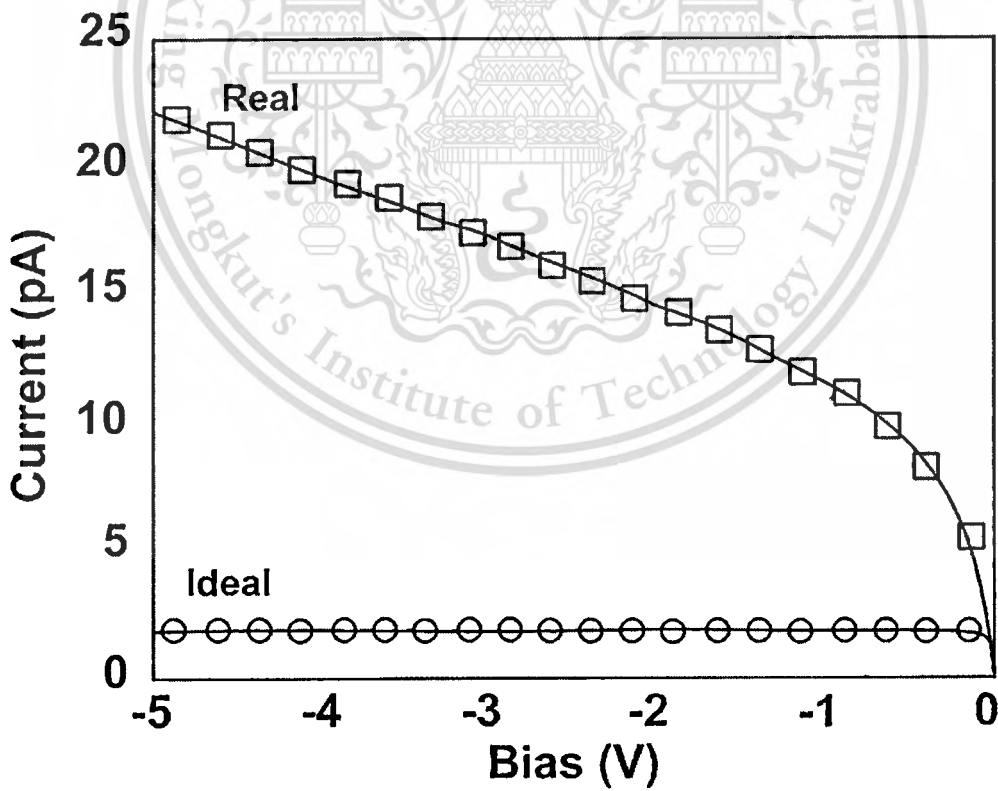


Fig. 2.7 The reverse current of ideal and reverse cases.

Form the Fig. 2.6 and 2.7 shows forward and reverse current of diode with difference bias voltage. Form Fig. 2.7 show the reverse biased junction mechanism of P-N diode, the leakage current (or reverse currents) is given by

$$I_R = I_d + I_{gb} + I_{gs} \quad (2.2)$$

$$I_{gb} = \frac{Aqn_iW_A}{\tau_g} \quad (2.3)$$

$$I_{gs} = Aqn_iS_g \quad (2.4)$$

$$S_g = \frac{S_r}{2 \cosh\left(\frac{E_{sT} - E_i}{kT}\right)} \quad (2.5)$$

Where I_d is the diffusion current, I_{gb} is the bulk generation, I_{gs} is the surface generation, W_A is the depletion width, S_g is the surface generation, S_r is the surface recombination, E_i is the energy intrinsic and E_{sT} is the energy level.

The forward current is given by

$$I_F = I_d + I_{rb} + I_{rs} \quad (2.6)$$

$$I_{rb} = I_{rbP} + I_{rbC} \quad (2.7)$$

$$I_{rs} = I_{rsP} + I_{rsC} \quad (2.8)$$

Where I_{rb} is the bulk recombination current, I_{rbP} is the peripheral bulk recombination current, I_{rbC} is the corner bulk recombination, I_{rs} is the surface recombination, I_{rsP} is the surface peripheral recombination current and I_{rsC} is the corner surface recombination current.

2.3.1.1 Activation energy (E_a)

The requirements for high-quality silicon substrates are extremely tight with respect to the control of grown-in or processing induced defect. There may still be a marked effect of the start material on the electrical characteristics of the device structure, like a capacitance or a P-N junction. The defects cause to reverse and forward diode characteristics. For example, the ratio of recombination and generation lifetime yields is principle the energy level with respect to mid map. Trapping levels (E_T) are dominant from

many cases such as silicon growth process and fabrication process. Trapping level is dependence of the temperature is given by

$$J_{dA} = GT^{3.4+i} \exp\left(-\frac{E_g}{kT}\right) \quad (2.9)$$

Where G is a constant value, E_g is the silicon band gap at 300 K (about 1.12 eV) and i is a small number (<1) related to the temperature dependence of the minority carrier mobility and the diffusion length.

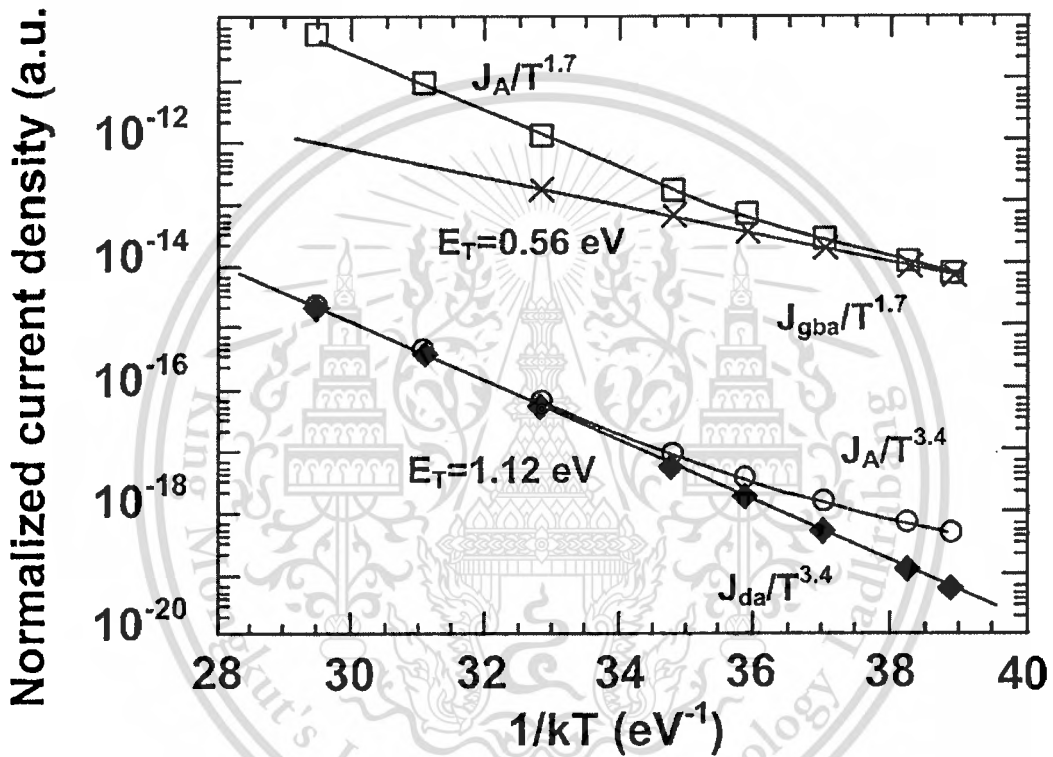


Fig. 2.8 Arrhenius plot of J_A verse $1/kT$.

In the contrast, assuming $E_T = E_g/2$ [45], the temperature variation of the area generation component for a R-G energy level in the upper half of the band gap becomes

$$J_A = J_{dA} + J_{gA} \quad (2.10)$$

$$J_{gA} = \frac{qn_i W}{\tau_g} \quad (2.11)$$

$$\therefore \tau_g = \tau_r \exp\left(\frac{E_T - E_i}{kT}\right) \quad (2.12)$$

Substituting C into B

$$J_{dA} = \frac{qn_i W^{1.7+\chi}}{\tau_r} \exp\left(-\frac{E_T}{kT}\right) \quad (2.13)$$

Where q is the elementary charge and χ is the small number (<1) to the temperature dependence of the depletion width.

The effects of the temperature on E_T and E_i is clear from Eq. 2.9 and 2.13. The Arrhenius plot of J_A versus $1/kT$ can find $-kT$ at lower temperature and $-E_g$ at higher temperature. From Fig. 2.8 is clear that extraction of E_T from the low temperature part of the curve is not straightforward and effected by the J_{dA} .

2.3.1.2 Carrier lifetime (τ)

We will classify the carrier lifetimes into 2 categories are recombination lifetimes and generation lifetimes [46]. The recombination lifetime (τ_r) applies when there are excess carriers in the semiconductor and recombination dominates. The generation lifetime (τ_g) applies when there is a paucity of carriers, as in the space-charge region (scr) of a reverse-biased device and the device tries to attain equilibrium. The concept of electron and hole lifetimes in semiconductor is, in principle, very straightforward. However, in practice there are generally as many lifetime values for a given device as there are measurement techniques. While some methods give numerical values that differ little, others differ greatly. A survey of lifetime measurement technique in 1968 yielded 300 papers published during the period from 1959 to 1967. Instead of discussing the various lifetimes in general, the concepts of recombination and generation lifetimes will be discussed, so that all lifetime fall into one or the other of these two categories.

Recombination lifetime

Recombination lifetime applies when excess carriers, introduced by light or forward bias P-N junction shown in Fig. 2.9. The recombination lifetime, τ_r , can be calculated from the area diffusion current density (J_{dA}). Current density can be obtained from the forward I-V characteristics method or combine the reverse I-V and C-V characteristics. From the Eq. 2.14 assume that the current in the lowly doped region dominates J_{dA} , $N_D \gg N_A$ and $L_n = \sqrt{D_n \tau_r}$, then τ_r can calculate from Eq. 2.15

$$I_0 = I_d = qn_i^2 A \left(\frac{D_n}{L_n N_A} + \frac{D_p}{L_p N_D} \right) \quad 2.14$$

$$\tau_r = \left(\frac{qn_i^2}{J_{dA} N_A} \sqrt{D_n} \right)^2 \quad 2.15$$

$$D_n = \mu_n \frac{kT}{q} \quad 2.16$$

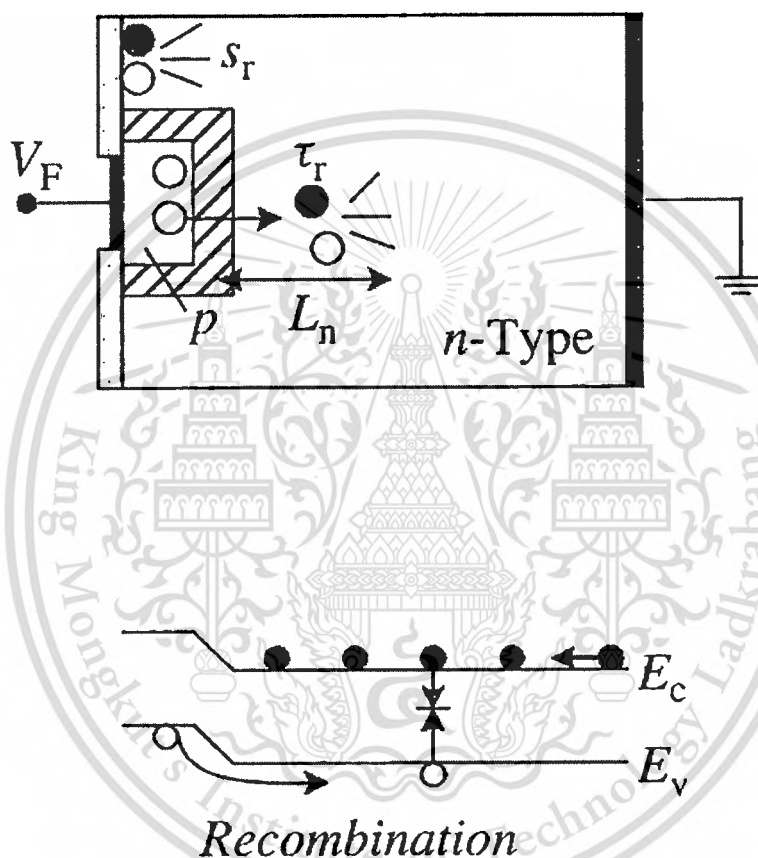


Fig. 2.9 Recombination mechanisms of diode.

Where μ_n is the electron mobility, D_n is the electron diffusion coefficient, D_p is the hole diffusion coefficient, L_n is the diffusion length correspond with an N_A is the carrier concentration of silicon substrate, A is the area of device, n_i is the intrinsic carrier concentration, N_A is the acceptor density, N_D is the donor density, I_0 is the leakage current and I_d is the diffusion current.

Generation lifetime

The generation lifetime, τ_g , applies when there is a paucity of carriers, as in the SCR of reverse bias device. The generation lifetime is time that it takes on average to generate time of the carrier in silicon bulk shown in Fig. 2.10. Thus generation lifetime is a misnomer, since the creation of an ehp is measured and generation time would be more appropriate. Nevertheless, the term “generation lifetime” is commonly accepted.

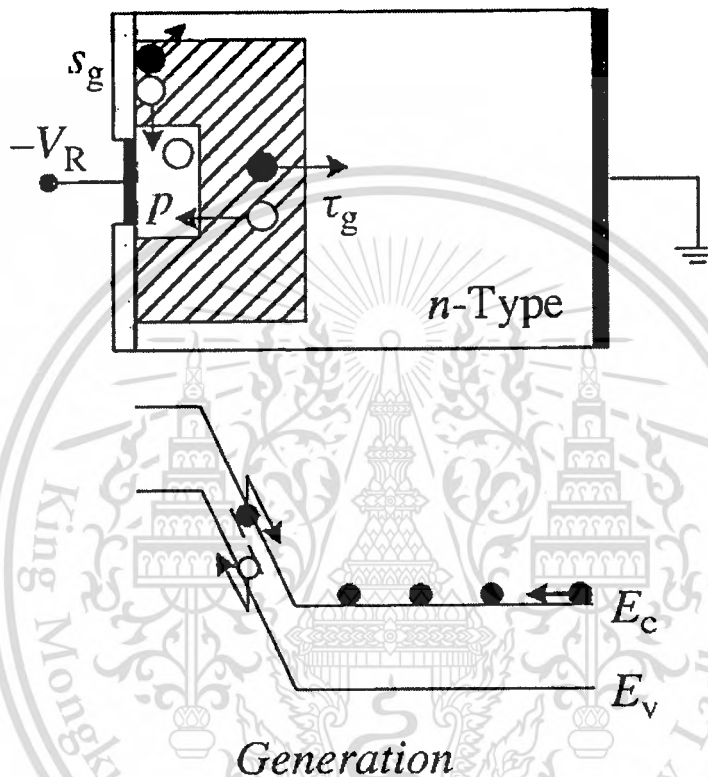


Fig. 2.10 Generation mechanism in the term of reverse-biased.

The generation lifetime can be calculate from Eq. 2.17

$$\tau_g = \frac{qn_i W_A}{(J_A - J_{dA})} \quad (2.17)$$

Where q is the Boltzmann constant, W_A is the depletion width and J_A is the current density.

2.3.1.3 Series resistance (R_s)

The neutral n and p region have finite resistances so the actual P-N junction will include a series resistance shown in Fig. 2.11.

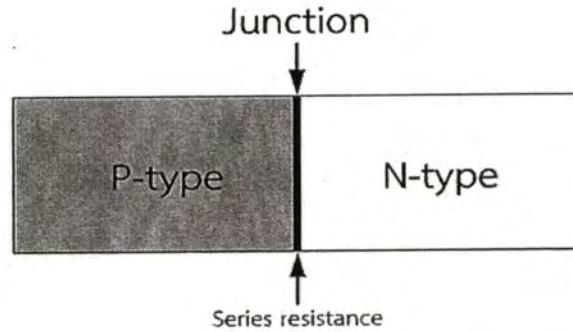


Fig. 2.11 Series resistance in P-N junction.

The deviation of the forward and reverse current in a real diode from the ideal case is shown in Fig. 2.12. The forward current corresponding with a forward bias close to V_{bi} , the reduction of the current in the region (Fig. 2.12) is determined by the series resistance (R_s).

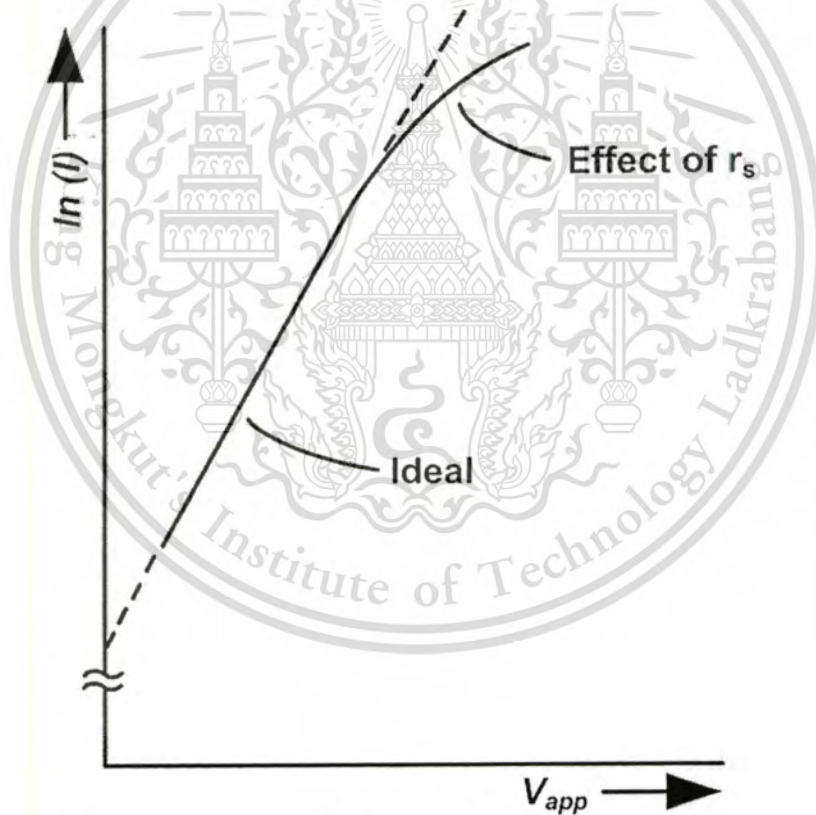


Fig. 2.12 Forward bias characteristics of P-N diode showing the effect of series resistance.

A semiconductor diode can be represented by the equivalent circuit on Fig. 2.13, consist of an ideal diode in series with series resistance (R_s). When the current flows through the device, the diode terminal voltage V is

$$V = V_d + I R_s \quad (2.18)$$

With series resistance Eq. 2.18 becomes

$$I = I_0 \left(e^{q(V - I R_s)/nkT} - 1 \right) \quad (2.19)$$

The current in P-N diode is due to two components are space-charge region (*scr*) recombination/generation and quasi-neutral region (*qnr*) recombination/generation, leading to the I-V relation is

$$I = I_{0,scr} \left(e^{q(V - I R_s)/nkT} - 1 \right) + I_{0,qnr} \left(e^{q(V - I R_s)/nkT} - 1 \right) \quad (2.20)$$

From the Eq. 2.20 is plot in Fig. 13 for the forward bias.

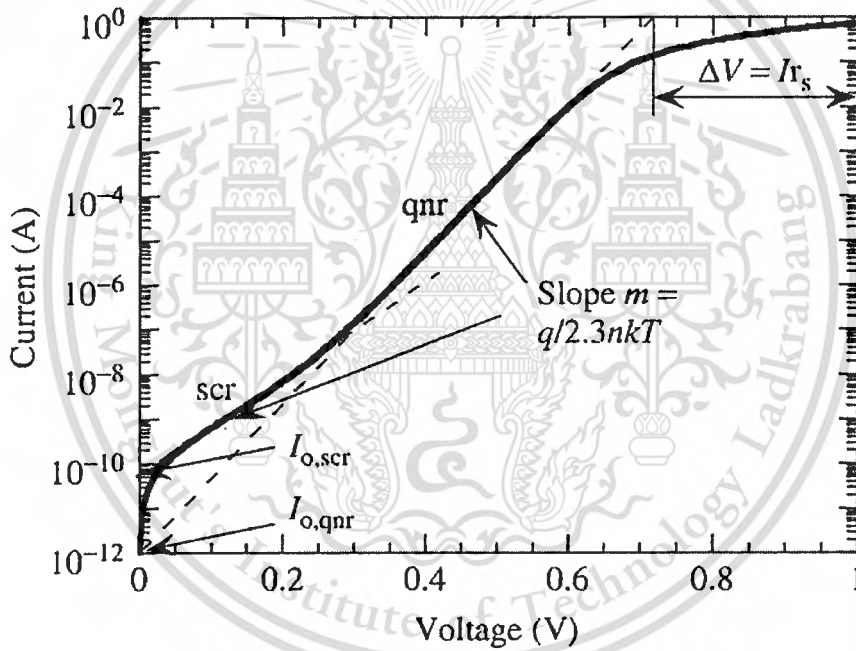


Fig. 2.13 Current versus voltage for P-N diode with the effect of series resistance.

The series resistance causes the forward current to deviate from the ideal diode and effects to measured junction capacitance. The series resistance have the effect to forward current at high bias voltage ($0.6 < R_s < 1V$) Shown in Fig. 2.13.

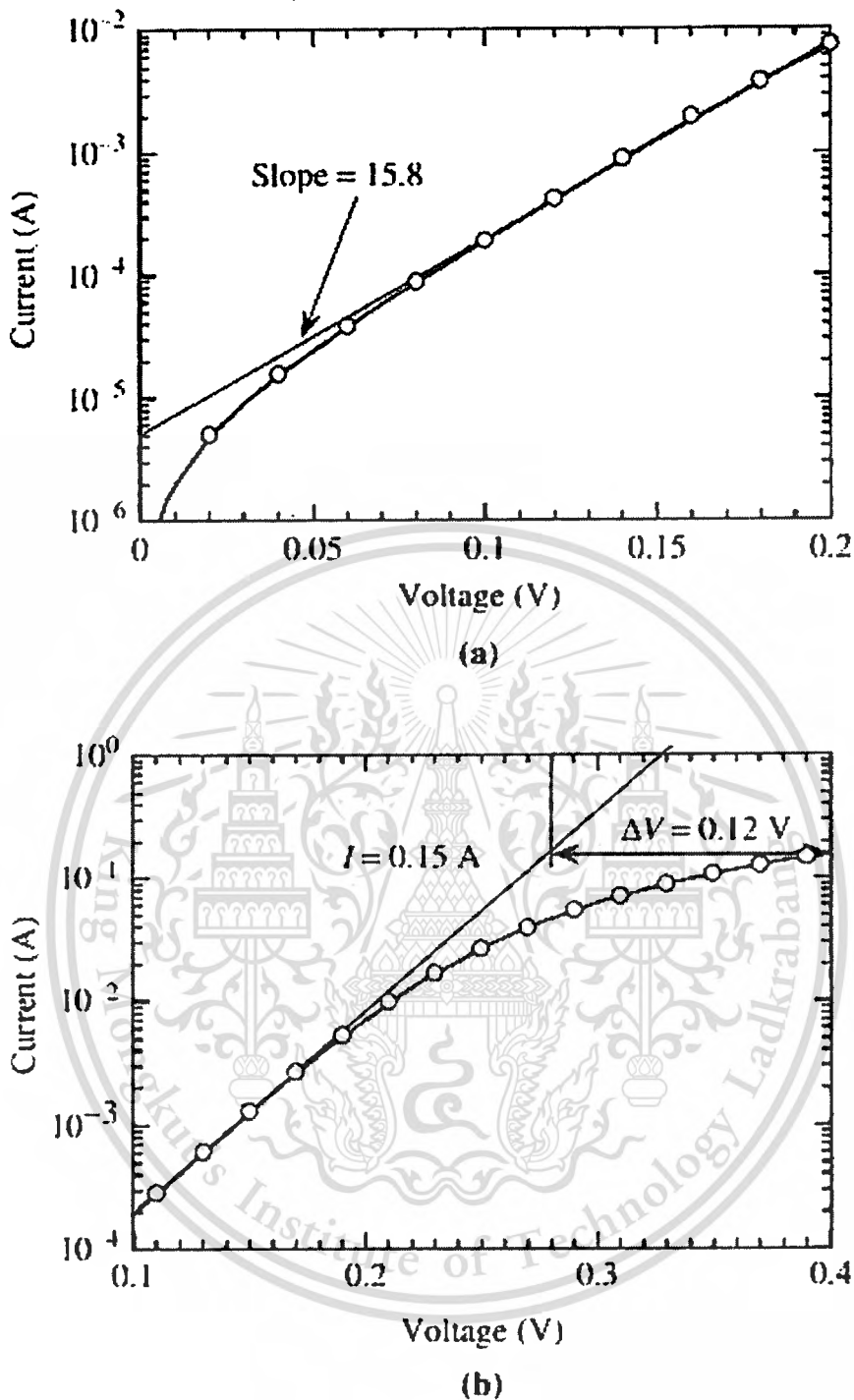


Fig. 2.14 The relation between semi-log current and voltage (a) shows the part of I-V curve where R_s is negligible (b) shows the part of the R_s -dominated curve.

Knowing I_0 , the plot V/I versus $[\ln((I-I_0)/I_0)]/I$ can be constructed as shown in Fig. 2.15, R_s can be found with the slope of kT/q .

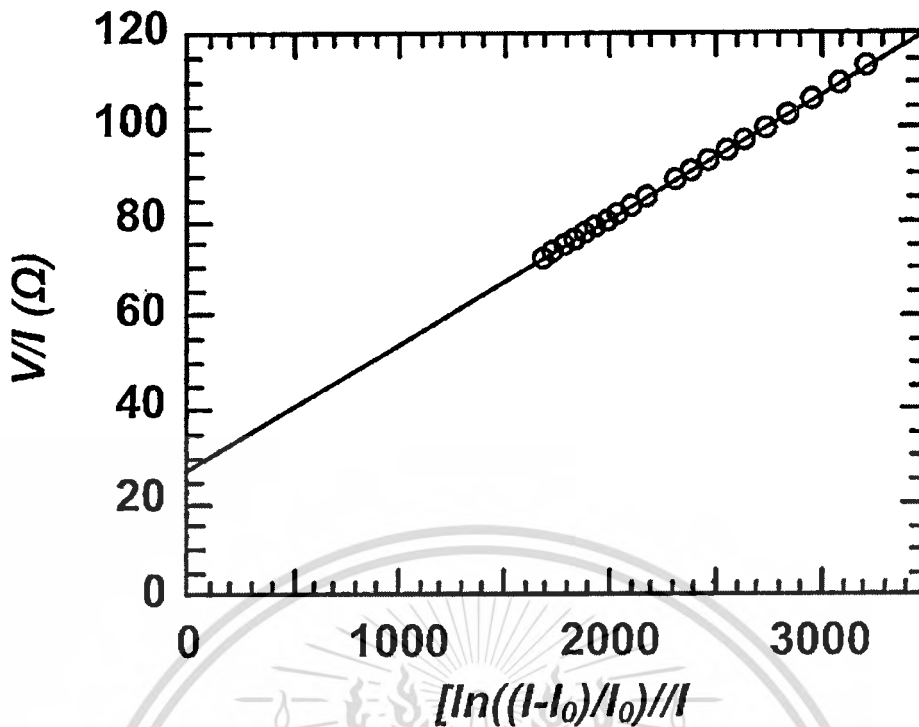


Fig. 2.15 Series resistance of P-N diode.

2.3.2 Capacitance-voltage characteristics (C-V)

The capacitance-voltage technique that width of a reverse-biased of a semiconductor junction device depends on the applied voltage. The capacitance associated with the charge variation in the depletion layer is call the junction, while the capacitance associated with the excess carrier in the quasi-neutral region is called the diffusion capacitance. The capacitance are obtained by calculation the change in charge for a change in bias voltage,

$$C = \frac{dQ}{dV} \quad (2.21)$$

The junction capacitance is calculated using the expression for the parallel plate capacitance. When applied small voltage variations one finds that charge is only added and removed at the edge of the depletion region. Therefore, the capacitance depends on the dielectric constant of plate,

$$C_j = \frac{\epsilon_s}{W} = \sqrt{\frac{q\epsilon_s}{2(\phi_i - V_a)} \frac{N_a N_d}{N_a + N_d}} \quad (2.22)$$

Where C_j is the junction capacitance, N_a is the acceptor concentration, N_d is the donor concentration, V_o is the bias voltage, ϵ is the silicon permittivity and W is the depletion width. [47]

Diffusion capacitance is the capacitance due to transport of charge carriers between two plates of a device. If the applied voltage changes to a different value and the current changes to a different value, a different amount of charge will be in transit in the new circumstances. The change in the amount of transiting charge divided by the change in the voltage causing it is the diffusion capacitance. The diffusion capacitance can calculate by

$$C_{diff} = \frac{dQ}{dV} = \frac{dI(V)}{dV} \tau_F \quad (2.23)$$

Where C_{diff} is the diffusion capacitance and τ_F is the forward transit time. [48]

2.3.2.1 Depletion width (W)

The depletion width of P-N diode can be found from

$$W_A = \frac{\epsilon_{si}}{C_A} \quad (2.24)$$

From the condition of charge (the total negative charge in the P-side depletion region exactly balance the total positive charge in the N-side depletion region), can write

$$w_p N_a = w_n N_d \quad (2.25)$$

Where W_p and W_n are the widths of the p-side and n-side charged regions, respectively. In addition, one can express the total of depletion width W as

$$W = w_p + w_n \quad (2.26)$$

$$W_p = \sqrt{\frac{2\epsilon_{si}}{q} \left(\frac{N_D}{N_A(N_A + N_D)} \right) (V_{bi} - V)} \quad (2.27)$$

$$W_n = \sqrt{\frac{2\epsilon_{si}}{q} \left(\frac{N_A}{N_D(N_A + N_D)} \right) (V_{bi} - V)} \quad (2.28)$$

2.3.2.2 Carrier concentration (N)

The carrier concentration is one of most-importance parameter of semiconductor. The concentration can doped with difference type and dose of impurities to vary its resistivity.

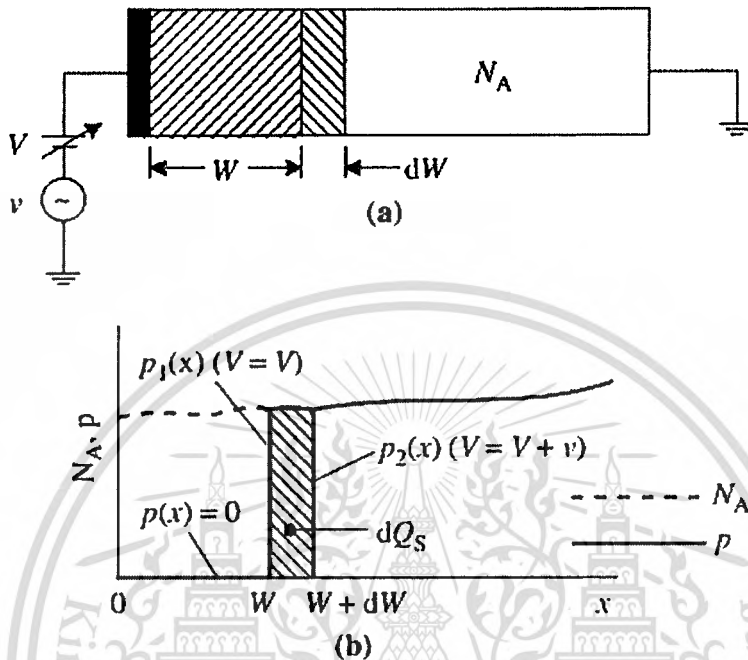


Fig. 2.16 (a) A reverse-biased Schottky diode, and (b) the doping density and majority carrier density profiles in the depletion approximation.

The concentration in junction depth can calculate by

$$N(W) \doteq \frac{C^3}{qK_s \epsilon_0 A^2 dC/dV} = \frac{2}{qK_s \epsilon_0 A^2 d(1/C^2)/dV} \quad (2.29)$$

Using the identity

$$d(1/C^2)/dV = -(2/C^3)dC/dV \quad (2.30)$$

Where A is the area of device, N is doping density, V is the dc bias, W is the space-charge region, ϵ_0 is the permittivity of free space. We consider the Schottky barrier diode of Fig. 2.16.

Chapter 3

Device fabrication and Design of experiment

This chapter presents the fabrication process of P-N junction diode using CMOS technology and design of experiment for the effect of X-ray radiation on the electrical characteristics. The plan for this project is shown in Fig. 3.1

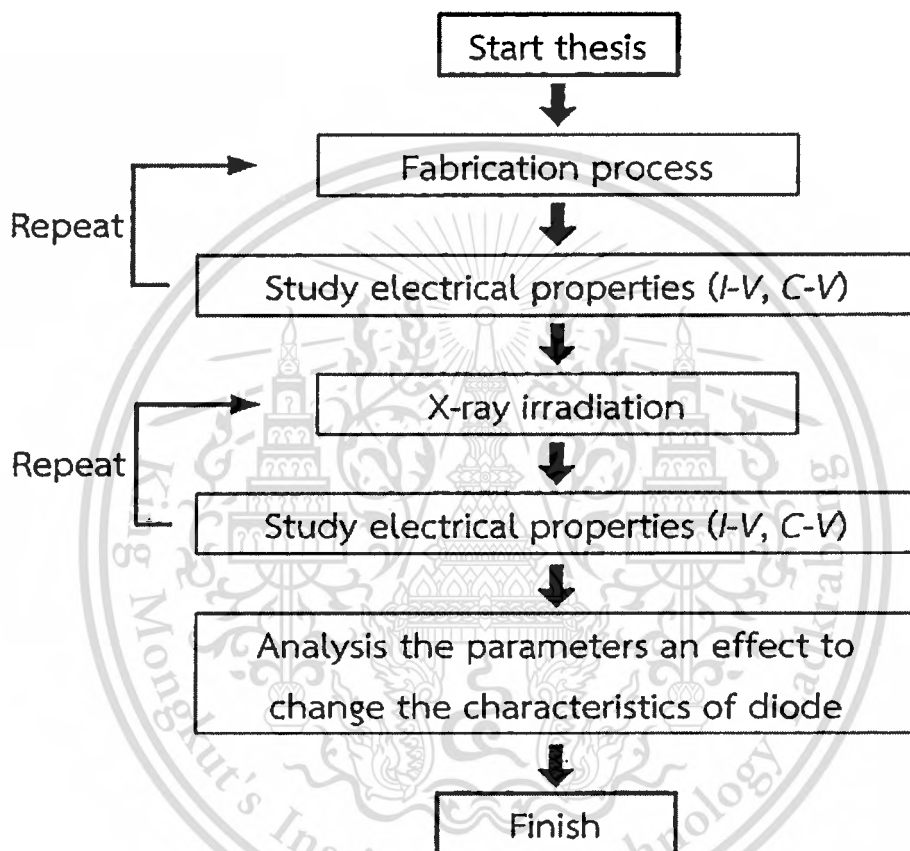


Fig. 3.1 The plan for this thesis.

3.1 Device fabrication

The processing of the shallow P-N junction diodes was done using CMOS technology by the Thai Microelectronics Center (TMEC), Thailand. The P-N junction diodes were fabricated using an n-type (P doped) single crystal silicon wafer with a (111) surface orientation, 650 mm thick and 120–135 $\Omega\text{-cm}$ of resistivity. The wafer was cleaned with an ultra-sonic bath to remove organic contaminants. The diode

process module consists of (i) the deposition of the oxide covered substrate and the dry-etching of the active area, (ii) the implantation of phosphorus at an energy of 120 kV and dosage of $1 \times 10^{16} \text{ cm}^{-2}$ for ohmic contact on the backside wafer, (iii) the implantation of boron at the same energy and dose on the front side of wafer, (iv) after the implantation, it was followed by a thermal annealing at $1050 \text{ }^\circ\text{C}$ for 60 min, resulting in a junction depth of about $1 \text{ }\mu\text{m}$ and (v) the Al metal-deposition, $1 \text{ }\mu\text{m}$ thick [49,50], on both the front and back sides [51]. After that the wafer was diced into separate devices. Finally, the fully assembled chip was installed into a prototype circuit board (PCB) before the finishing connections were made, the fabrication process of P-N diode is shown in Fig. 3.2.

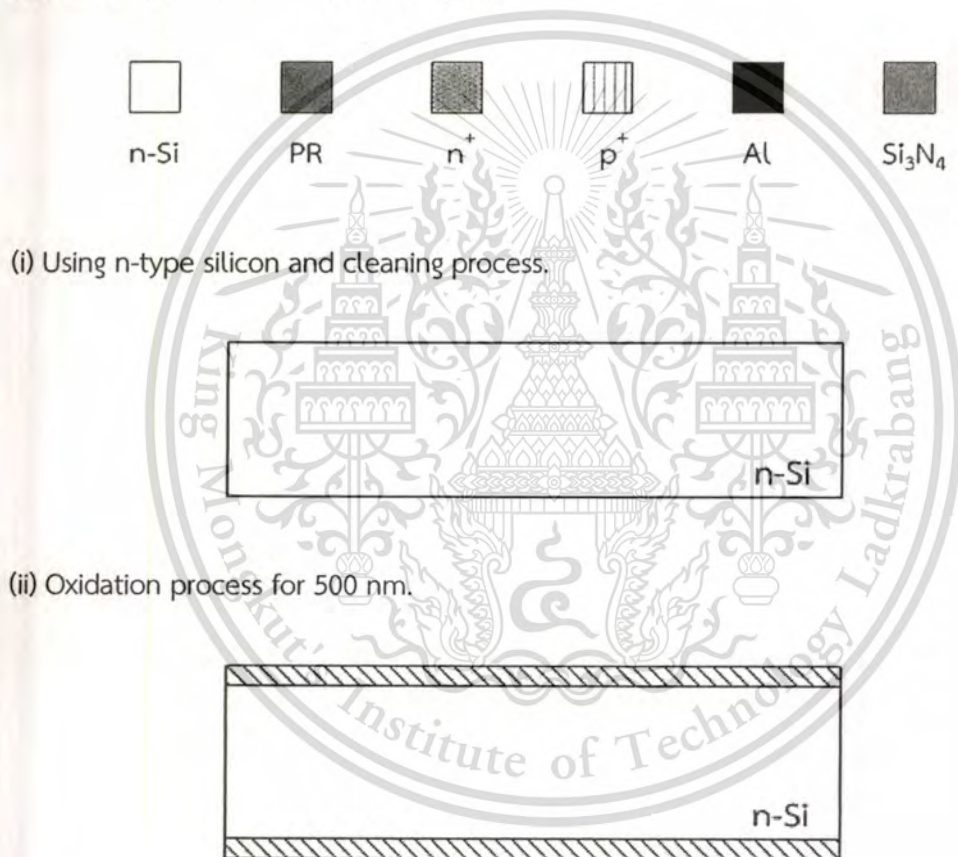
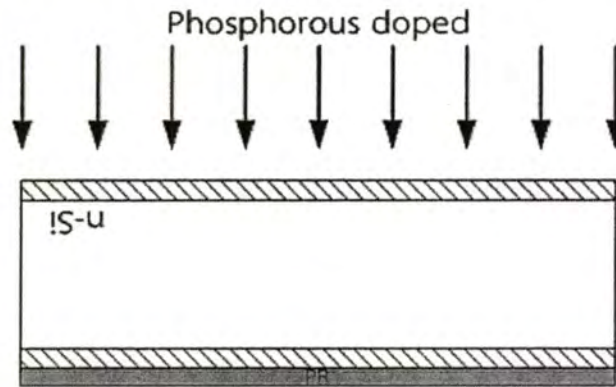
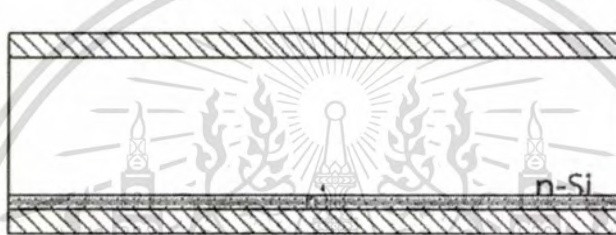


Fig. 3.2 The process flow of P-N diode fabrication using CMOS technology at TMEC.

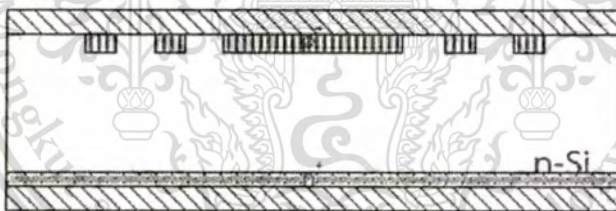
(iii) Photolithography and ion implantation of phosphorus (n^+) on the back side.



(iv) After phosphorus doping on the back side



(v) Photolithography and ion implantation of boron (p^+) on front side.



(vi) PECVD oxide for $1.5 \mu\text{m}$.

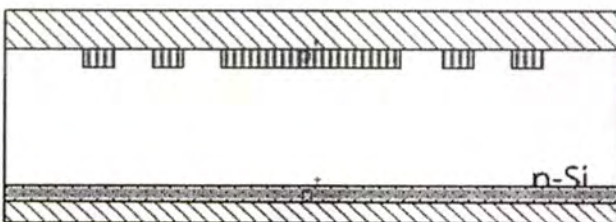
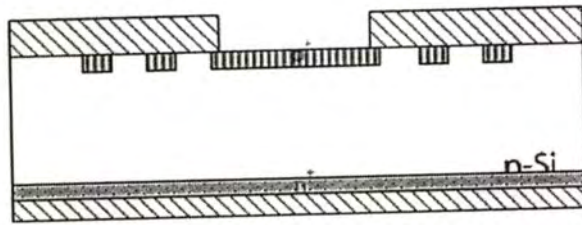
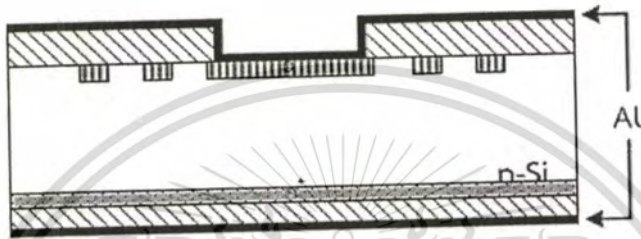


Fig. 3.2 The process flow of P-N diode fabrication using CMOS technology at TMEC.
(Cont. 1)

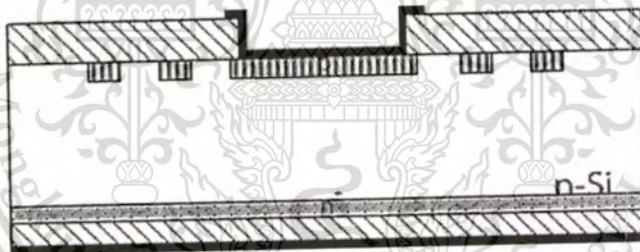
(vii) Photolithography before dry etching of SiO_2 .



(viii) Deposited Al for $1\ \mu\text{m}$.



(ix) Patterning Al.



(x) PECVD Silicon Nitride for 500 nm on the front side.

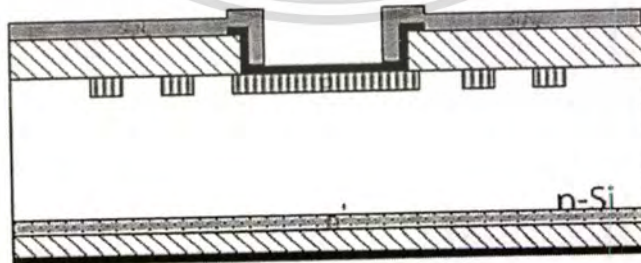


Fig. 3.2 The process flow of P-N diode fabrication using CMOS technology at TMEC.
(Cont. 2)

(xiii) Dicing process.

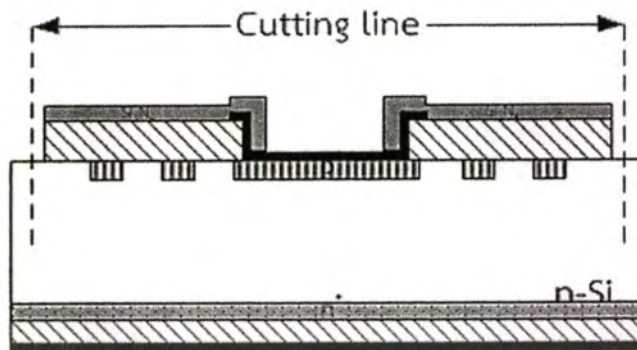


Fig. 3.2 The process flow of P-N diode fabrication using CMOS technology at TMEC.
(Cont. 3)

3.2 Experiment

After fabrication, the P-N diodes were irradiated by X-ray radiation at different energy levels and times. The P-N diode after fabrication as shown in Fig. 3.3

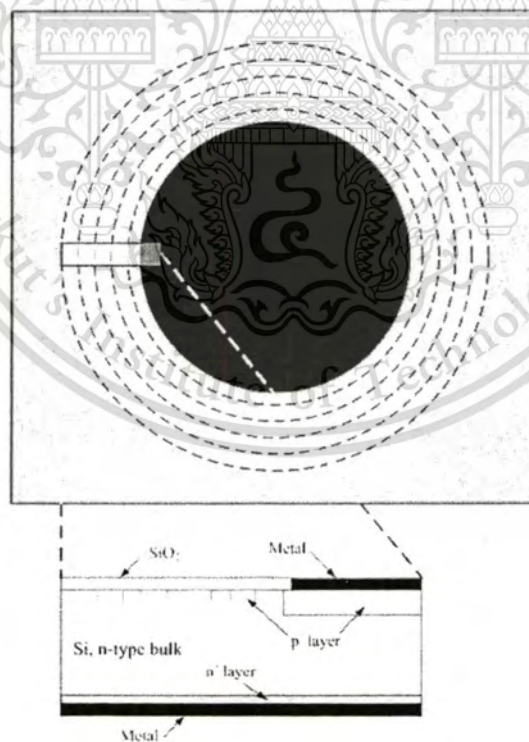


Fig. 3.3 P-N diode after fabrication.

This material is reserved for educational use only, not allowed for commercial use.

Forbidden to modify the content, and cite the document when use.

This experiment choose P-N diode to study the effect of X-ray irradiation on the electrical characteristics because P-N is similar structure and popular device to use in many application. The X-ray energy have wide range but the most energy have in range 40 to 70 keV, therefore, this thesis use the X-ray energy in this range.

The devices are irradiated by X-ray radiation at various levels of energy and time shows as shown in Fig. 3.4. The X-ray energy were 40, 55 and 70 keV for 5, 55 and 205 second.

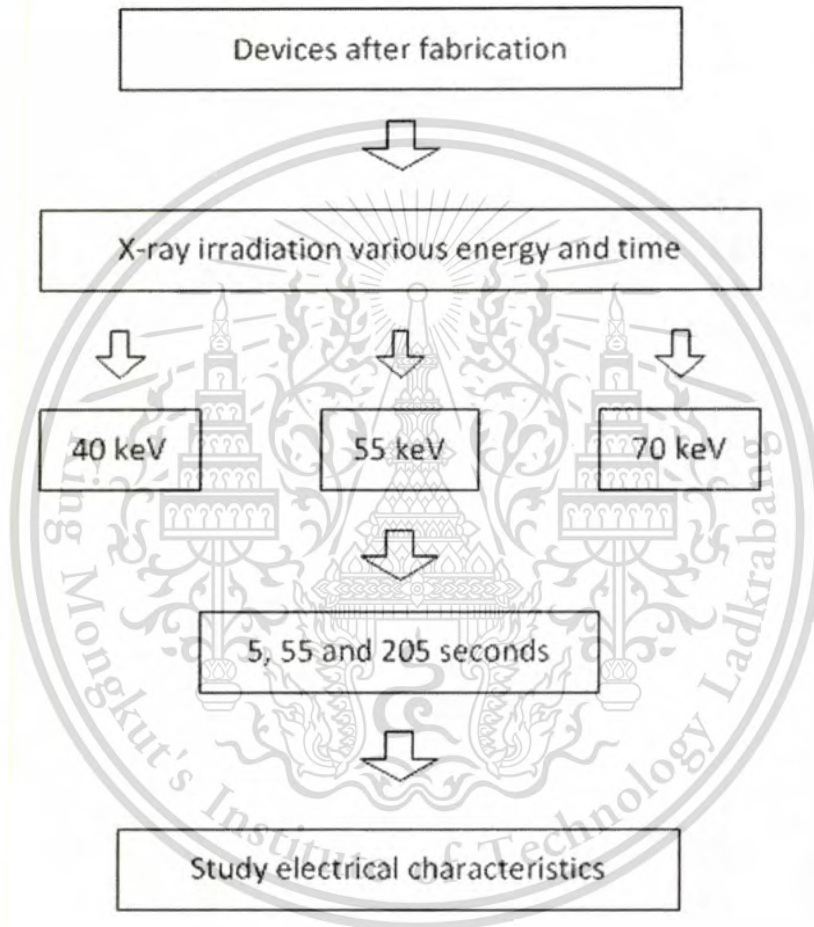


Fig. 3.4 Experiment diagram for the study of the effect of X-ray radiation on electrical characteristics of P-N diode.

After fabrication the electrical properties of P-N junction diodes were characterized by using Cascade Microtech Model M150 probe station at TMEC as shown in Fig. 3.5. The I-V and C-V characteristics were studied from -10 V to 1 V. The

devices were studied before and after irradiations by X-ray. The X-ray energy and exposure times is shown in Table. 3.1.

Table. 3.1 X-ray radiation at various levels of energy and times.

Energy	40 keV	55 keV	70 keV
Time	5 sec	5 sec	5 sec
	55 sec	55 sec	55 sec
	205 sec	205 sec	205 sec

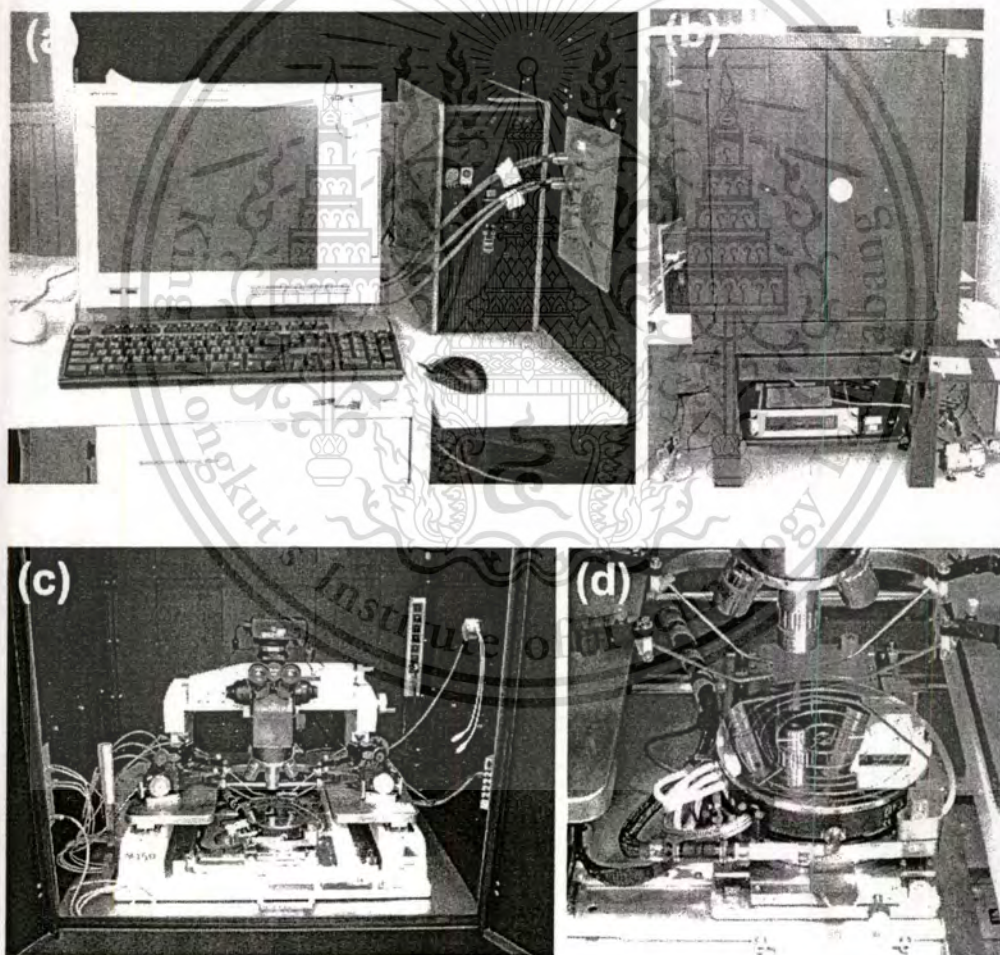


Fig. 3.5 Probe station at TMEC (a), (b) the Cascade Microtech Model M150 (c) I-V probe station and (d). chunk of probe station.

This material is reserved for educational use only, not allowed for commercial use.

Forbidden to modify the content, and cite the document when use.

Fig. 3.6 shows the X-ray irradiation machine (C-arm Siemens Siremobil Compact 650 135) at King Mongkut's University of Technology North Bangkok, Thailand.

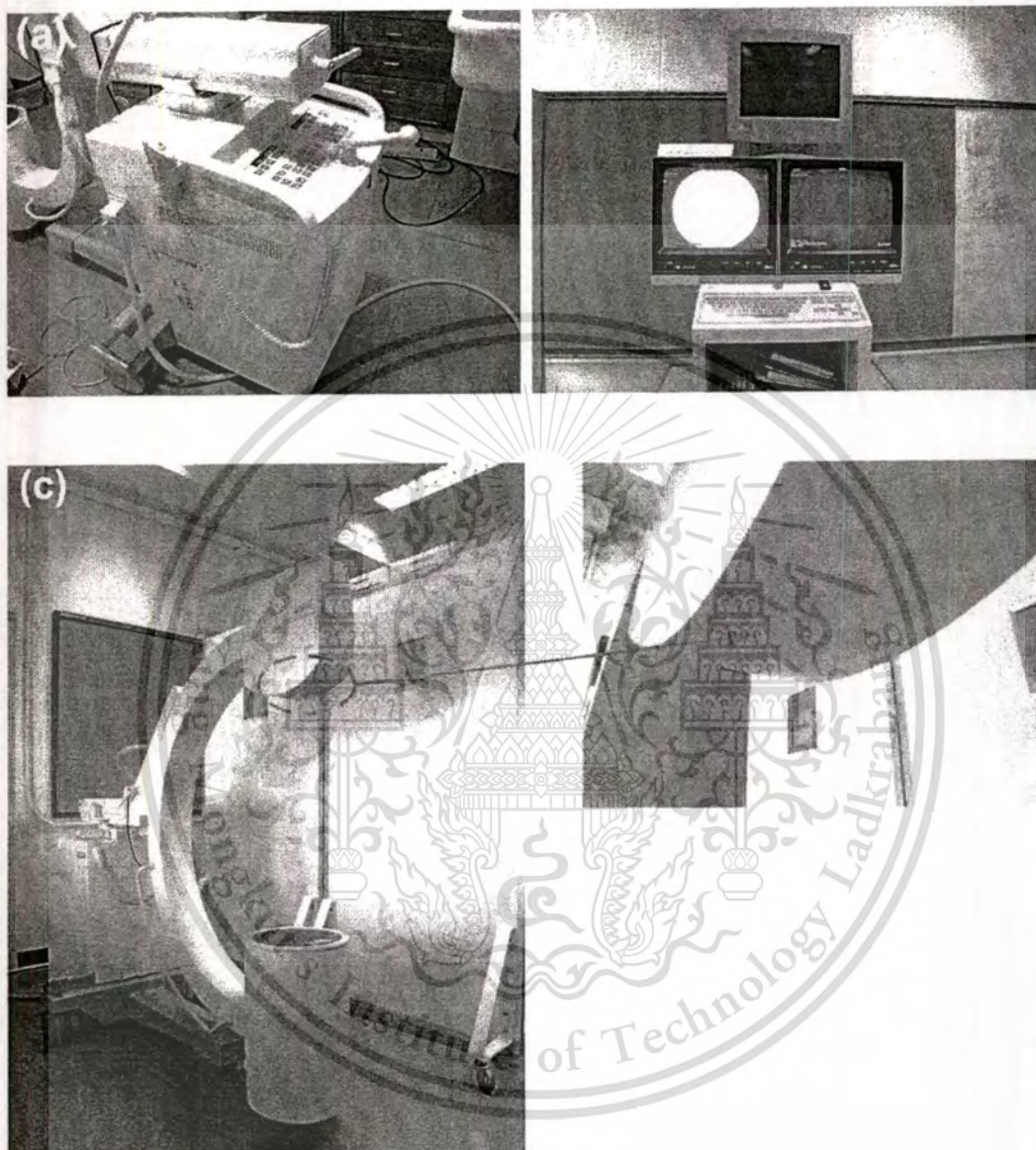


Fig. 3.6 X-ray radiation machine (C-arm Siemens Siremobil Compact 650 135) (a) control systems, (b) monitor and (c) point of X-ray irradiate.

Chapter 4

Results and Discussions

This chapter presents the results and discussion of the effect of X-ray on the electrical properties of P-N junction diode difference energy and dose. The electrical properties of P-N diode consist of I-V and C-V characteristics.

4.1 Current-voltage characteristics (I-V)

Fig. 4.1 shows the experimental semi-log forward and reverse-bias characteristics of the P-N junction diodes. The diode parameters were determined from the I-V characteristics, which are usually described using the P-N junction theory.

$$I = I_0 \exp\left(\frac{qV}{nkT}\right) \quad (4.1)$$

Here I is the current, q is the electron charge, V is the applied voltage, T is the absolute temperature, k is the Boltzmann constant, n is the ideality factor of P-N junction diodes, and I_0 is the saturation current. For values of V greater than nkT/q , the ideality factor from Eq. (4.1) can be written as described [52,53] by

$$n = \left[\frac{q}{kT} \right] \left[\frac{dV}{d \ln I} \right] \quad (4.2)$$

Also the voltage dependent ideality factor $n(V)$ can be written using Eq. (4.2) as

$$n(V) = \frac{qV}{[kT \ln(I/I_0)]} \quad (4.3)$$

From Eq. (4.1) I_0 is the saturation current. The saturation current under the reverse bias is the combination of the diffusion current (I_d) and the generation current (I_g) that are generated in the depletion region, as presented in Eq. (4.4).

$$I_0 = I_d + \frac{Aq n_i W}{\tau_g} \quad (4.4)$$

Here n_i is the intrinsic carrier concentration, τ_g is the carrier generation lifetime, and W is the depletion width. The carrier generation lifetime is given by Eq. (4.5).

$$\tau_g = \frac{Aq n_i W}{(I_0 - I_d)} \quad (4.5)$$

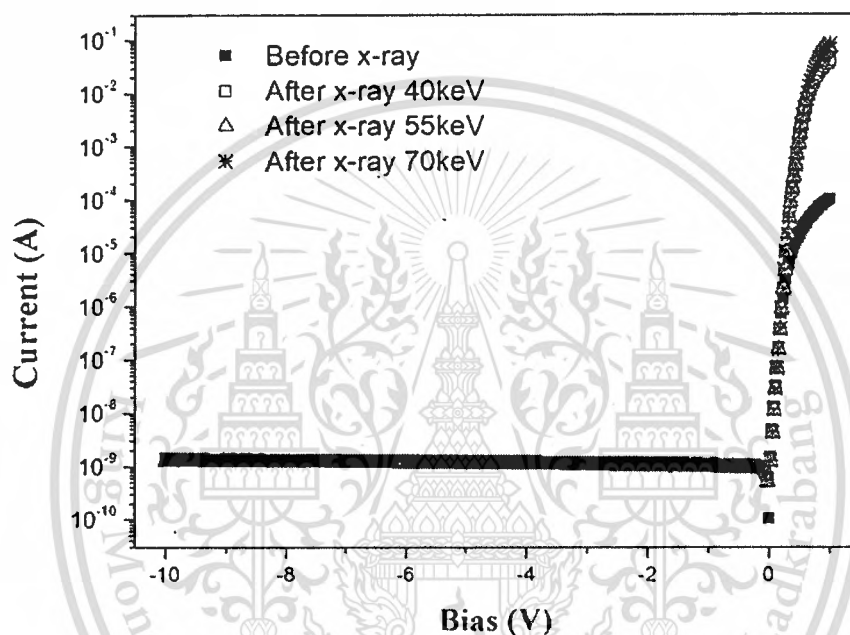


Fig. 4.1 The forward and reverse bias current vs voltage characteristics of the P-N junction diodes.

4.1.1 Forward bias

The experimental semi-log forward bias characteristics of the P-N junction diodes are shown in Fig. 4.2.

From this figure the forward current after irradiation is increased about 3 to 4 orders of magnitude. This was especially apparent when the analyzed forward current at 70 keV showed the higher forward current. The obtained result shows that a 70 keV exposure has an excellent performance on improving the diode characteristics. This result is very promising for further investigation.

From Fig. 4.2 the forward current are increased about 3 orders of magnitude for 40, 55 and 70 keV various times with bias 0.6-1 V, this results are deference the effects of electron, photon and neutron radiation on device base on silicon [54]. Form the graph show that this is a new result by using radiation to improve the electrical properties of the diode. The changes in forward current possibly are occurred by many cause such as series resistance (R_s) [55], Ideality factor (η) [56], recombination lifetime (τ_r) [57].

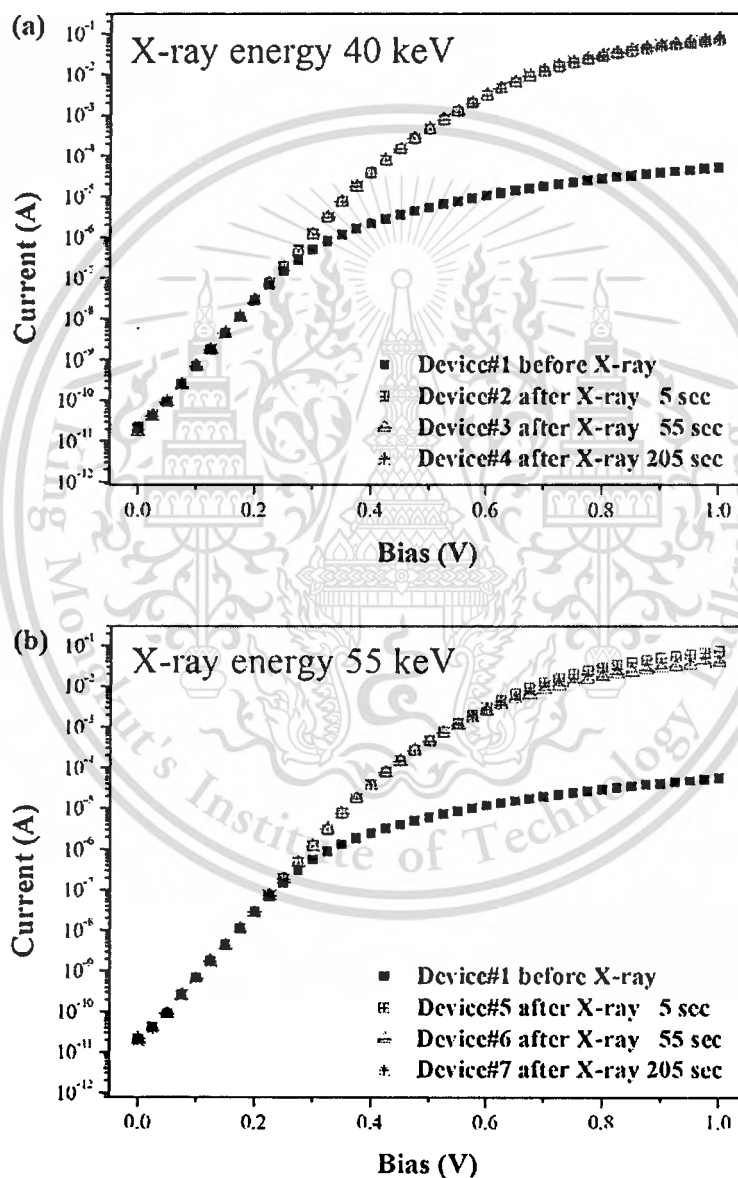


Fig. 4.2. Forward I-V characteristics of the P-N junction diodes for different energy and dose.

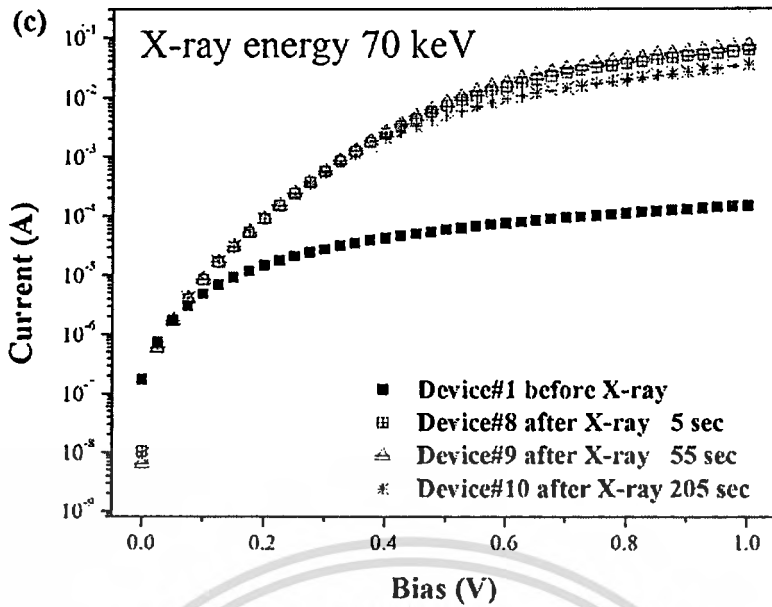


Fig. 4.2. Forward I-V characteristics of the P-N junction diodes for different energy and dose. (Cont.)

4.1.1.1 Series resistance (R_s)

The change of the forward current seems to be caused by a series resistance reduction that affected the ideality factor of the diode.

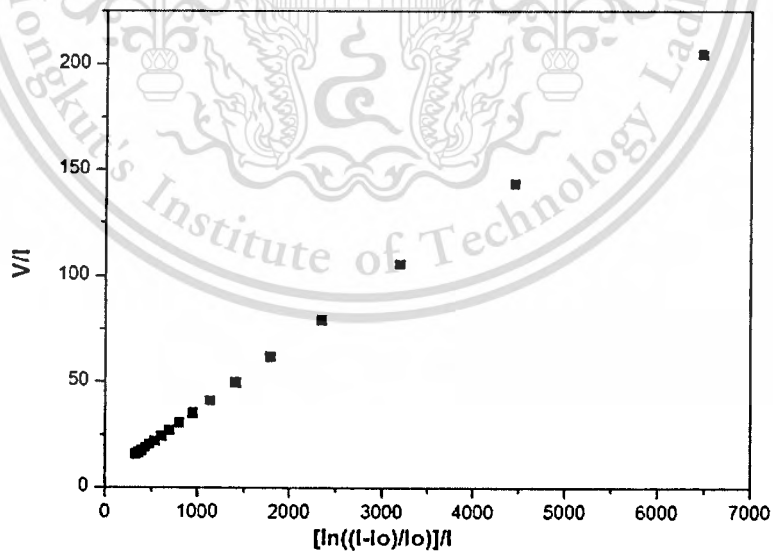


Fig 4.3. A plot V/I vs. $[\ln((I-I_0)/I_0)]/I$ obtained from forward bias current-voltage characteristic of P-N diode.

The effect of the series resistance is usually modeled with series combination of a diode and resistor, R_s , in which the voltage V_d across the diode can be expressed in terms of the total voltage drop V across the diode and the resistance, R_s . Thus, $V_d = V - IR_s$ and Eq. (4.1) can be expressed as

$$I = I_0 \exp \left[\frac{q(V - IR_s)}{nkT} \right] \quad (4.6)$$

By rewriting Eq. (4.6) using the Chung's method this equation can be presented as in Eq. (4.7) [58]

$$\frac{dV}{d \ln(I)} = IR_s + \frac{nkT}{q} \quad (4.7)$$

Table. 4.1. Series resistance of P-N junction diodes various energy and times.

Time (sec)	Series resistance (Ω)		
	40 keV	55 keV	70 keV
Before (non-irradiation)	9560	9570	9640
5	6.4	7.6	4.4
55	5.3	6.3	3.3
205	4.5	6.3	5

Table. 4.2. Sheet resistance of P-N junction diodes before and after exposure by X-ray.

	Front metal ($m\Omega/\square$)	Boron doped region (Ω/\square)	Silicon bulk (Ω/\square)	Back contact ($m\Omega/\square$)
Before (non-irradiation)	59	12.15	2232	55
After	58	12.11	2187	53

From $dV/d\ln(I)$ vs I plots, the series resistance is shown in Table. 4.1. Therefore, by using this model, the results show a dramatic reduction in the overall parasitic series resistance from several $k\Omega$ to a few $k\Omega$ when the diode has been irradiated by X-rays. The series resistance of P-N junction diodes can possibly be divided into 4 parts which they are front metal contact, boron doped region, silicon bulk, and back contact. The individual sheet resistivity measurement has also been performed by using the 4-point probe technique on each part [59-60].

The sheet resistances of the 4 parts before and after exposure by X-rays are shown in Table 4.2, where the front metal, boron doped region, silicon bulk and back contact were separately fabricated. There are no significant changed in the sheet resistance of metal contact and boron dope region. This implies that there is permanent modification of the base materials by the X-ray irradiation. Therefore, this confirms that the X-ray irradiation has mainly influenced the silicon bulk condition. The sheet resistance of metal or aluminum contact data before and after soft X-ray irradiation is given in Table. 4.2, where the sheet resistance of metal is a little changed after irradiation. Results show that soft X-ray irradiation is not effect of the metal contacts. In the case of surface/interface oxide can be explained by the capacitance-voltage (C-V) characteristics, in which the capacitances of P-N junction diode are not changed after irradiation as shown in Fig. 4.4, which means that the soft X-ray irradiation is not effect of interface oxide.

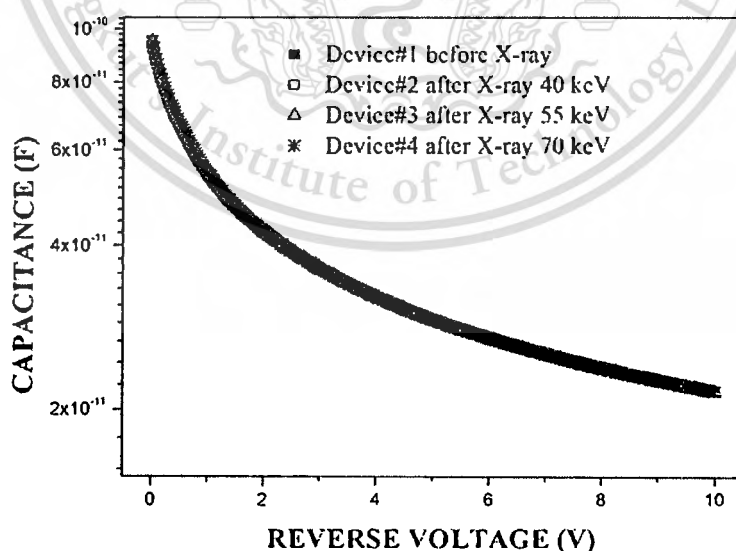


Fig. 4.4 Capacitance-voltage characteristics of P-N diode.

4.1.1.2 Ideality factor (η)

The ideality factor is an effect to forward current of diode. This parameter can examine the type of current between recombination or diffusion current. In the case of diffusion current are generate by many case such as doping concentration and epitaxial interface, on the other hand, recombination current are generate by trapping center or defects in bulk of the wafer. The ideality factor are in range shows, 1 (diffusion current) \ll Ideality factor \ll 2 (recombination current). When the diffusion current near 1 shows low defects and near 2 is many defects in silicon bulk. One of the ideality factor calculated method is developed by plot J vs. V will be linear. It is found that at $J=0$, which the slope of qv/mT is present in Fig. 4.5. The ideality factor after irradiation are a little change, therefore, this parameter may not cause to the leakage current of P-N diode.

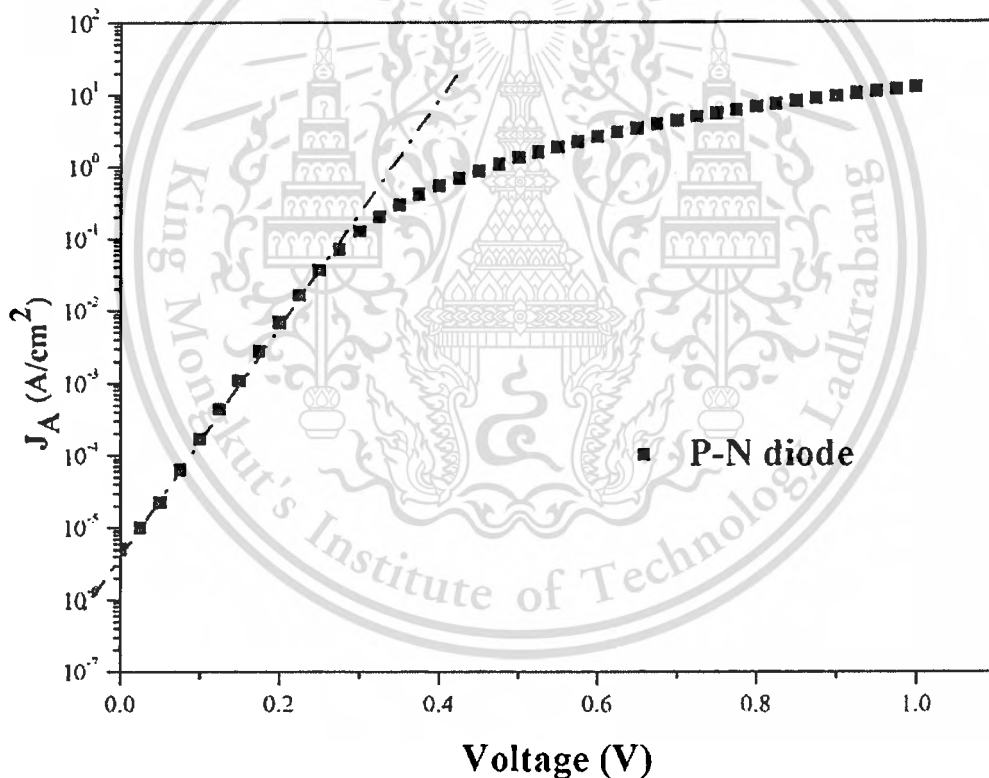


Fig. 4.5 A plot J_A vs. V obtained from forward bias current-voltage characteristics of P-N diode.

Table 4.3 shows the ideality factor of P-N diode before and after irradiation by X-ray various energy and times.

Energy (keV) \ Time (sec)	40	55	70
Before (non-irradiation)	1.05	1.06	1.05
5	1.03	1.04	1.04
55	1.03	10.2	1.03
205	1.03	1.03	1.03

4.1.1.3 Recombination lifetime (τ_r)

Recombination lifetime is a one important parameters cause to change the forward current of P-N diode. The trapping center or defects in silicon bulk can generate by many cases such high energy irradiation and CZ process. Normally, the recombination lifetime can be calculate from the current density (J_A) in the term of forward bias, which are calculated by

$$I_F = I_d + I_{rb} + I_{rs} \quad (4.8)$$

$$I_0 = I_d = qn_i^2 A \left(\frac{D_n}{L_n N_A} + \frac{D_p}{L_p N_D} \right) \quad (4.9)$$

$$L_n = \sqrt{D_n \tau_r} \quad (4.10)$$

$$\tau_r = \left(\frac{qn_i^2}{J_{dA} N_A} \sqrt{D_n} \right)^2 \quad (4.11)$$

$$D_n = \mu_n \frac{kT}{q} \quad (4.12)$$

Where τ_r is the recombination lifetime, N_A and N_D are the carrier concentration, J_{dA} is the current density, D_n and D_p are the diffusion coefficient of electrons in the p-side and holes in n-side, respectively.

The recombination lifetime are shown in Table. 4.4. From Eq. 4.8-4.12 the

recombination lifetime have an effect to forward current. The recombination lifetimes after irradiation are a little decrease.

Table. 4.4 The recombination lifetime of P-N diode.

Energy (keV) Time (sec)	Recombination lifetime (τ_r) (μsec)		
	40	55	70
Before (non-irradiation)	0.297	0.299	0.299
5	0.292	0.295	0.299
55	0.292	0.295	0.305
205	0.290	0.292	0.307

4.1.1.4 Build in voltage (V_{bi})

The build in voltage of P-N diode can be found from the intercept of plot I versus V , as shown in Fig. 4.6.

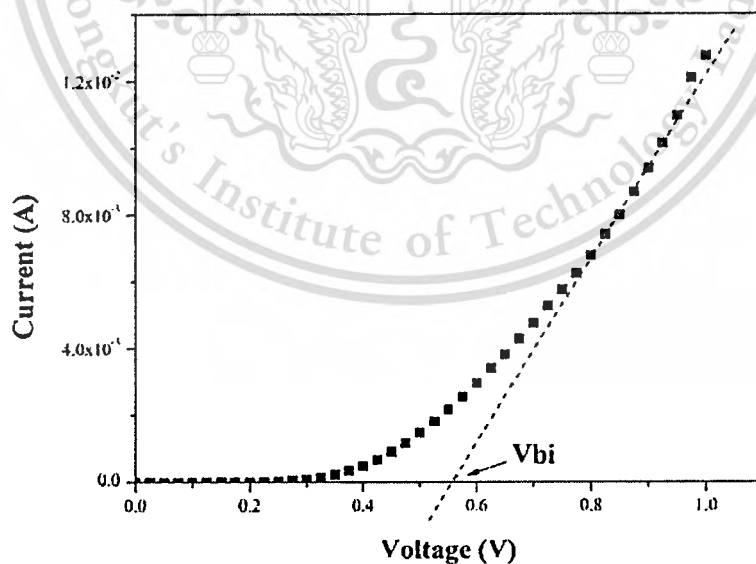


Fig. 4.6 The relation between I vs. V for found V_{bi} .

The build in voltage of P-N diode are in range 0.4 to 0.7 V. The build in voltage before and after X-ray irradiation are shown in Table 4.5. From this figure, the build in voltage after irradiation are not change, therefore, X-ray radiation cannot change characterization between metal and silicon.

Table. 4.5 build in voltage of P-N diode.

Energy (keV) \ Time (sec)	Build in voltage (eV)		
	40	55	70
Before (non-irradiation)	0.55	0.54	0.54
5	0.54	0.54	0.55
55	0.55	0.55	0.53
205	0.53	0.54	0.54

4.1.2 Reverse bias

The current-voltage characteristics of the diodes with different doses shown in Fig. 4.7.

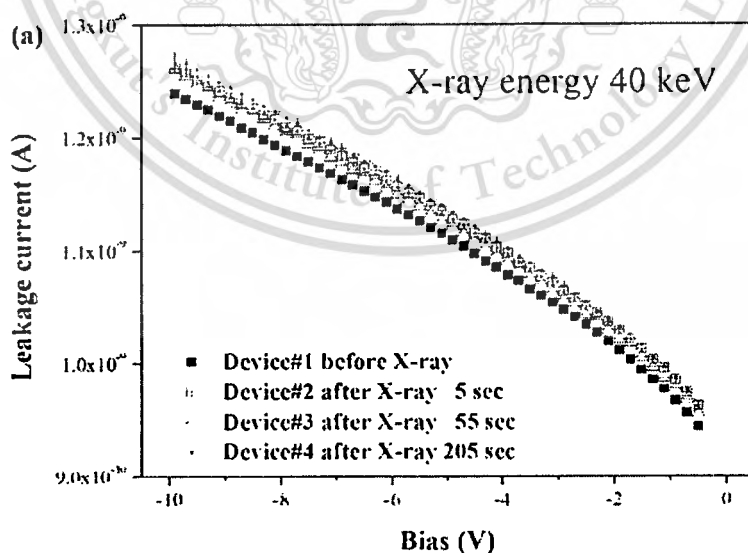


Fig. 4.7. Leakage current of diode before and after irradiated.

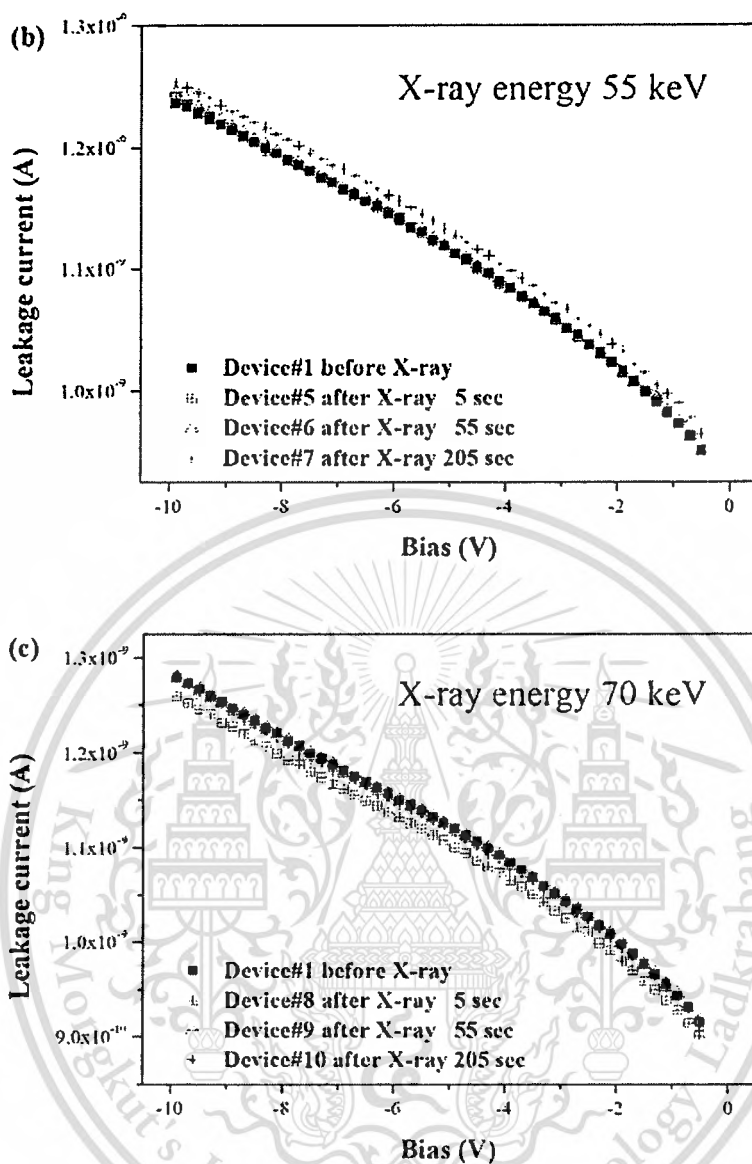


Fig. 4.7. Leakage current of diode before and after irradiated. (Cont.)

From the Fig. 4 shows the leakage current versus voltage before and after X-ray irradiation at 40 keV and 55 keV slightly increases with the increasing diode.

Therefore, increasing of leakage current at higher reverse bias are increase up to many parameters such as activation energy (E_a), generation lifetime (τ_g), diffusion current (I_d) and generation current (I_g).

4.1.2.1 Activation energy (E_a)

From Eq. 4.4, 4.9 the activation energy is an important parameter cause to change the diffusion current. A general relation between a physical variable and its activation energy. can be applied to the leakage current of a P-N junction, according to

$$I_R(T) \propto \exp(-E_a / kT) \quad (4.13)$$

With I_R is the reverse current, k is the Boltzmann constant, T is the absolute temperature.

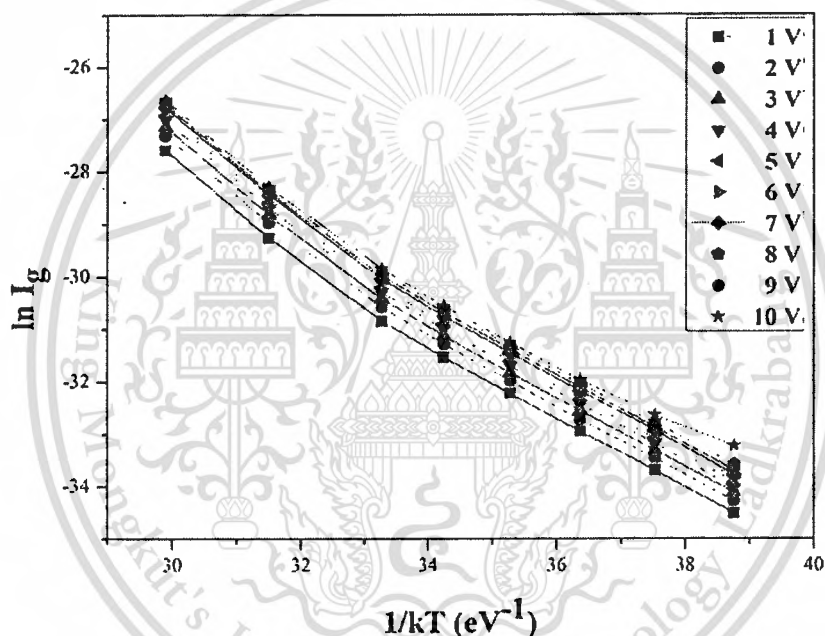


Fig. 4.8 Arrhenius plot of generation current vs. temperature of the difference bias.

The slope of an Arrhenius plot, $I_R(T)$ vs. $1/kT$ yields the activation energy (E_a) [61]. Fig. 4.8 shows example of the effect of difference temperature corrections on the activation energy from Arrhenius plot of generation current versus the temperature of the difference bias.

The activation energy of P-N diode with difference various energy and exposure times shown in Fig. 4.9.

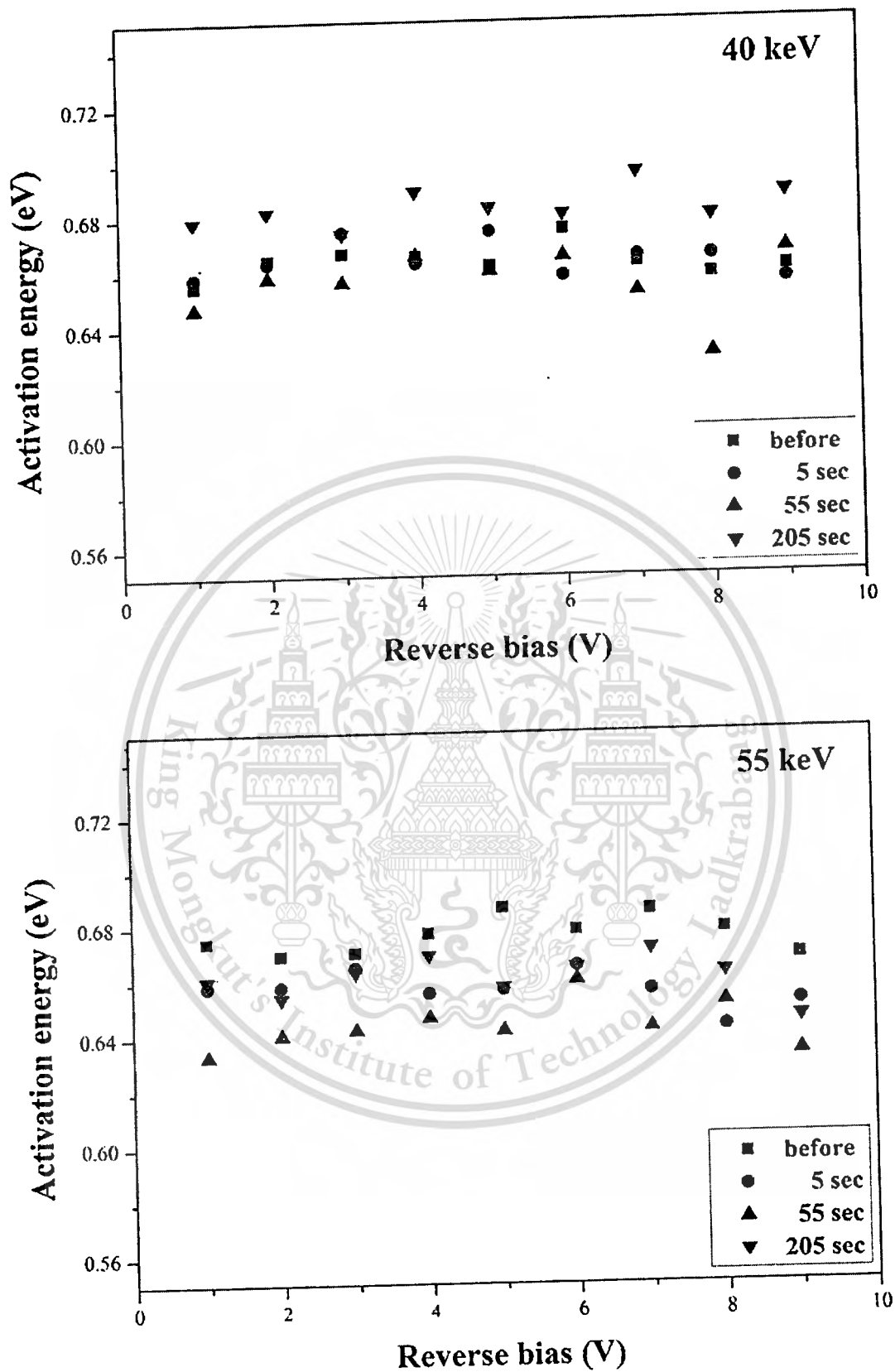


Fig. 4.9 The value of the activation energy versus bias voltage.

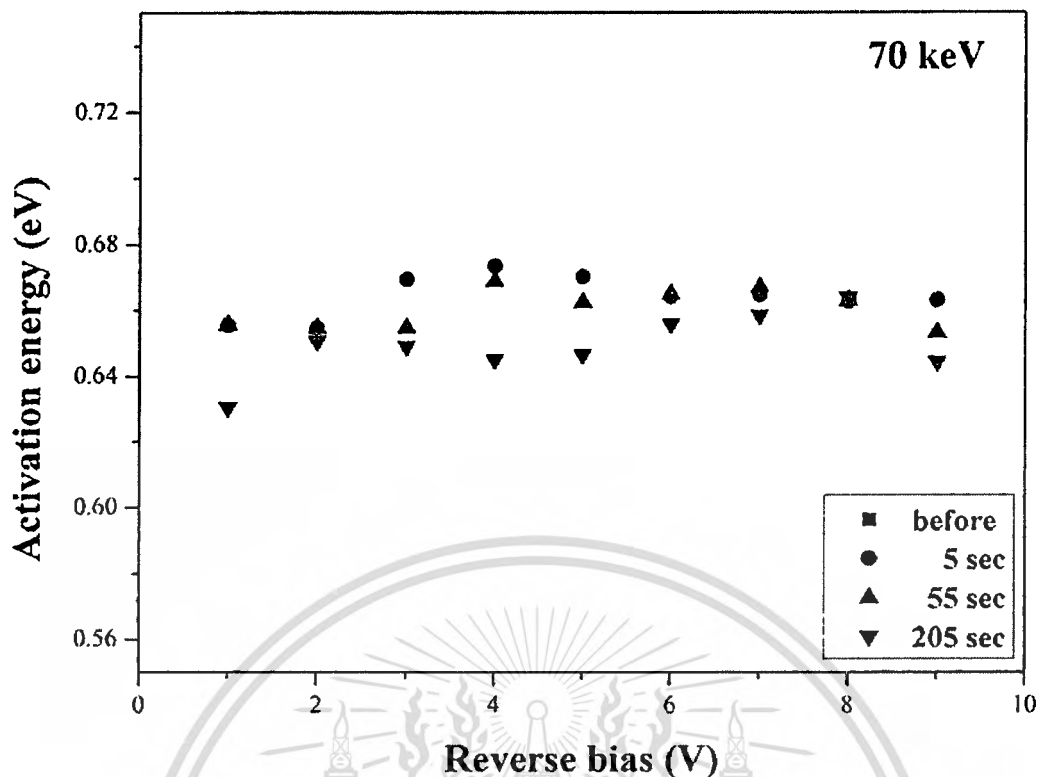


Fig. 4.9 The value of the activation energy versus bias voltage. (Cont.)

Form Fig. 4.9 shows that the activation energy after irradiate 40 keV are decrease about 0.02 eV at 55 sec and increase about 0.02 at 205 sec, 55 keV of exposure all activation are decrease about 0.02 to 0.05 eV and 70 keV the activation energy are change about 0.01 to 0.03 eV. Form the result shows that the activation energy of P-N diode after X-ray irradiated are a little change about 0.01 to 0.05. Although, the activation energy are change after irradiate but it cannot confirm of the important parameter to change the leakage current because it is both defects.

4.1.2.2 Diffusion current (I_d)

From Eq. 4.8, I_d is the diffusion current can find by the intersection of 2 parameter between leakage current (I_0) and depletion width (W) shown in Fig. 4.11.

The diffusion current examine by using technique from Fig. 4.11 are shown in Table. 4.7. The diffusion current after irradiation difference energy and times are increase about 30 pA at 40 and 55 keV, on the other hand, the diffusion current are decreased about 30 pA at 70 keV.

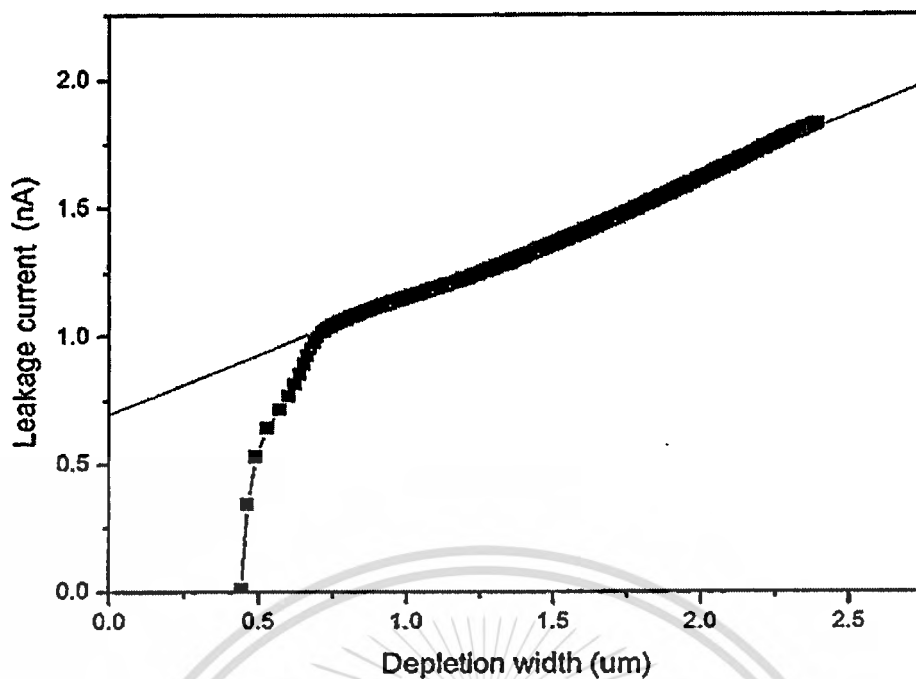


Fig 4.10 The leakage current versus the depletion width of the silicon p-n junction diode.

Table 4.6. The diffusion current of diode before and after irradiation at difference energy and times.

		Diffusion current (nA)		
		40	55	70
Time (s)	Energy (keV)			
		40	55	70
	Before (non-irradiation)	0.62	0.61	0.61
	5	0.64	0.63	0.61
	55	0.64	0.64	0.59
	205	0.65	0.64	0.58

The diffusion current increase at 40 and 55 keV shows that the X-ray are induced some problems in silicon bulk, on the other hand, at 70 keV the diffusion current are decrease because X-ray can removed the problems in silicon bulk.

4.1.2.3 Carrier generation lifetime (τ_g)

The carrier generation lifetime is one of important parameter cause to leakage current. Generation lifetime is the average time of electron-hole to generate. The X-ray irradiate can cause to the leakage current of P-N diode shows in Fig. 4.7. From Fig. 4.7 leakage current after irradiation at 40 and 55 keV are increase, on the other hand, 70 keV are decrease. The effects may relate to the defects. These defects can be studied from the generation lifetime. The generation lifetime can also be calculated using Eq. 4.14 which is exactly in the form of the Eq. 4.4 reversed slope.

$$\tau_g = Aqn_iW / (I_0 - I_d) \quad (4.14)$$

The curve of generation lifetime, which are calculated from Eq. 4.14 versus the depletion width from difference X-ray irradiation energy and time are shown in Fig. 4.10. From Fig. 4.10 shows that the generation lifetime at 40 keV are decrease after irradiated, on the other hand, the generation lifetime at 55 and 70 keV for 5 sec are increase, in contrast, 55 and 205 sec are decrease.

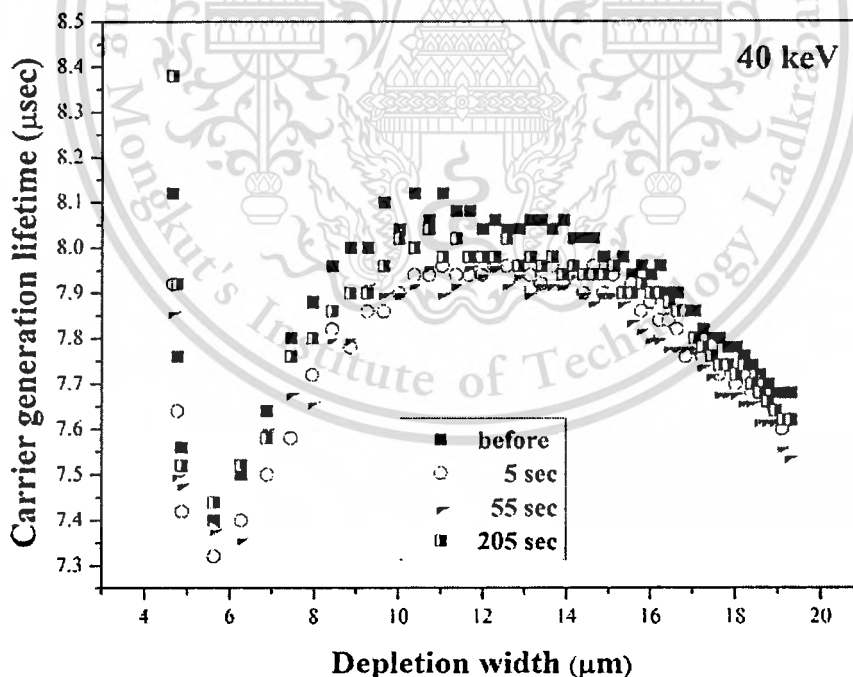


Fig. 4.11 The generation lifetime of P-N diode before and after X-ray irradiation.

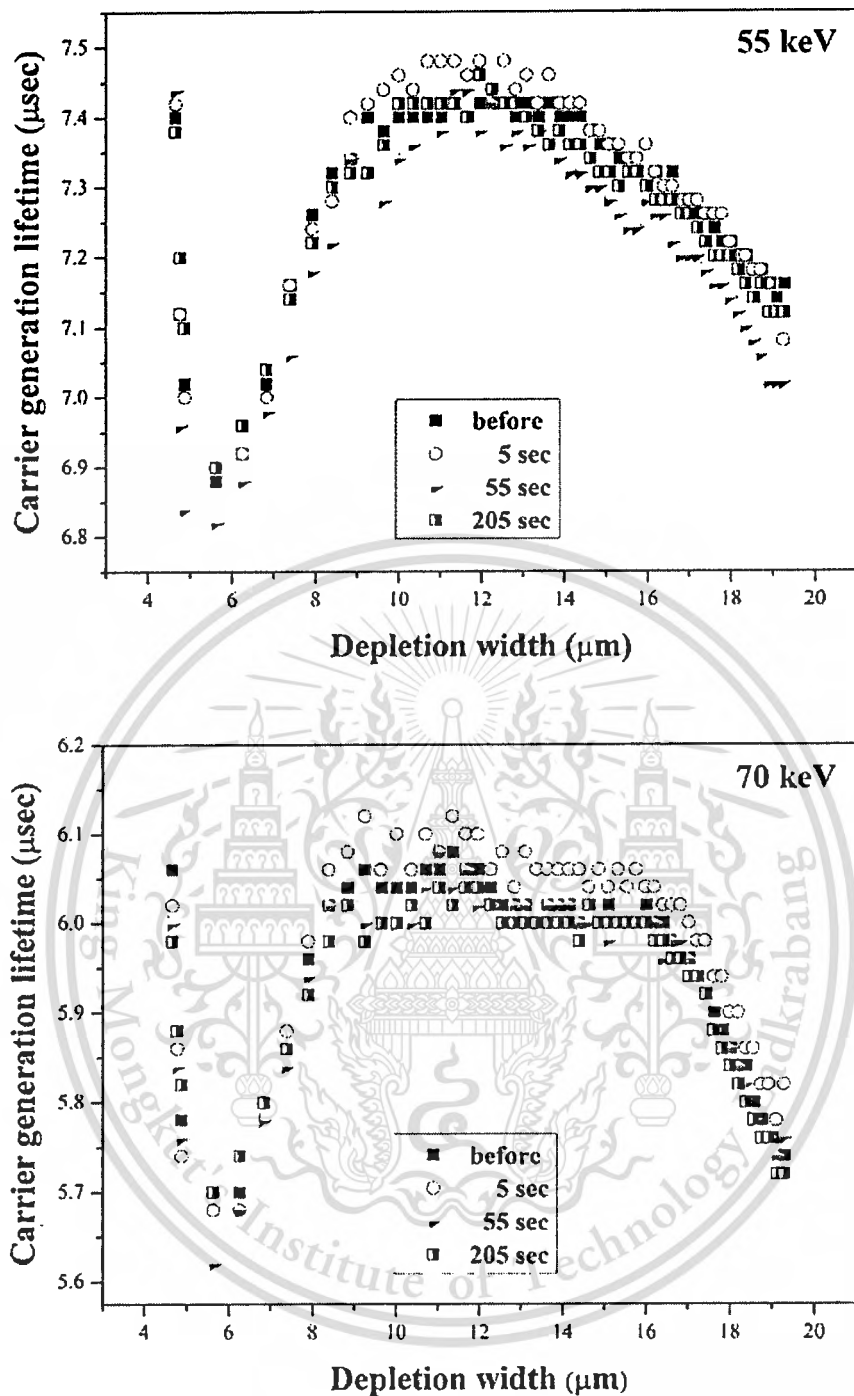


Fig. 4.11 The generation lifetime of P-N diode before and after X-ray irradiation.
(Cont.)

The generation lifetime averages from Fig. 4.10 are shown in Table 4.6. The leakage current of the diode before and after irradiation have a trend decrease and increase relation with the generation lifetime.

Table 4.7. The average generation lifetime from Fig. 4.12.

Energy (keV) Time (sec)	Carrier generation lifetime (τ_g) (μsec)		
	40	55	70
Before (non-irradiation)	6.96	6.44	6.84
5	6.88	6.45	6.89
55	6.90	6.40	6.82
205	6.86	6.36	6.85

4.2 Capacitance-voltage characteristics (C-V)

The capacitance-voltage characteristic is an important to study the properties of P-N diode.

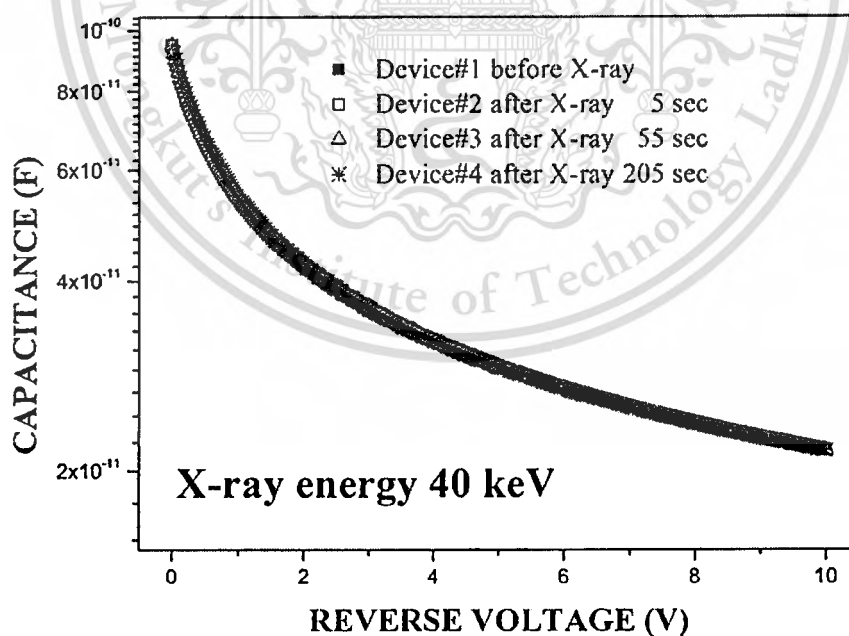


Fig. 4.12 Capacitance-voltage characteristics of P-N diode.

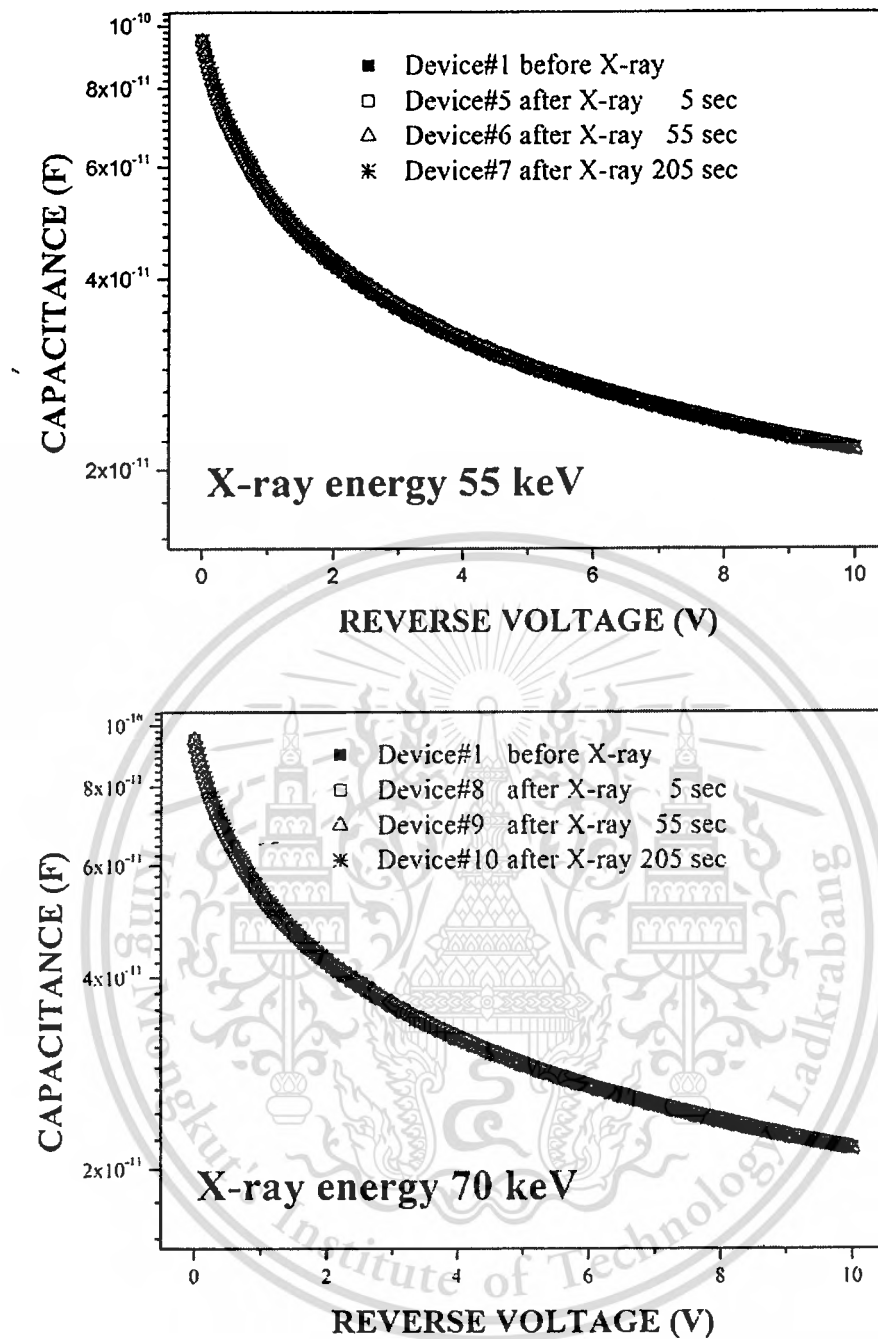


Fig. 4.12 Capacitance-voltage characteristics of P-N diode. (Cont.)

The Capacitance-voltage characteristics of the P-N diode before and after the X-ray irradiation are shown in Fig. 4.15, revealing an unchanged capacitance, originating from a radiation induced dopant deactivation in the Si layer. From I-V characteristics were decreased at 70 keV of exposure.

The effect of X-ray irradiated on I-V characteristics have many caused such as X-ray induced defect in bulk structure, carrier generation lifetime were increased and carrier concentration were changed.

In this experiment, we investigated the carrier concentration of diode after irradiated by X-ray. The capacitance of a reverse-biased junction, when considered as a parallel plate capacitor, is

$$C = \frac{K_s \epsilon_0 A}{W} \quad (4.16)$$

4.2.1 Carrier concentration (N)

A change of the I-V characteristics after X-ray irradiation can be confirmed by measuring the doping concentration. The boron concentration after irradiation $[B_\phi]$ has been defined by $[B_\phi] = [B_0] - R_c \Phi$, where R_c is the boron removal rate and $[B_0]$ is the boron concentration before irradiation $[B]$. By knowing the boron concentration $[B]$ at a certain depth below the junction before and after irradiation, R_c at each state can be obtained from, $R_c = ([B_0] - [B_\phi]) / \Phi$.

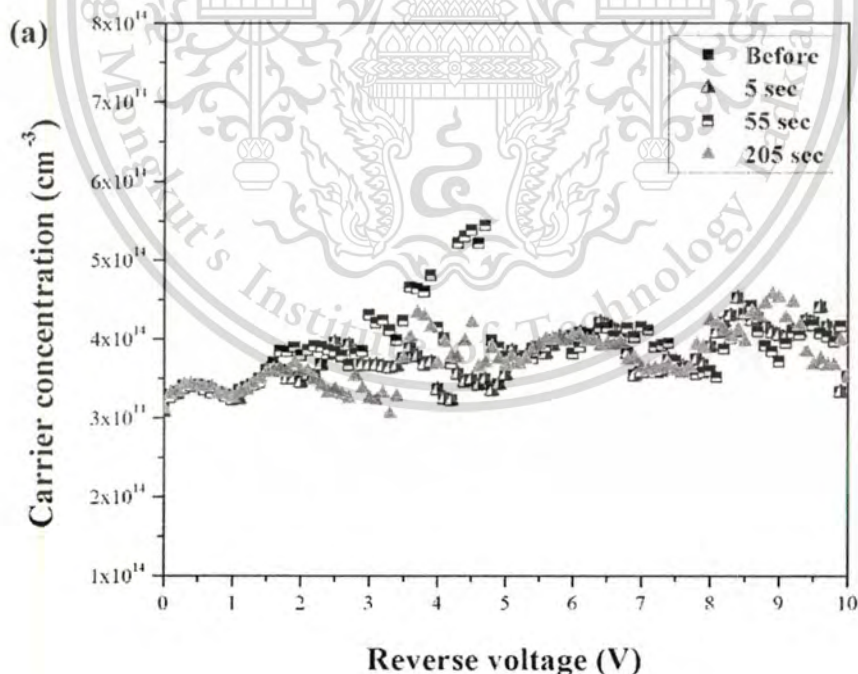


Fig. 4.12 Carrier concentration of diode at (a) 40 kV, (b) 55 kV and (c) 70 keV.

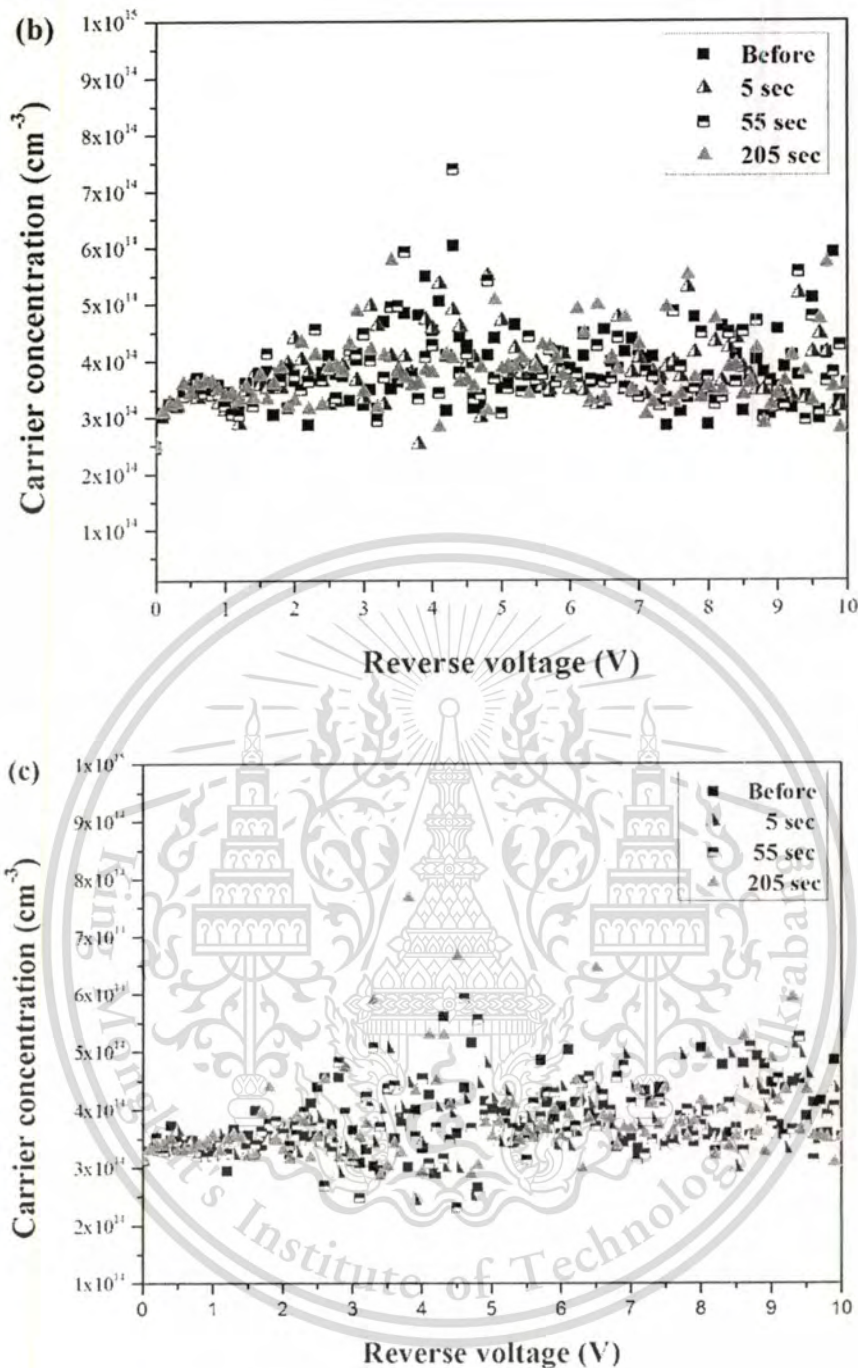


Fig. 4.12 Carrier concentration of diode at (a) 40 kV, (b) 55 kV and (c) 70 keV. (Cont.)

Usually, [B] is derived from the derivative of $1/C^2$ versus V_R . It found that [B] had been reduced after X-ray irradiation. In this case [B], which is obtained from C-V characteristics, has only the value within W. Fig 4.16 shows doping concentration of

P-N diode before and after irradiation. From Fig. 4.16, the doping concentration before and after irradiation at 40, 55 and 70 kV have only minor change [65].

The average concentration of 40, 55 and 70 kV were about $3-4 \times 10^{14} \text{ cm}^{-3}$, but it notices that there are maximum peaks of concentration at -5V bias were about $5.5 \times 10^{14} \text{ cm}^{-3}$, $1.2 \times 10^{15} \text{ cm}^{-3}$ and $1.2 \times 10^{15} \text{ cm}^{-3}$ at 40, 55 and 70 kV, respectively.

4.2.2 Build in voltage (V_{bi})

From the I-V characteristics can calculate the build in voltage of the P-N diode. The I-V characteristics may effect of the resistance to change the V_{bi} .

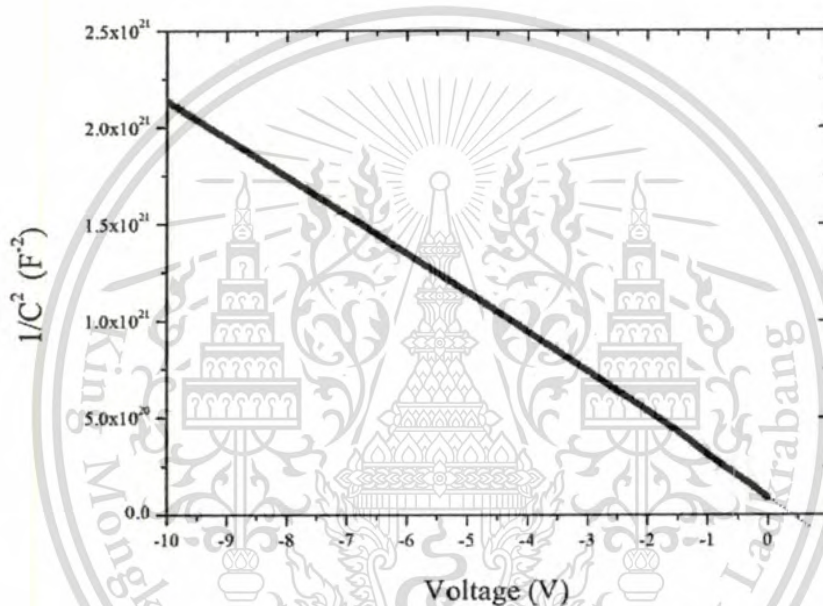


Fig. 4.14 Graph relation between $1/C^2$ vs. V .

Therefore, the capacitance-voltage characteristic is a one of technique to found V_{bi} by plot $1/C^2$ vs. V shown in Fig. 4.17. The build in voltage of P-N diode before and after irradiation are not change, V_{bi} are in range 0.4-0.7 V.

4.2.3 Depletion width (W)

Depletion width of P-N diode can be found from Eq. 4.17

$$W = \frac{\epsilon_{Si}}{C} \quad (4.17)$$

From Fig. 4.18 the depletion width of P-N diodes are not change after irradiation by X-ray with various energy and times. The depletion width at -10 V have about 19 μm . Therefore, X-ray radiation are not effect to depletion width of P-N diodes.

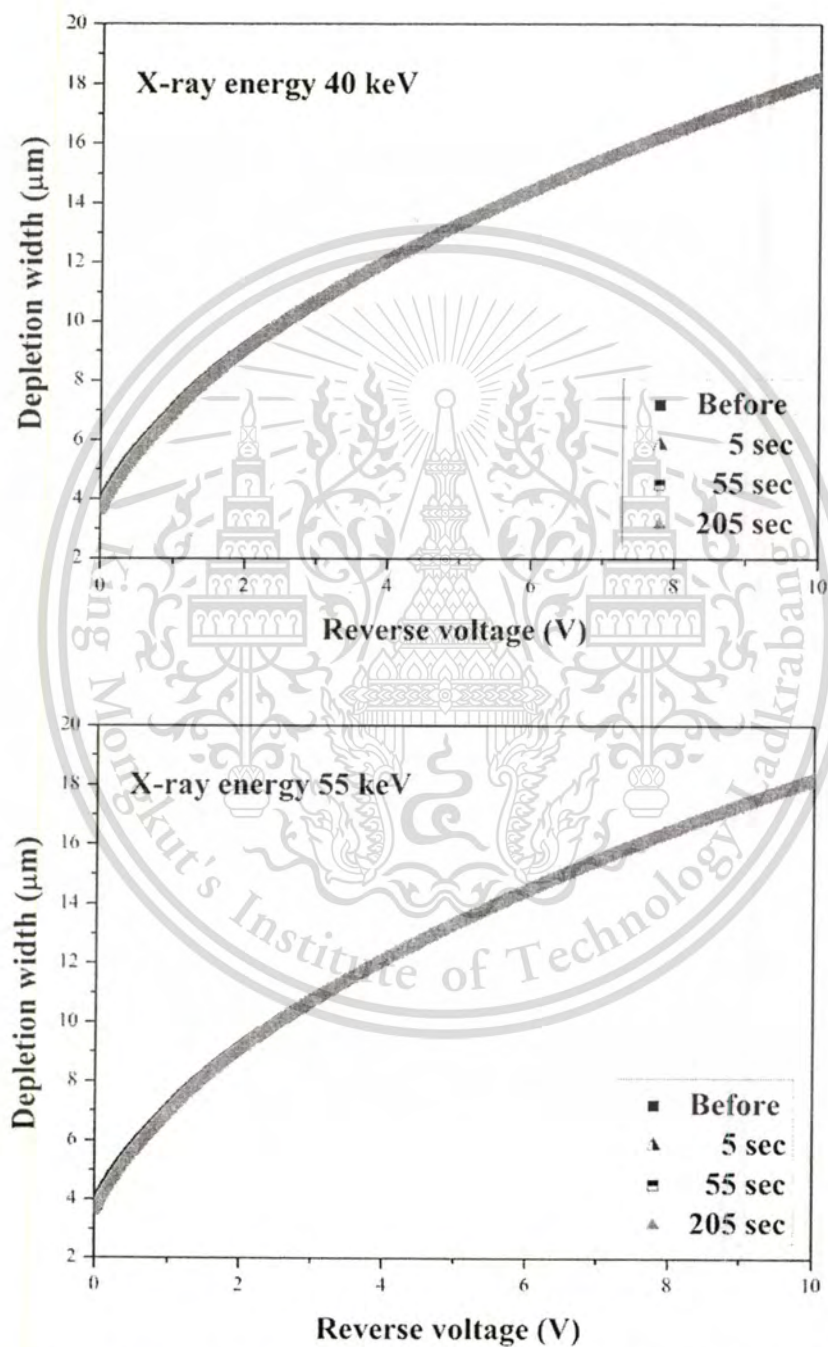


Fig. 4.15 The depletion width of diode compare before and after irradiation.

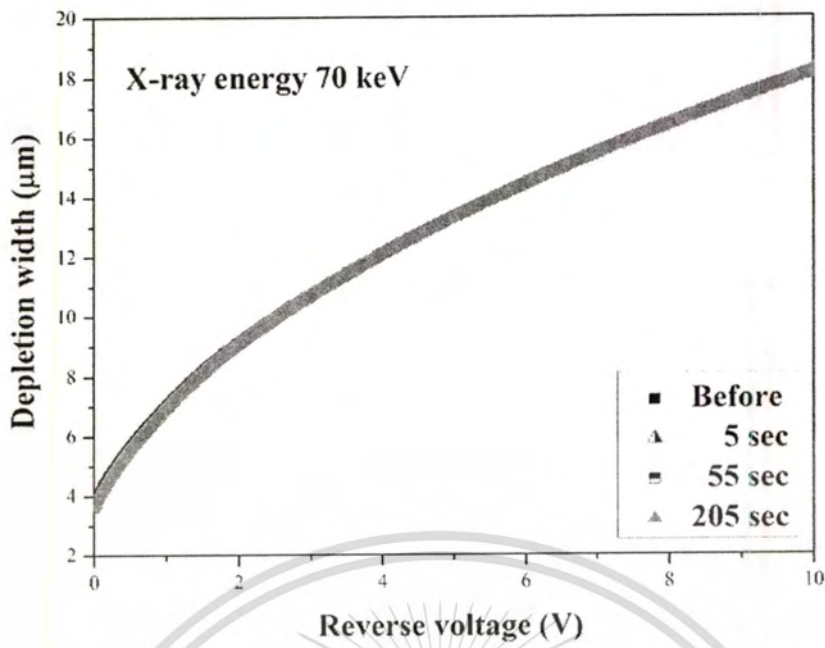
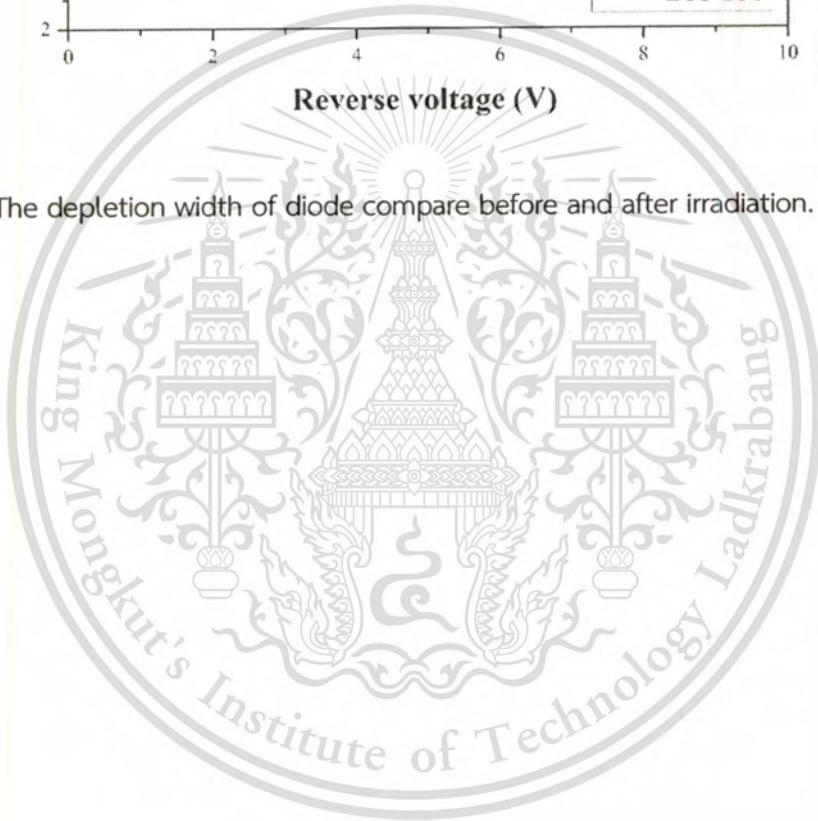


Fig. 4.15 The depletion width of diode compare before and after irradiation. (Cont.)



Chapter 5

Conclusion

This thesis are study the effect of X-ray irradiation on the electrical properties of P-N diode. The electrical properties of P-N diode are study such as current-voltage characteristics (I-V) and capacitance-voltage characteristics (C-V). X-ray radiations to use in this thesis are various energy and times, the energy various are 40, 55 and 70 keV with times 5, 55 and 205 second. The current-voltage (I-V) measurement was then performed using a HP4156B. The I-V characteristic results were measured on the wafer with a bias step of 25 mV from the reverse (VR) to forward (VF) voltage, in the range of -10 to +1V.

The results shows that reverse bias regime, leakage currents of 40 and 55 keV were slightly increased, while, the leakage current was found to decrease with 70 keV of exposure. In the forward bias regime, the forward current was increased about 3 orders of magnitude because of a dramatic reduction in the series resistance calculated by the standard model (from several $k\Omega$ to a few Ω). Capacitance-voltage characteristics are not change after irradiation. From the results, we have to found the effect of X-ray irradiation to the characteristics of P-N diode. The electrical properties of P-N diode have 2 characteristics are I-V and C-V characteristics. I-V characteristics are consist of 2 parts forward and reverse bias, the forward bias can be found many parameters to explain the effect of X-ray radiation such as carrier recombination lifetime (τ_r), forward current (I_f), series resistance (R_s), ideality factor (n) and build in voltage (V_{bi}). Reverse bias team are consist of leakage current (I_0), Diffusion current (I_d), activation energy (E_a), depletion width (W), carrier concentration (N) and carrier generation lifetime (τ_g). These results show the benefit of X-ray irradiation as the post-fabrication soft annealing process to cure high parasitic resistance of our low grade P-N junction diodes with the minimum cost and effort. In addition, the optimized condition of the X-ray irradiation may still be improved, where the evidence or mechanism of silicon bulk modification by the X-ray is required to study in details.

From the results show that the activation energy, build in voltage and carrier concentration are a little change, therefore, this parameter are not important parameter to change the leakage current. On the other hand, the carrier generation lifetime are decreased after irradiation, the change of carrier generation lifetime can cause to the leakage current because it is main parameters involved in the leakage current from equation 4.4. Moreover, the diffusion current is a one important

parameter of change the leakage current from equation 4.4, the diffusion current are decreased almost of all energy an times and except for 5 min at 70 keV. The leakage current are a little change by the relation with carrier generation lifetime and diffusion current. In forward bias term, the forward currents after irradiation are increase about 3 orders at 0.6 to 1.0 V. The ideality factor of the after exposed diode can be calculated and has a value around 1.03 which confirms that these diodes approached the ideal diode performance, the change of ideality factor shows that the current in forward bias team are the recombination current because the ideality nearly 1. Recombination lifetime are decrease at 40 and 55 keV while 70 keV are increase, in this case X-ray at 40 and 55 keV may generate defects and trap in silicon bulk. Therefore, this effects can cause to decrease recombination lifetime, on the other hand, 70 keV of exposure may reduce defects in silicon bulk. From the forward current are increase about 3 orders of magnitude can cause by reduce of series resistance because of a dramatic reduction in the series resistance calculated by the standard model (from several $k\Omega$ to a few Ω). The change in the forward current seems to be caused by a series resistance reduction that affected the ideality factor of the diode. The effect of the series resistance is usually modeled with series combination of a diode and resistor, R_s , in which the voltage V_{da} cross the diode can be expressed in terms of the total voltage drop V_a cross the diode and the resistance R_s . These results show that this is a promising method for manufacturing yield improvement with a minimum added cost and effort. In this experiment, both front and back sides were irradiated, in which the same electrical characteristics is obtained. By using the X-ray method, there is no silicon atom escaped from the lattice. On the other hand, this energy is sufficient to destroy the defect complexes in a semiconductor, in which the impurity atoms in these complexes can become electrically active.

The P-N junction diodes are improving the performance after irradiation by X-ray, the X-ray can treatment of some damage in silicon device. The damage in silicon device can cause by many case such as high-energy ion implantation, CZ wafer and contaminate in device fabrication. From the results the X-ray at 70 keV are suitable to use for improve the P-N junction diode because can decrease leakage current and improve the forward current. This research is important implications for the development of the semiconductor devices, which may reduce production costs and improve the efficiency of the device.

References

- [1] G. F. Dalla Betta, G. U. Pignatelli, G. Verzellesi, and M. Boscardin, "Si-Pin X-ray Detector Technology", *Nuclear Instruments and Methods in Physics Research A*, Vol. 395, pp. 344-349, 1997.
- [2] P. Hazdra, and H. Dorschner, "Radiation Defect Distribution in Silicon Irradiated with 600 keV Electron", *Nuclear Instruments and Methods in Physics Research B*, Vol. 201, pp. 513-519, 2003.
- [3] E. Gaubas, A. Uleckas, J. Chen, D. Yang, and J. Vanhellefont, "Study of Irradiation Induced Changes of Electrical and Functional Characteristics in Ge Doped Si Diodes", *Physica B*, Vol. 407, pp. 2998-3001, 2012.
- [4] M. A. Krivov, and S. V. Malyanov, "Effect of Roentgen Radiation on Germanium and Germanium P-N Junctions", *IZ Vestiya VUZ*, pp. 76-78, 1965.
- [5] N. Konofaos, E. K. Evangelou, F. Scholz, K. Zieger, and E. Aperathitis, "Electrical Characteristics and Carrier Transport Mechanisms of GaAs p/i/n Devices for Photovoltaic Applications", *Materials Science and Engineering B*, Vol. 80, pp. 152-155, 2000.
- [6] R. R. Sumathi, M. Udhayasankar, J. Kumar, P. Magudapathy, and K. G. M. Nair, "Effect of Proton Irradiation on the Characteristics of GaAs Schottky Barrier Diodes", *Physica B*, Vol. 308-310, pp. 1209-1212, 2001.
- [7] D. V. Kuskonov, H. Temkin, A. Osinsky, R. Gaska, and M. A. Khan, "Low-frequency Noise and Performance of GaN P-N Junction Photodetectors", *International Electron Devices Meeting (IEDM)*, pp. 759-762, 1997.
- [8] H. Ohyama, K. Takakura, M. Hanada, T. Nagano, K. Yoshino, T. Nakashima, S. Kuboyama, E. Simoen, and C. Claeys, "Degradation of GaN LEDs by Electron Irradiation", *Materials Science and Engineering B*, Vol. 173, pp. 57-60, 2010.
- [9] N. Wang, N. Zhang, and M. Wang, "Wireless Sensors in Agriculture and Food industry-Recent Development and Future Perspective", *Computers and Electronics in Agriculture*, Vol. 50, pp. 1-14, 2006.
- [10] C. Beinke, U. Oestreicher, A. Riecke, U. Kulka, V. Meineke, and H. Romm, "Interlaboratory Comparison to Validate the Dicentric Assay as a Cytogenetic Triage Tool for Medical Management of Radiation Accidents", *Radiation Measurement*, Vol. 46, pp. 929-935, 2011.

- [11] T. Osawa, "Solar Radiation Quantity Detecting Device for Automobile Air-Conditioner", *Environment International*, Vol. 18 (6), pp. 1-2, 1992.
- [12] D. Adliene, I. Cibulskaitė, and S. Meskinis, "Low Energy X-ray Radiation Impact on Coated Si Constructions", *Radiation Physics and Chemistry*, Vol. 79, pp. 1031-1038, 2010.
- [13] R. D. Harris, "Proton Irradiation of Silicon Schottky Barrier Power Diodes", *IEEE Transactions on Nuclear Science*, Vol. 53 (4), pp. 1995-2003, 2006.
- [14] A. Ruzin, G. Casse, M. Zanet, F. Lemeilleur, and Watts, "Comparison of Radiation Damage in Silicon Induced by Proton and Neutron Irradiation", *IEEE Transactions on Nuclear Science*, Vol. 46 (5), pp. 1310-1313, 1999.
- [15] A. M. Strel'chuk, V. V. Kozlovski, N. S. Savkina, M. G. Rastegaeva, and A. N. Andreev, "Influence of Proton Irradiation on Recombination Current in 6H-SiC PN Structures", *Materials Science and Engineering B*, Vol. 61, pp. 441-445, 1999.
- [16] A. Czerwinski, J. Katcki, J. Ratajczak, E. Simoen, A. Poyai, C. Claeys, and H. Ohyama, "Impact of Fast-neutron Irradiation on the Silicon P-N Junction Leakage and Role of the Diffusion Reverse Current", *Nuclear Instruments and Methods in Physics Research B*, Vol. 186, pp. 166-170, 2002.
- [17] K. Takakura, K. Hayama, D. Watanabe, H. Ohyama, T. Kudou, K. Shigaki, S. Matsuda, S. Kuboyama, T. Kishikawa, E. Simoen, and C. Claeys, "Radiation Defects and degradation of Si Photodiodes Irradiated by Neutrons at Low Temperature", *Physica B*, Vol. 376-377, pp. 403-406, 2006.
- [18] K. W. Jang, B. S. Lee, and J. H. Moon, "Development and Characterization of the Integrated Fiber-Optic Radiation Sensor for the Simultaneous Detection of Neutrons and Gamma Rays", *Applied Radiation and Isotopes*, Vol. 69, pp. 711-715, 2011.
- [19] M. Angelone, M. Pillon, R. Faccini, D. Pinci, W. Baldini, R. Calabrese, G. Cibinetto, A. C. Ramusino, R. Malaguti, and M. Pozzati, "Silicon Photo-multiplier Hardness Tests with a Beam Controlled Neutron Source", *Nuclear Instruments and Methods in Physics Research A*, Vol. 623, pp. 921-926, 2010.
- [20] H. Ohyama, K. Hayama, K. Takakura, T. Jono, E. Simoen, and C. Claeys, "Effect of Irradiation Temperature on Radiation Damage in Electron-irradiated MOS FETs", *Microelectronic Engineering*, Vol. 66, pp. 530-535, 2003.

- [21] J. Vobecky, P. Hazdra, O. Humbel, and N. Galster, "Crossing Point Current of Electron and Proton Irradiated Power P-i -N Diodes", *Microelectronic Reliability*, Vol. 40, pp. 427-433, 2000.
- [22] Y. Unno, M. Takahata, H. Maeohmichi, F. Hinode, T. Akagi, T. Aso, M. Daigo, J. Dewitt, D. Dorfan, T. Dubbs, M. Frautschi, A. Grillo, C. Haber, T. Handa, T. Hatakenaka, B. Hubbard, H. Iwasaki, Y. Iwata, D. Kaplan, S. Kashigin, I. Kipnis, S. Kobayashi, T. Kohriki, T. Kondo, W. Droeger, J. Matthews, H. Miyata, A. Murakami, K. Noble, K. O'Shaughnessy, T. Ohmoto, T. Ohsugi, H. Ohyama, T. Pulliam, J. Rahn, W. A. Rowe, G. G. W. Sadrozinski, A. Seiden, J. Siegrist, E. Spencer, H. Spieler, R. Takashima, N. Tamura, S. Terada, M. Tezuka, A. Webster, R. Wichmann, M. Wilder, and M. Yoshikawa, "Beam Tests of a Double-sided Silicon Strip Detector with Fast Binary Readout Electronics before and after Proton-irradiation", *Nuclear Instruments and Methods in Physics Research A*, Vol. 383, pp. 211-222, 1996.
- [23] K. Hayama, K. Takakura, K. shigaki, H. Ohyama, J. M. Rafi, A. Mercha, E. Simoen, and C. Claeys, "Impact on the Back Gate Degradation in Partially Depleted SOI n-MOSFETs by 2-MeV Electron Irradiation", *Microelectronics Reliability*, Vol. 46, pp. 1731-1735, 2006.
- [24] M. A. Krivov, S. V. Malyanov, and V. I. Gaman, "The Effect of X-rays on Silicon and Silicon P-N Junctions", *Izvestiya VUZ*, Vol. 10, pp. 150-152, 1967.
- [25] G. F. D. Betta, G. U. Pignatel, G. Verzellesi, and M. Boscardin, "Si-PIN X-ray Detector Technology", *Nuclear Instruments and Methods in Physics Research A*, Vol. 395, pp. 344-348.
- [26] K. Hayama, H. Ohyama, E. Simoen, C. Claeys, A. Poyai, T. Miura, and K. Kobayashi, "Radiation Defects in STI Silicon Diodes and Their Effects on Device Performance", *Physica B*, Vol. 308-310, pp. 1217-1221, 2001.
- [27] B. J. Baliga, "Comparison of Gold, Platinum, and Electron Irradiation for Controlling Lifetime in Power Rectifiers", *IEEE Transaction on Electron Devices*, Vol. 24 (6), pp. 685-688, 1977.
- [28] P. Hazdra, and H. Dorschner, "Radiation Defect Distribution in Silicon Irradiated with 600 keV Electron", *Nuclear Instrument and Methods in Physics Research B*, Vol. 201, pp. 513-519, 2003.

- [29] M. Pattabi, S. Krishnam, and G. Sanjeev, "Studies on the Temperature Dependence of I-V and C-V Characteristics of Electron Irradiated Silicon Photo-detectors", *Solar Energy Material & Solar Cells*, Vol. 91, pp. 1521-1524, 2007.
- [30] R. Korde, A. Ojha, R. Braasch, T. C. English, "The Effect of Neutron Irradiation on Silicon Photodiodes", *IEEE Transactions on Nuclear Science*, Vol. 36 (6), 2169-2175, 1989.
- [31] N. Croitoru, A. Gambirasio, P. G. Rancoita, and A. Seidman, "Current-voltage and Impedance Characteristics of Neutron Irradiated Silicon Detectors at Fluence up to 10^{16} n/cm²", *Nuclear Instrument and Methods in Physics Research B*, Vol. 111, pp. 297-302, 1996.
- [32] M. A. Krivov, and G. I. Potakhova, "The Effect of X-rays on the Electrophysical Properties of Silicon and Silicon P-N Junctions", *IZ Vestiya VUZ*, No. 6, pp. 55-61, 1966.
- [33] The Berkeley Atmospheric CO₂ Observation Network. "Infrared Radiation." [Online]. Available : <http://beacon.berkeley.edu/GHGs/InfraredRadiation.aspx>. 2012.
- [34] R. Russell. "X-ray Radiation." [Online]. Available : http://www.windows2universe.org/physical_science/magnetism/em_xray.html. 2005.
- [35] Princeton University. "Radiation Properties." [Online] Available : <http://web.princeton.edu/sites/ehs/osradtraining/radiationproperties/radiationproperties.htm>. 2008.
- [36] I. Kaplan. *Nuclear Physics*. 2nd ED. Addison-Wesley Publishing Company. 1977.
- [37] P. Sathyavathi, P. S. Bhave, and V. N. Bhoraskar, "Irradiation Effects of 35 MeV Lithium and 70 MeV Oxygen Ions on the Hole Lifetime and the Forward Current of Silicon Diodes", *Solid State Communications*, Vol. 106 (11), pp. 755-758, 1998.
- [38] S. E. Boqushevich, I. I. Uqolev, "Inorganic EPR Dosimeter for Medical Radiology", *Applied Radiation and Isotopes*, Vol. 52 (5), pp. 1217-1219, 2000.
- [39] S. Z. Xin, Y. J. Song, C. Lv, Y. K. Rui, F. S. Zhang, W. Xu, D. Wu, S. Wu, J. Zhong, D. L. Chen, Q. Chen, and F. T. Peng, "Application of Synchrotron Radiation X-ray Fluorescence to Investigate the Distribution of Mineral Elements in Different Organs of Greenhouse Spinach", *Horticultural Science*, Vol. 36, pp. 133-139, 2009.
- [40] Authority of the Minister of Health. *Radiation Protection and Safety for Industrial X-ray Equipment*. Her Majesty the Queen in Right of Canada, 2003.
- [41] U. K. Mishra, and J. Singh. *Semiconductor Device Physics and Design*. Springer, 2008.

- [42] G. E. McGuire. *Characterization of Semiconductor Materials*. Noyes Publications, 1989.
- [43] D. K. Schroder. *Semiconductor Material and Device Characterization*. New Jersey, John Wiley & Sons., Hoboken, 2006.
- [44] D. A. Neamen. *Semiconductor Physics and Devices*. McGraw-Hill Companies, 2003.
- [45] A. Poyai. 2002. "Defect Assessment in Advanced Semiconductor Materials and Device." Ph.D. Thesis of Katholieke Universiteit Leuven.
- [46] D. K. Schroder, "The Concept of Generation and Recombination Lifetimes in Semiconductors", *IEEE Transactions on Electron Devices*, Vol. 29, pp. 1336-1338, 1982.
- [47] J. V. Zeghbrock. "The P-N Junction Capacitance." [Online] Available : <http://ecee.colorado.edu/~bart/book/pncap.htm#diffusion>. 1997.
- [48] W. Liu. *MOSFET Models for Spice Simulation*. New York: Wiley-Interscience, 2001.
- [49] H. Ohyama, T. Hirao, E. Simoen, C. Claeys, S. Onoda, Y. Takami, and H. Itoh, "Impact of Lattice Defects on the Performance Degradation of Si Photodiodes by High-temperature Gamma and Electron Irradiation. *Physica B*, Vol. 308-310, pp. 1226-1229, 2001.
- [50] H. Ohyama, E. Simoen, C. Claeys, K. Takakura, H. Matsuoka, T. Jono, J. Uemura, and T. Kishikawa, "Radiation Damage in Si Photodiodes by High-temperature Irradiation. *Physica E*, Vol. 16, pp. 533-538, 2003.
- [51] P. Rujanapich, A. Poyai, I. Sriphanachai, P. Pengpad, C. Hruanan, S. Sophitpan, S. Ueamapong, and W. Titiroonguang, "Activation Energy Analysis of P-N Junction X-ray Direct Detector", *ITC-CSCC-2010*, Vol. 1, pp. 257-260, 2010.
- [52] B. Sahin, H. C. Etin, and E. Ayyildiz, "The effect of Series Resistance on Capacitance-voltage Characteristics of Schottky Barrier Diodes", *Solid State Communication*, Vol. 135, pp. 490-495, 2005.
- [53] H. Ohyama, K. Kobayashi, J. Vanhellefont, E. Simoen, C. Claeys, T. Hirao, and S. Onoda, "Induced Lattice Defects in InGaAs Photodiodes by High-temperature Electron Irradiation", *Physica B*, Vol. 340-342, pp. 337-340, 2003.
- [54] P. P. Allport, P. S. L. Booth, C. Green, A. Greenall, J. N. Jackson, T. J. Jones, J. D. Richardson, S. M. I. Garcia, N. A. Smith, P. R. Turner, M. P. Wormald, "Annealing Effects on Irradiated n^+n Silicon Detectors", *Nuclear Instruments and Methods in Physics Research A*, Vol. 420, pp. 473-480, 1999.

- [55] K. Cinar, C. Coskun, S. Aydogan, H. Asil, and E. Gur, "The Effect of the Electron Irradiation on the Series Resistance of Au/Ni/6H-SiC and Au/Ni/4H-SiC Schottky Contacts", *Nuclear Instruments and Methods in Physics Research B*, Vol. 268, pp. 616-621, 2010.
- [56] A. Poyai, E. Simoen, C. Claeys, and A. Czerwinsky, "Silicon Substrate Effects on the Current-voltage Characteristics of Advanced P-N Junction Diodes", *Materials Science and Engineering*, Vol. 73, pp. 191-196, 2000.
- [57] A. Poyai, E. Simoen, C. Claeys, R. Rooyackers, and G. Badenes, "Lifetime Study in Advance Isolation Techniques", *Materials Science in Semiconductor Processing*, Vol. 4, pp. 137-139, 2001.
- [58] S. C. Cheung, and N. W. Cheung, "Extraction of Schottky Diode Parameters from Forward Current-voltage Characteristics", *Applied Physical Letters*, Vol 49, pp. 85, 1986.
- [59] I. Srithanachai, S. Ueamanapong, A. Poyai, S. Niemcharoen, and P. P. Yupapin, "An Experimental Investigation of P-N Diode Electrical Characteristics by Soft X-ray Annealing Method", *Optics & Laser Technology*, Vol. 44, pp. 636-639, 2012.
- [60] J. Prabket, I. Srithanachai, S. Ueamanapong, A. Poyai, W. Titiroongruang, S. Niemcharoen, P. P. Yupapin, "An Improvement of Electrical Characteristics of P-N Diode by X-ray Irradiation Method", *Scientific Research and Essays*, Vol. 71 (11), pp. 1230-1236, 2012.
- [61] I. Srithanachai, S. Ueamanapong, P. Rujanapich, N. Atiwongsangthong, S. Niemcharoen, A. Poyai, and W. Titiroongruang, "Defects Study by Activation Energy Profile for Lowering Leakage Current in P-N Junction", *Materials Science Forum*, Vol. 695, pp. 569-572, 2011.
- [62] A. Poyai, E. Simoen, and C. Claeys, "Hole-trapping-related Transients in Shallow n^+p Junctions Fabricated in a High-energy Boron-implanted p Well", *Applied Physics Letters*, Vol. 78, pp. 949, 2001.
- [63] J. M. Hinckley, and J. Singh, "High-field Thermal Noise of Holes in Silicon: The Effect of Valence Band Anisotropy", *Journal of Applied Physics*, Vol. 80 (12), pp. 6766, 1996.

- [64] H. Su, H. Wang, T. Xu, and R. Zong, "Role of Shallow Si/SiO₂ Interface State on High Frequency Channel Noise in n-Channel Metal-oxide-semiconductor Field Effect Transistors", *Applied Physics Letters*, Vol. 95, pp. 123508, 2009.
- [65] H. Jin, W. E. Jellett, Z. Chum, K. J. Weber, A. W. Blakers, and P. J. Smith, "The Effect of Boron Diffusions on the Defect Density and Recombination at the (111) Silicon-Silicon Oxide Interface", *Applied Physics Letters*, Vol. 92, pp. 1221091-3, 2008.



Appendix



This material is reserved for educational use only, not allowed for commercial use.

Forbidden to modify the content, and cite the document when use.



This material is reserved for educational use only, not allowed for commercial use.

Forbidden to modify the content, and cite the document when use.

X-ray radiation generator at KMUTNB

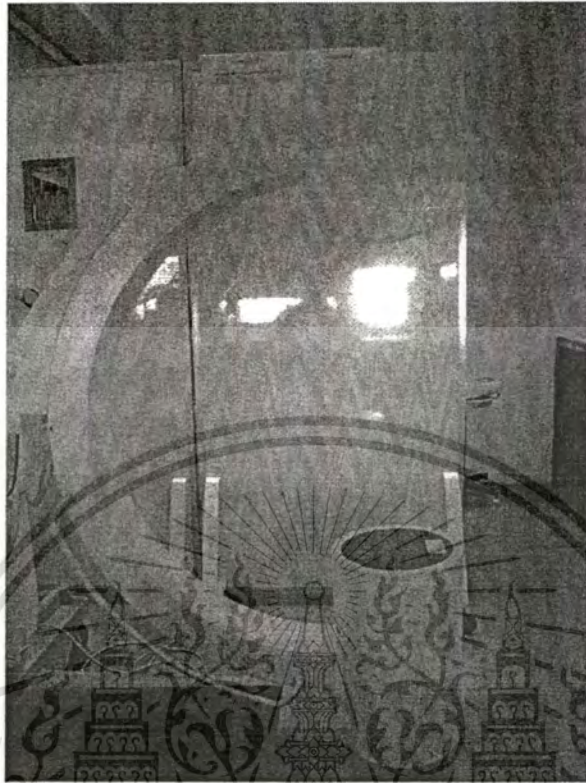


Fig. A1 C-arm of X-ray radiation generator.



Fig. A2 Monitor shows the image of device.



Fig. A3 Point of the device for X-ray generator.



Fig. A4 Control part of the X-ray generator.

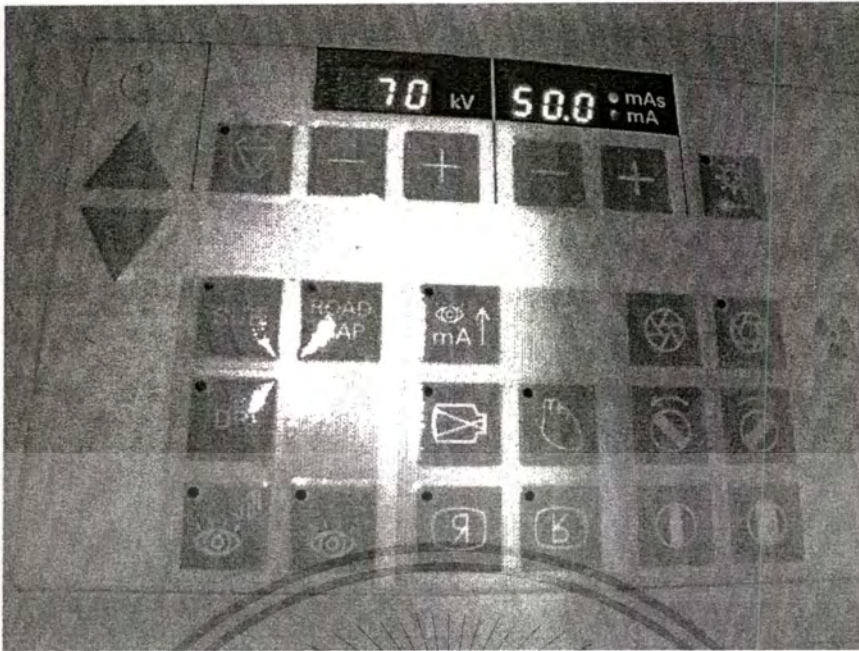
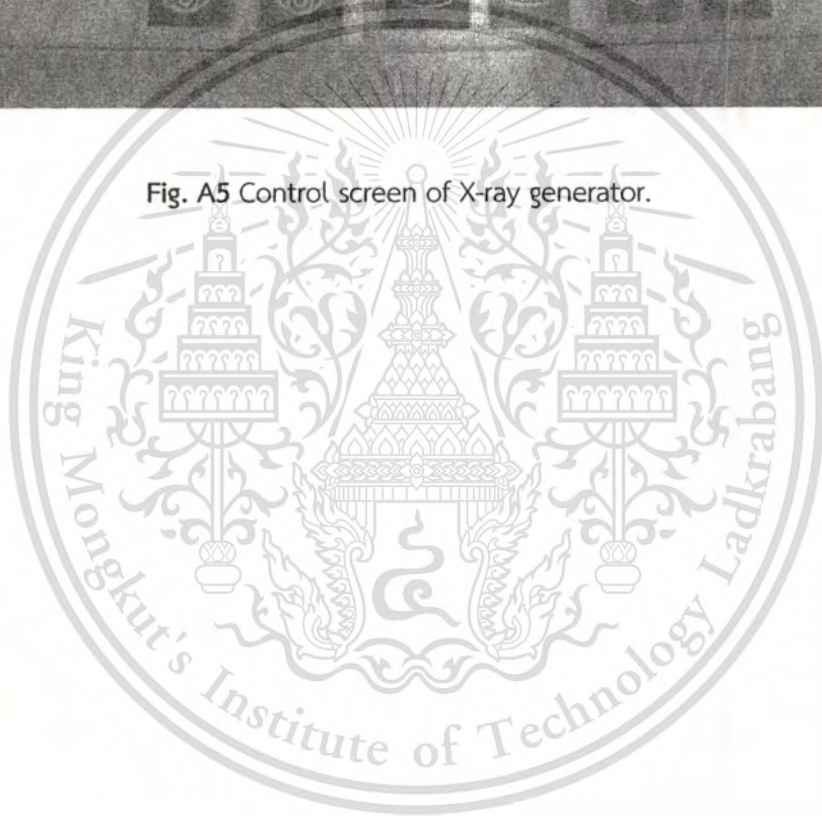


Fig. A5 Control screen of X-ray generator.



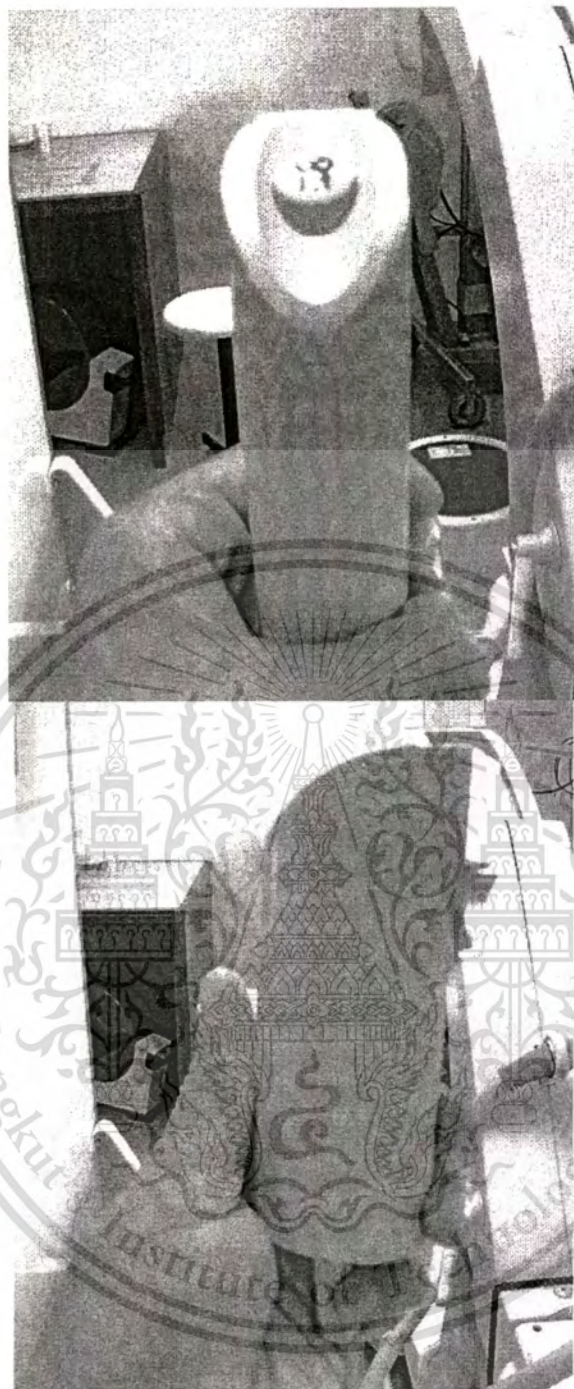


Fig. A6 Hand switch to control the emission of X-rays.

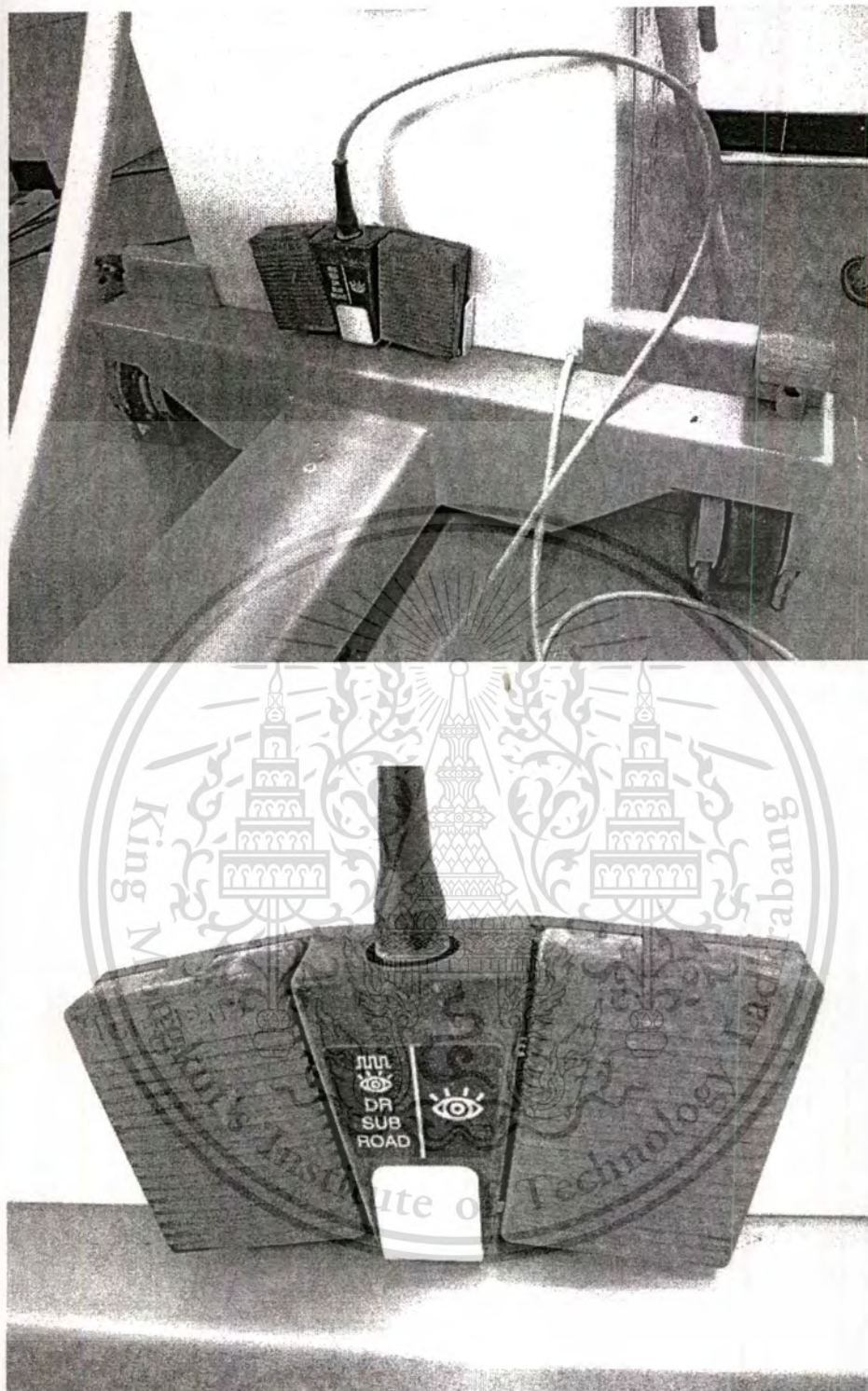


Fig. A7 Foot switch to control the emission of X-rays.

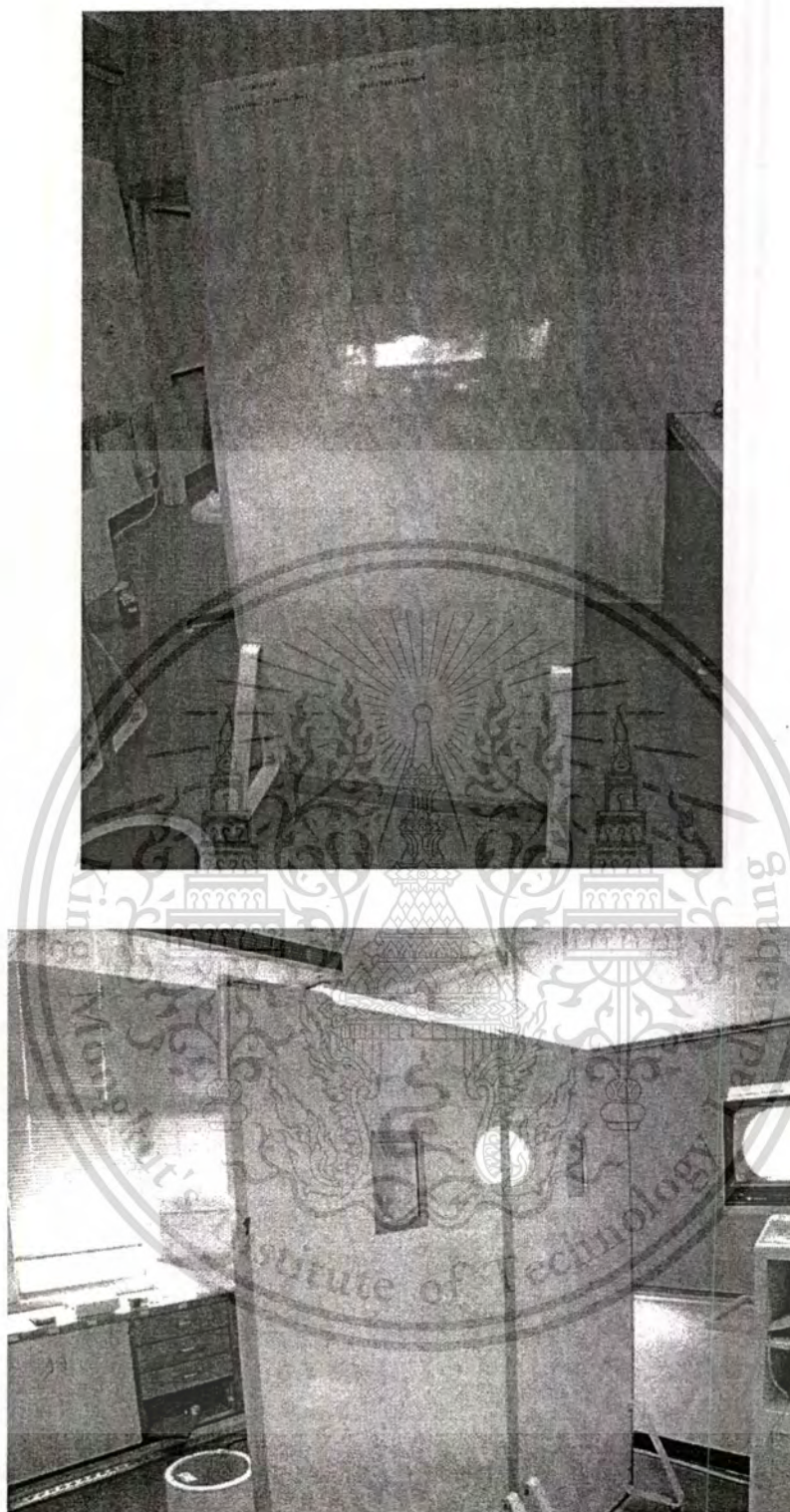


Fig. A8 Lead board for block X-rays.

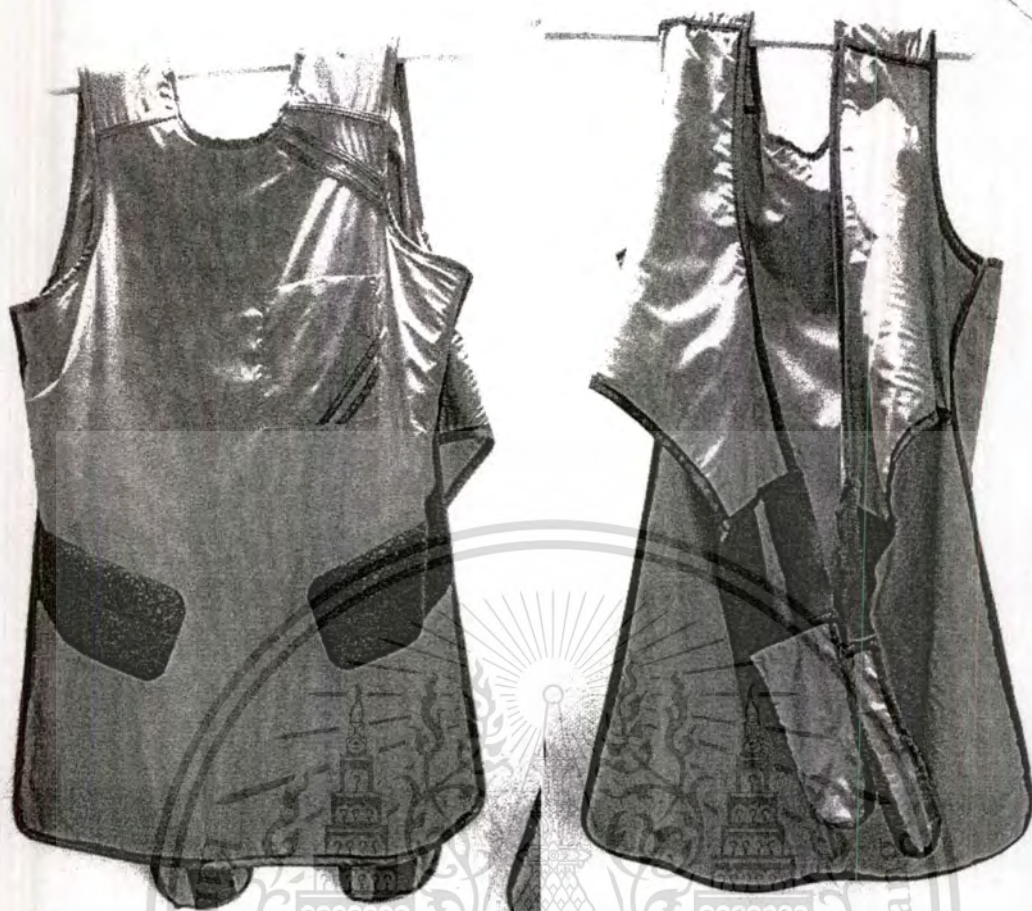


Fig. A9 Radiation jacket.

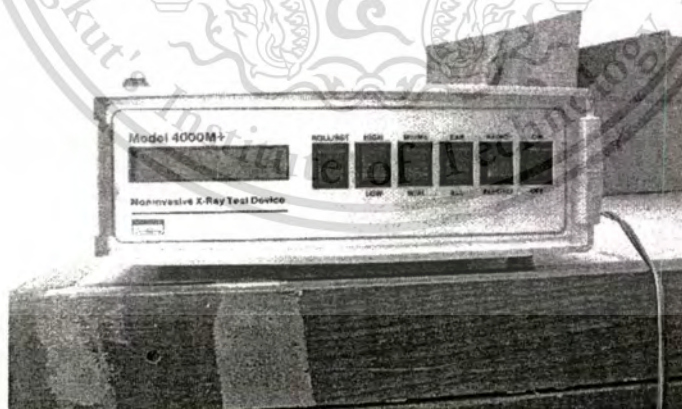


Fig. A10 Noninvasive X-ray test device.

This material is reserved for educational use only, not allowed for commercial use.

Forbidden to modify the content, and cite the document when use.

X-ray generator at Chulalongkorn University

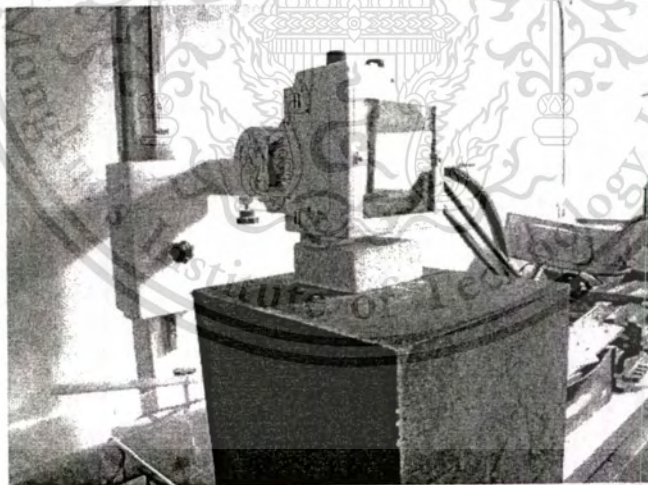
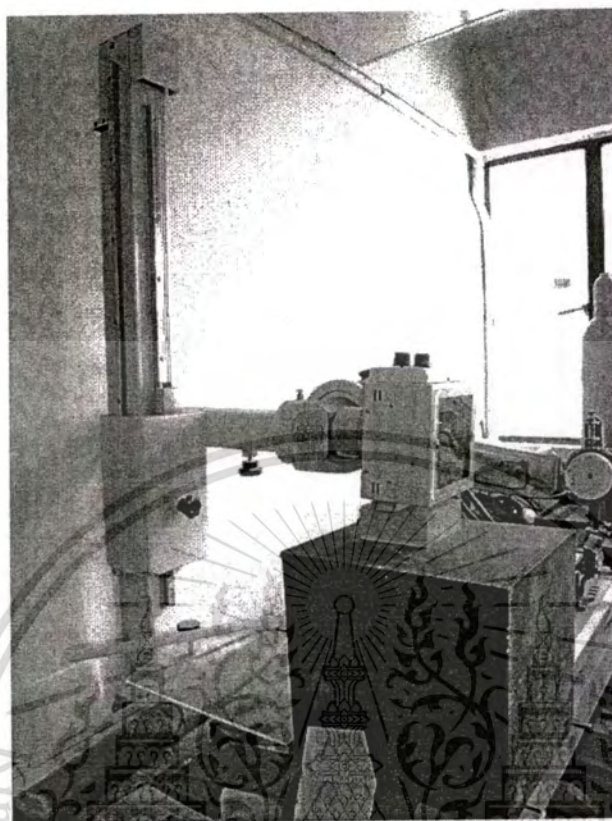


Fig. A11 X-ray generator at CU.

This material is reserved for educational use only, not allowed for commercial use.

Forbidden to modify the content, and cite the document when use.

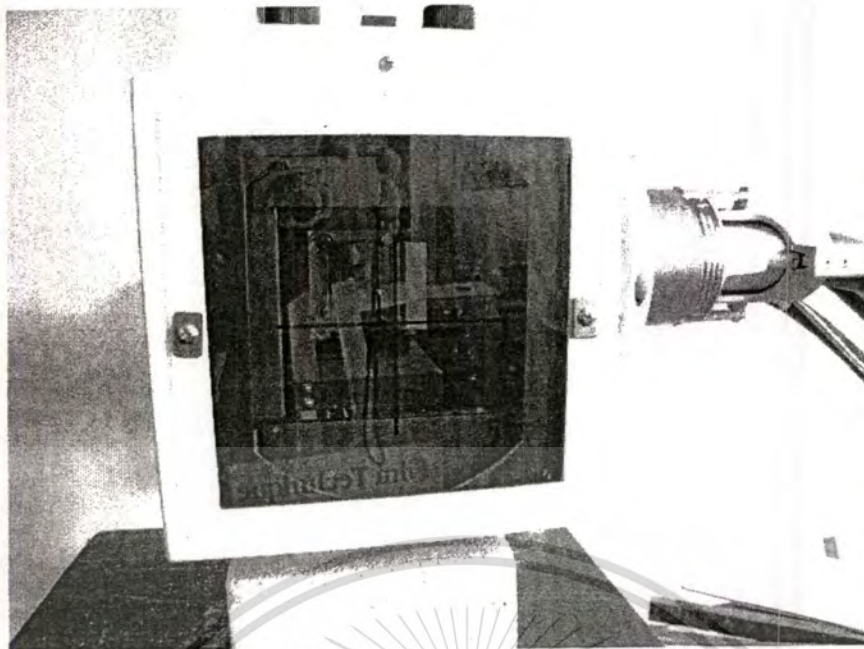


Fig. A12 Point of the device on X-ray generator.

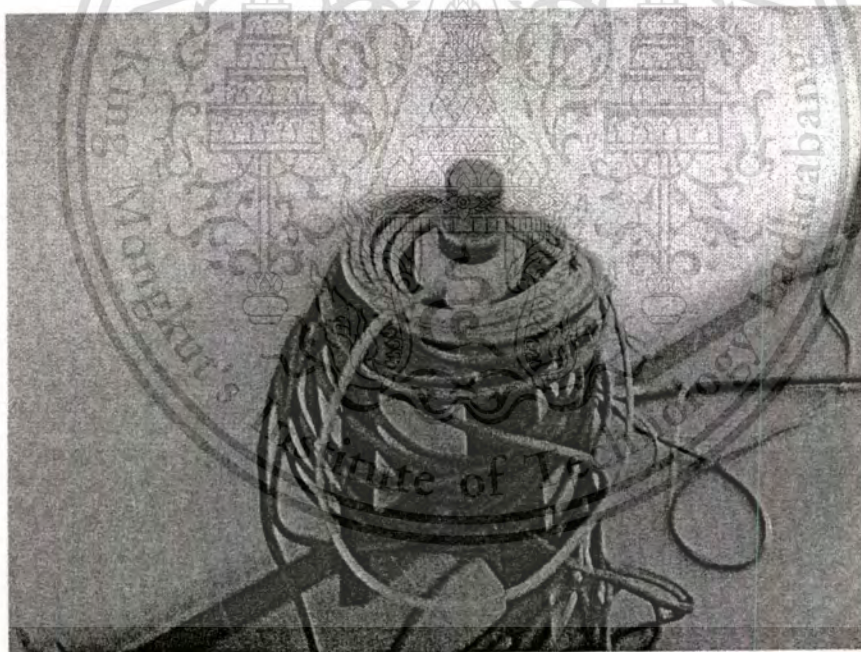


Fig. A13 Aram of X-rays.

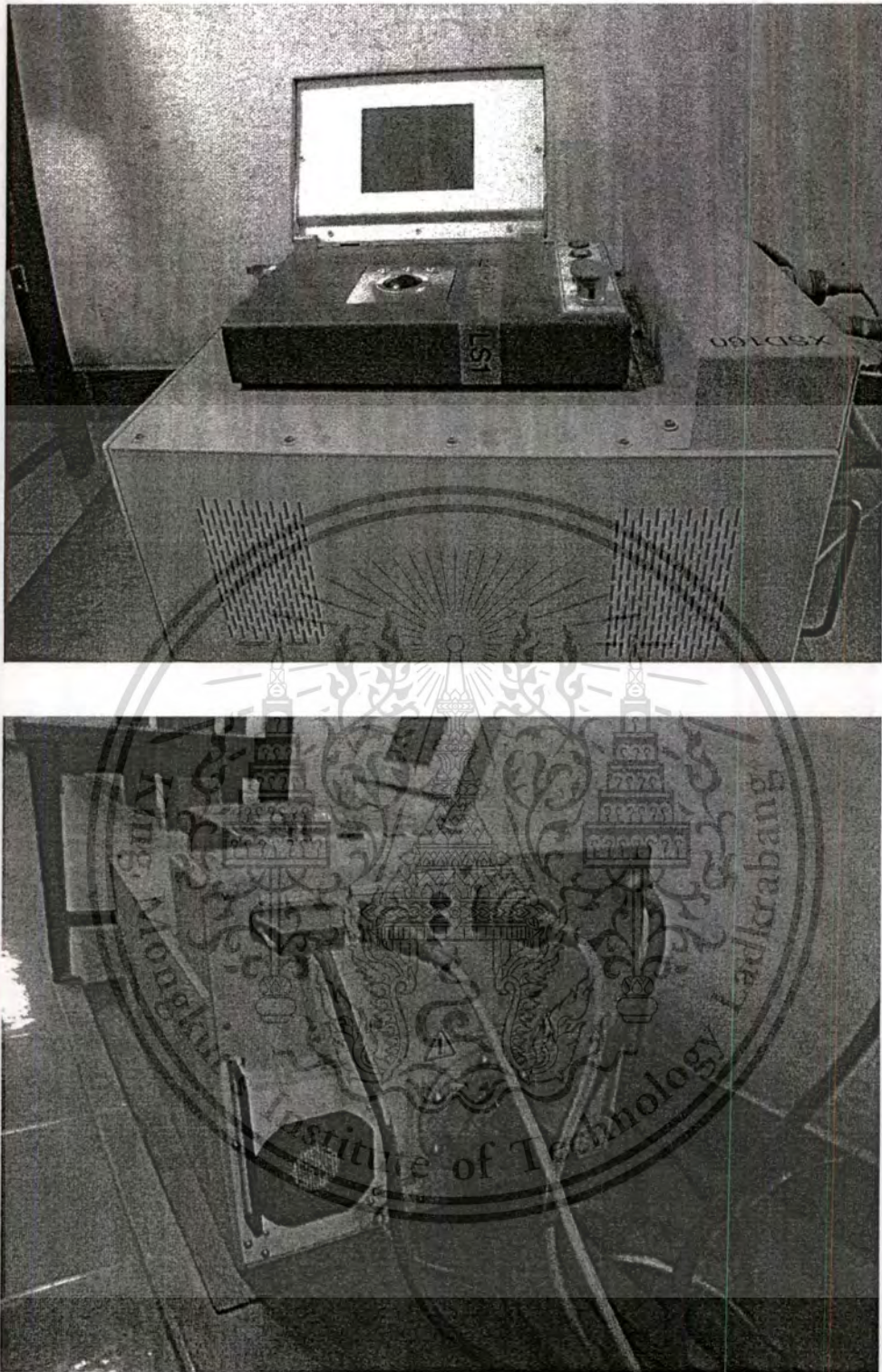


Fig. A14 Control part of X-rays at CU.

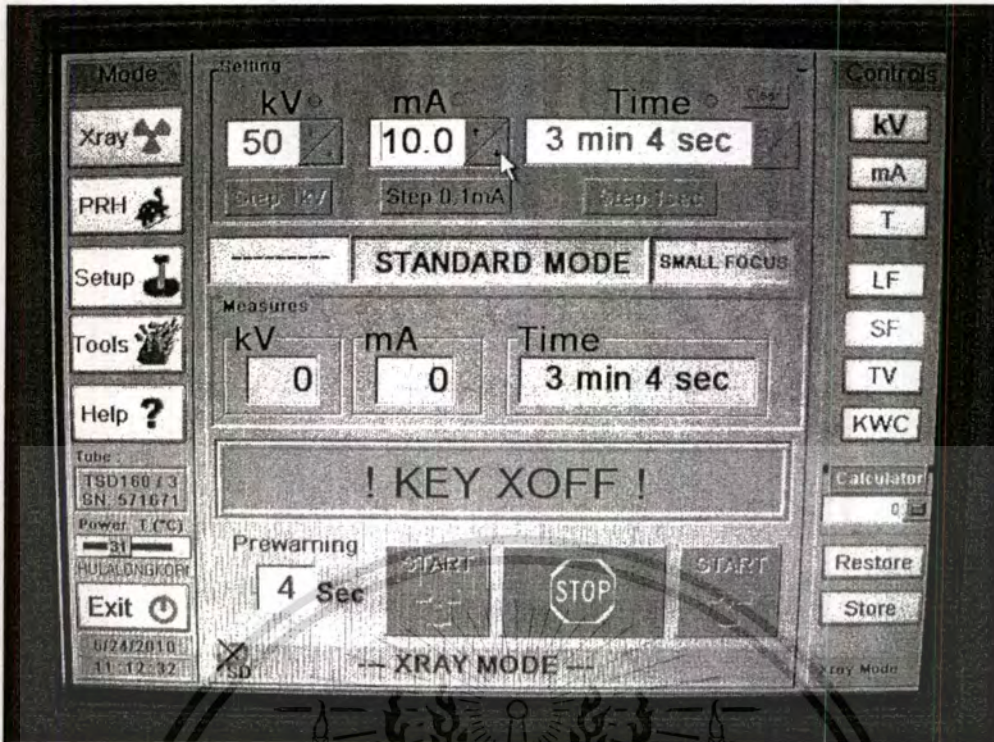


Fig. A15 Screen control of X-rays.

Deep Level Transient Spectroscopy (DLTS) at Mahidol University

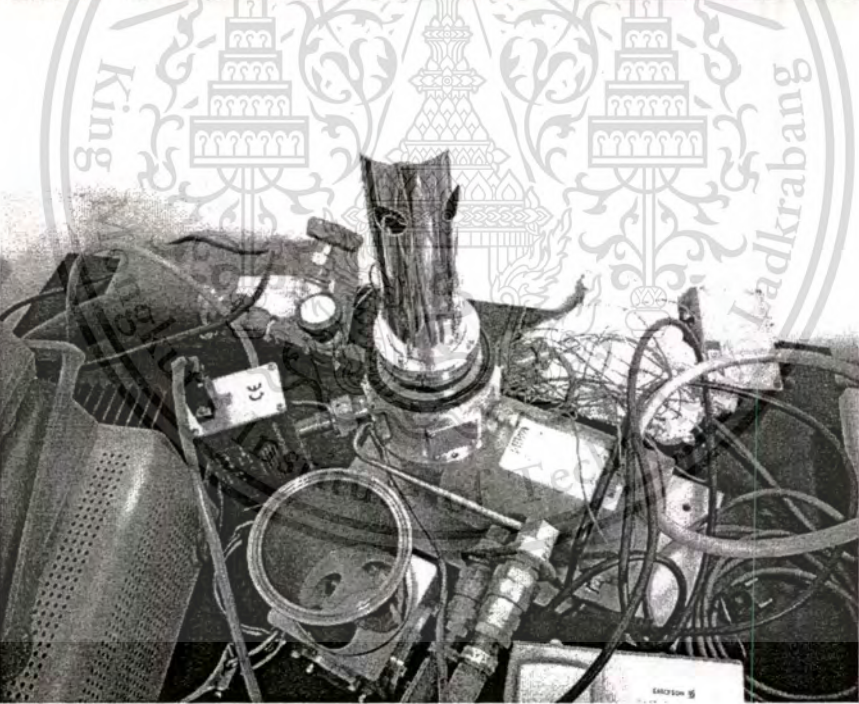


Fig. A16 DLTS systems at MU.

This material is reserved for educational use only, not allowed for commercial use.

Forbidden to modify the content, and cite the document when use.

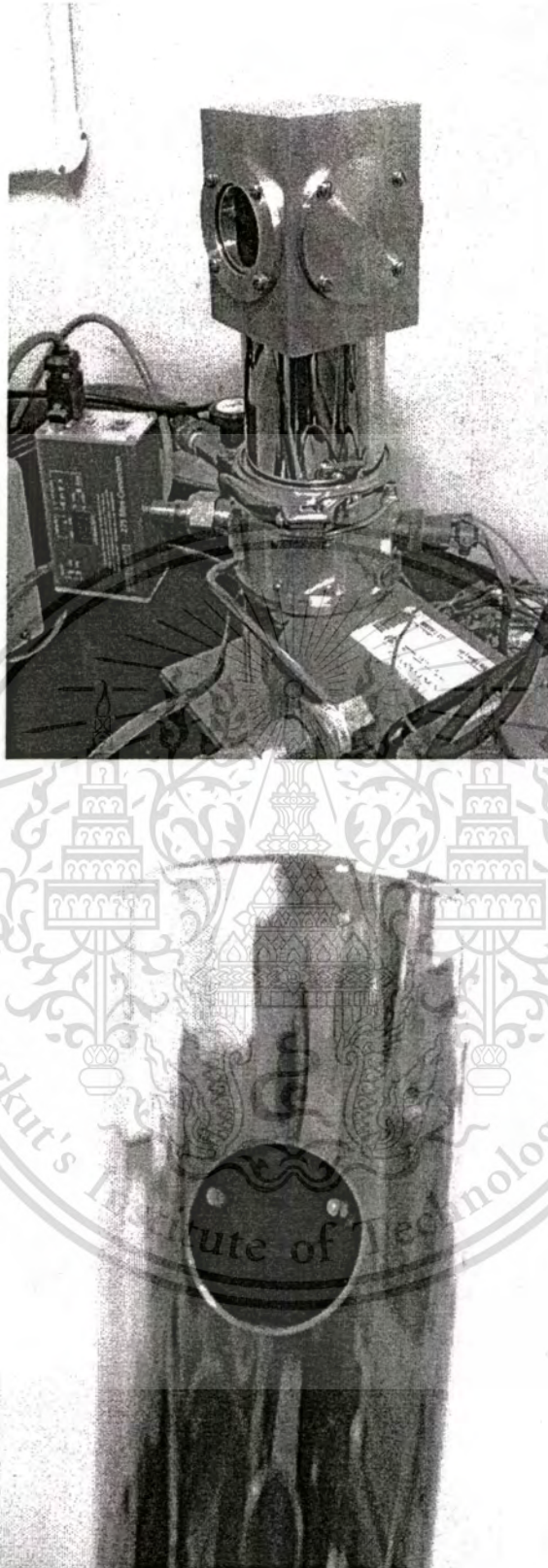


Fig. A17 Vacuum system of DLTS.

This material is reserved for educational use only, not allowed for commercial use.

Forbidden to modify the content, and cite the document when use.

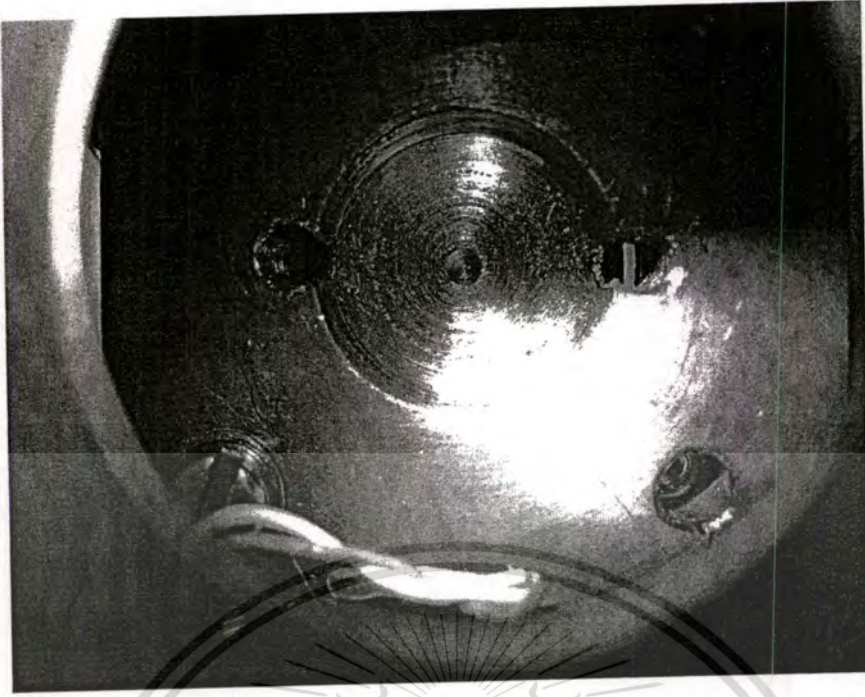


Fig. A17 Vacuum system of DLTS. (Cont.)

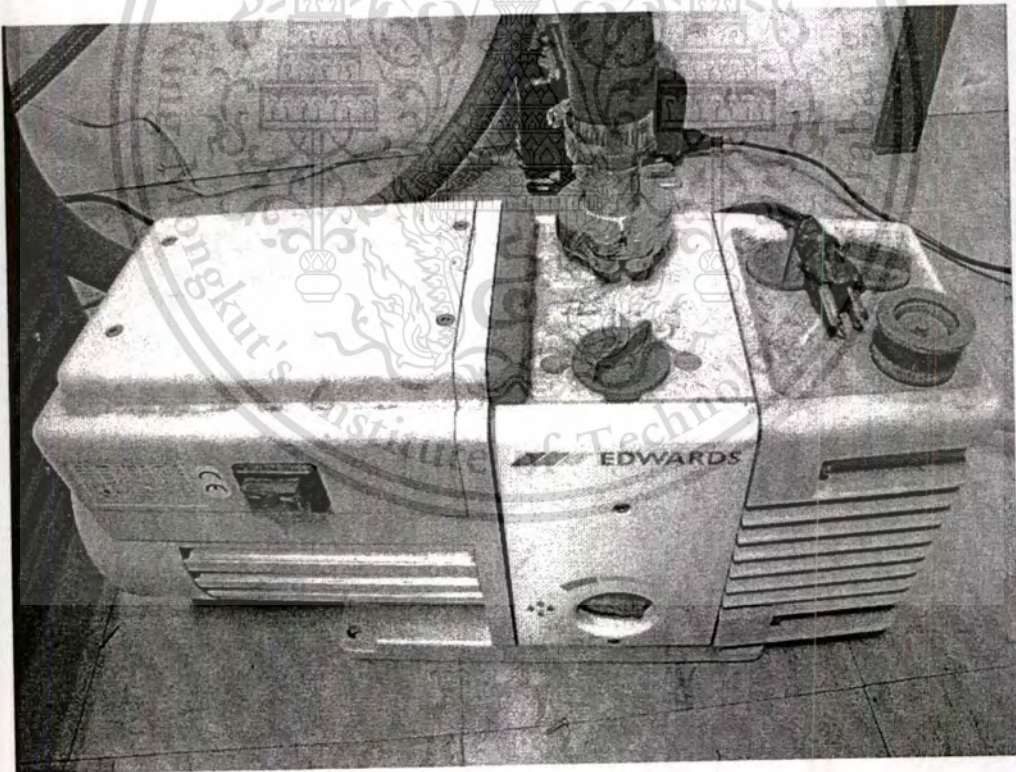


Fig. A18 Turbo pump for use in vacuum system.



CMOS Technology for Device Fabrication at TMEC

Bay 1 at TMEC (Class XX)

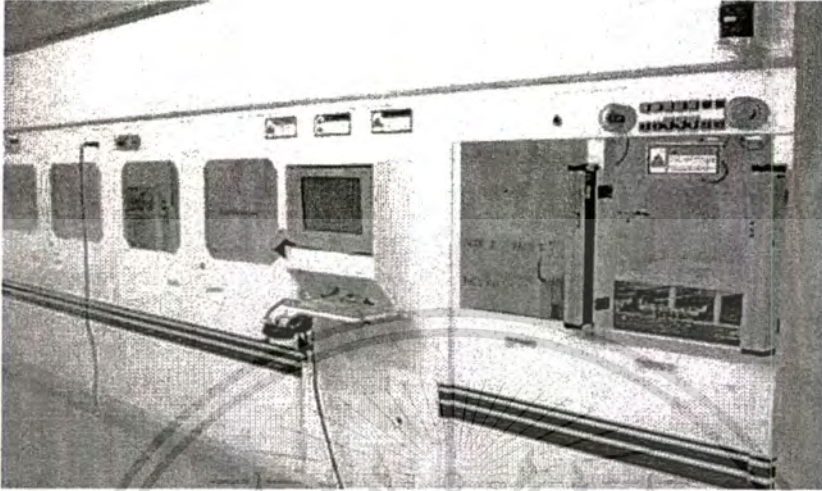


Fig. B1 Automotive wet bench.



Fig. B2 SVG TMX 2604 Diffusion Furnace

This material is reserved for educational use only, not allowed for commercial use.

Forbidden to modify the content, and cite the document when use.

Bay 2 at TMEC (Class XX)

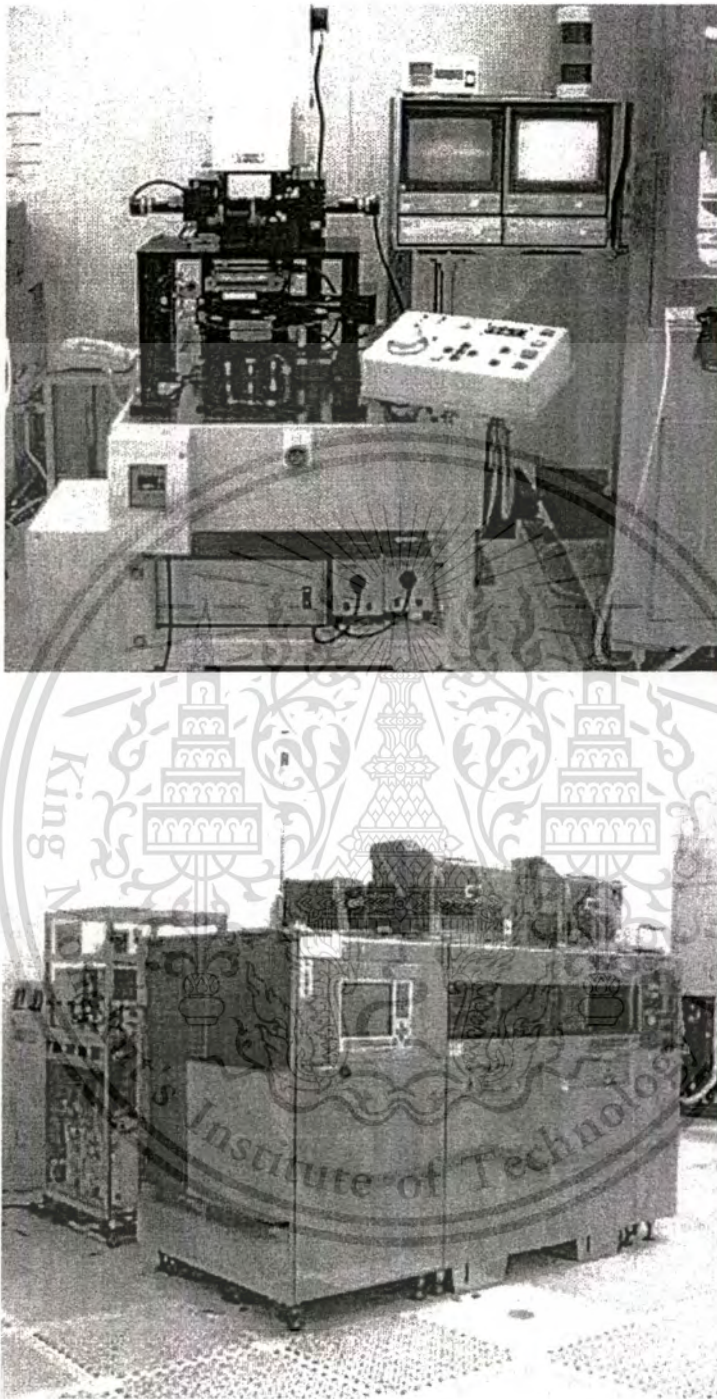


Fig. B3 Mask aligner and PR coating machine.

This material is reserved for educational use only, not allowed for commercial use.

Forbidden to modify the content, and cite the document when use.

Bay 3 at TMEC (Class XX)



Fig. B4 Sputter machine.

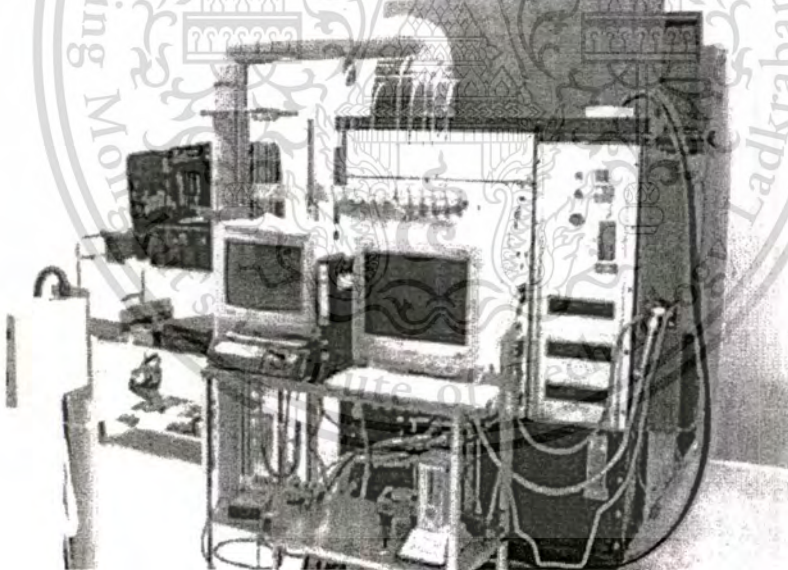


Fig. B5 Mark II Dry Etcher.



This material is reserved for educational use only, not allowed for commercial use.

Forbidden to modify the content, and cite the document when use.



An experimental investigation of P–N diode electrical characteristics by soft X-ray annealing method

Itsara Srithanachai^{a,*}, Surada Ueamanapong^a, Amporn Poyai^b, Surasak Niemcharoen^a, Preecha P. Yupapin^c

^a Department of Electronics Engineering, Faculty of Engineering, King Mongkut's Institute of Technology Ladkrabang, Chalongsing Road, Ladkrabang, Bangkok 10520, Thailand

^b Thai Microelectronics Center (TMEC), 51/4 Moo 1, Wang-Takden District, Amphur Muang, Chachoengsao 24000, Thailand

^c Nanoscale Science and Engineering Research Alliance (NSERA), Faculty of Science, King Mongkut's Institute of Technology Ladkrabang, Bangkok 10520, Thailand

ARTICLE INFO

Article history:
Received 3 June 2011
Received in revised form 7 September 2011
Accepted 13 September 2011
Available online 28 September 2011

Keywords:
P–N junction diodes
Soft X-ray annealing
Series resistance
Ideality factor

ABSTRACT

We present new experimental results for the electrical behaviors of P–N junction diodes irradiated by X-rays. The current–voltage (I – V) characteristics of the P–N junction diodes were measured at room temperature. The reverse and forward current before and after irradiation can be explained relative to the following parameters: carrier generation lifetime (τ_g), ideality factor (n), series resistance (R_s), and sheet resistance (ρ). After irradiation at 40 and 55 keV, a small increment in the diode leakage current was seen, while at 70 keV of exposure, the leakage current was slightly decreased. On the other hand, the forward current was dramatically increased by about three orders of magnitude. In addition, the series resistance of the diodes was confirmed to be positively modified by the use of the soft X-ray annealing method.

© 2011 Elsevier Ltd. All rights reserved.

1. Introduction

P–N junction diodes are important devices widely used in many applications including measurement [1], communication [2], security [3] and photodiode [4]. P–N junction diodes are widely used for detecting the photo spectrum because they exhibit high performance for detection in a wide spectrum range with cut off wavelengths ranging from UV to far-IR [5,6]. To further improve these properties, many researchers have worked to improve the performance of P–N junction diodes, where generally a good diode should have a low leakage current and a high forward current. In this work, the tested diodes were fabricated by the Microelectronic Center (TMEC), Thailand, in which the underperformance diodes, especially, the high leakage and low forward current were chosen as targets to investigate. Commonly, the leakage current of a P–N junction diode is one of the main parameters that affect the device performance where the leakage current is caused by defects which exist in the semiconductor bulk [7,8]. Many research projects have already been undertaken to improve diode performance, for instance, using proton, neutron and electron irradiation on the diodes [9–11]. In this work, the general diode is designed for X-ray irradiation effect, where the electrical characteristics are the

objective of study. Results obtained have shown that the diodes after X-ray irradiation have low leakage current and high forward current for the reversed and forward biased voltages, respectively. Therefore, this concept can be used for improving the performance of photodiode because a good photodiode should have low leakage and high forward currents. We have investigated the effect of the electrical characteristics of P–N junction diodes compared before and after irradiation by X-ray annealing. In this study, the designed diode is used for soft X-ray annealing. Therefore, this structure may not be appropriate for P–N junction diodes characteristic investigations. From our system, the soft X-ray annealing cost is 3 times less than the thermal annealing cost. The measured decrease in the leakage current and dramatic increase in the forward current could provide a significant benefit for future applications.

2. Experimental arrangement

The processing of the shallow P–N junction diodes was done using CMOS technology by the Thai Microelectronics Center (TMEC), Thailand. The P–N junction diodes were fabricated using an n -type (P doped) single crystal silicon wafer with a (111) surface orientation, 650 μm thick and 120–135 Ωcm resistivity. The wafer was cleaned with an ultra-sonic wash to remove organic contaminants. The diode process module consists of (i) the deposition of the oxide covered substrate and the dry-etching of the active area,

* Corresponding author. Tel.: +66 81173 2050.
E-mail address: srithanachai@gmail.com (I. Srithanachai).

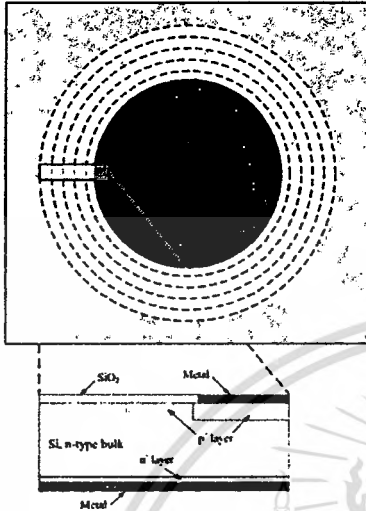


Fig. 1. Structure of the multi-ring gated diode devices used in the study. The bottom picture is zooming on the cross section in the marked region.

Table 1
Dose of X-ray irradiation on P-N junction diodes.

Group 1: 40 keV		Group 2: 55 keV		Group 3: 70 keV	
Number	Dose (roentgen)	Number	Dose (roentgen)	Number	Dose (roentgen)
Device#1	0	Device#1	0	Device#1	0
Device#2	7.0E+04	Device#5	4.5E+05	Device#8	4.9E+06
Device#3	7.8E+05	Device#6	5.3E+06	Device#9	5.4E+07
Device#4	2.9E+06	Device#7	1.9E+07	Device#10	2.0E+08

(ii) the implantation of phosphorus at an energy of 120 keV and dosage of $1 \times 10^{16} \text{ cm}^{-2}$ for ohmic contact on the backside wafer, (iii) the implantation of boron at the same energy, (iv) dose on front side wafer, where the implantation was followed by a thermal annealing at 1050 °C for 60 min, resulting in a junction depth of about 1 μm and (v) the Al metal-deposition, 1 μm thick [12,13], on both the front and back sides [14]. After that the wafer was transferred to the sawing process. Finally, the fully assembled chip was installed onto a prototype circuit board (PCB) before the finishing connections were made, as is shown in Fig. 1.

The diodes were irradiated by X-ray for various energies and exposure dosages, as shown in Table 1. The current-voltage (*I-V*) measurement was then performed using a HP4156B. The *I-V* characteristic results were measured on the wafer with a bias step of 25 mV from the reverse (V_R) to forward (V_F) voltage, in the range of -10 to $+1$ V.

3. Result and discussion

Fig. 2 shows the experimental semi-log forward and reverse-bias characteristics of the P-N junction diodes. The diode parameters were determined from the *I-V* characteristics, which are usually described using the thermionic emission theory.

$$I = I_0 \exp(qV/nkT) \tag{1}$$

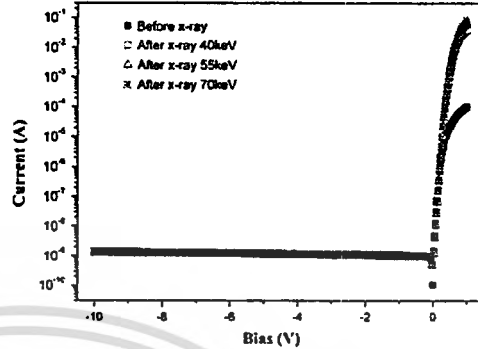


Fig. 2. The forward and reverse bias current vs voltage characteristics of the P-N junction diodes.

Here *I* is the current, *q* is the electron charge, *V* the applied voltage, *T* the absolute temperature, *k* the Boltzmann constant, *n* the ideality factor of P-N junction diodes, and *I*₀ is the saturation current. For values of *V* greater than nkT/q , the ideality factor from Eq. (1) can be written as described in [15,16] by

$$n = (q/kT) [dV/d \ln I] \tag{2}$$

Also the voltage dependent ideality factor *n(V)* can be written using Eq. (2) as

$$n(V) = qV/kT \ln(I/I_0) \tag{3}$$

From Eq. (1) *I*₀ is the saturation current. The saturation current under the reverse bias is the combination of the diffusion current (*I*_d) and the generation current (*I*_g) that are generated in the depletion region, as presented in Eq. (4).

$$I_0 = I_d + Aq n_i W / \tau_g \tag{4}$$

Here *n*_i is the intrinsic carrier concentration, τ_g is the carrier generation lifetime, and *W* is the depletion width. The carrier generation lifetime is given by Eq. (5).

$$\tau_g = Aq n_i W / (I_0 - I_d) \tag{5}$$

Fig. 3 shows the *I-V* characteristics of the diodes with different doses, where the leakage current versus voltage before and after X-ray irradiation at 40 keV and 55 keV slightly increases with the increasing dose [17]. This result clearly shows the impact of the X-ray irradiation at a higher reverse bias in the case of the 70 keV exposed energy, where the leakage current after exposure is slightly decreased. The change in the leakage current depends on the carrier generation lifetime. The carrier generation lifetime can be calculated using Eq. (5), which is changed after irradiated by X-ray. In our former work, a longer operation lifetime was achieved for lower dose operation. This can also be due to defects annealed by the X-ray. The prolonging diode lifetime, the longer exposure after a typical sensing operation may be a concern.

The experimental semi-log forward bias characteristics of the P-N junction diodes are shown in Fig. 4. From this figure the forward current after irradiation is increased about three orders of magnitude. This was especially apparent when the analyzed reverse and forward current at 70 keV showed the lower leakage and higher forward current. The obtained result shows that a 70 keV exposure has an excellent performance on improving the

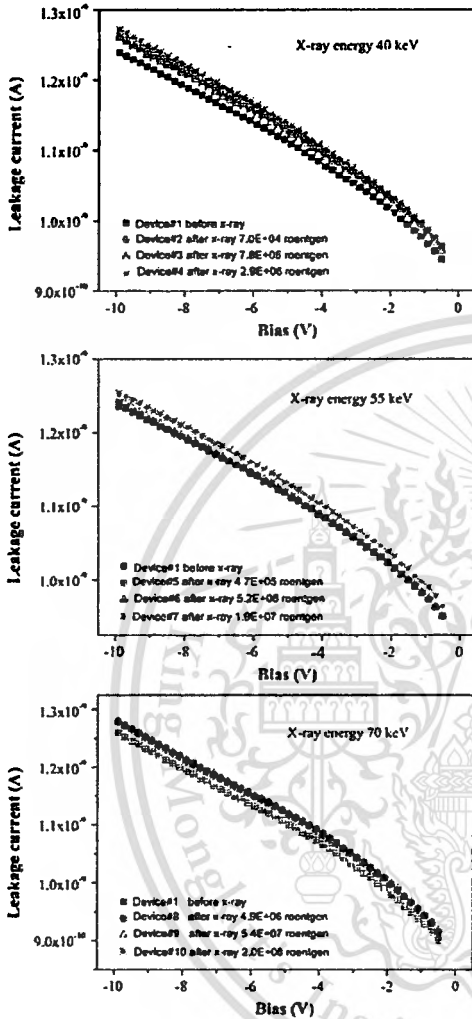


Fig. 3. Leakage current of diode before and after irradiated with various energy and exposure dose.

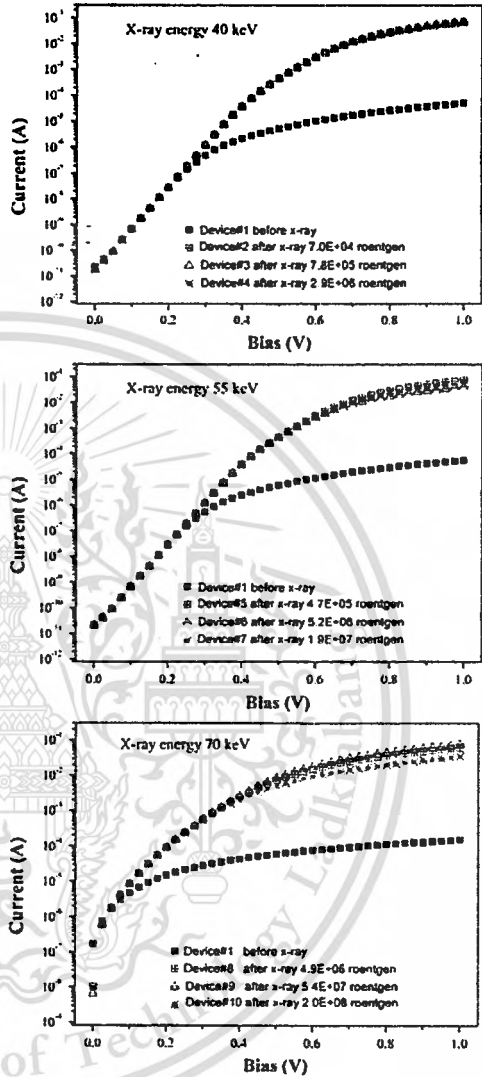


Fig. 4. Forward *I*-*V* characteristics of the P-N junction diodes for different energies and doses.

diode characteristics. This result is very promising for further investigation.

The change in the forward current seems to be caused by a series resistance reduction that affected the ideality factor of the diode. The effect of the series resistance is usually modeled with series combination of a diode and resistor, R_s , in which the voltage V_d across the diode can be expressed in terms of the total voltage drop V across the diode and the resistance R_s . Thus, $V_d = V - IR_s$ and Eq. (1) can be expressed as

$$I = I_0 \exp(q(V - IR_s)/nkT) \tag{6}$$

By rewriting Eq. (6) using the Chung's method this equation can be presented as in Eq. (7) [18]

$$dV/d\ln(I) = IR_s + nkT/q \tag{7}$$

Eq. (7) predicts a straight line for the data of the downward curvature region of the forward bias *I*-*V* characteristics. The slope and *y*-axis intercept of a plot $dV/d\ln(I)$ versus *I* will give R_s and nkT/q , respectively.

Table 2
Series resistance of P–N junction diodes various dose at 70 keV.

Dose (roentgen)	Series resistance (Ω)
Before = 0	9640
$4.9E+06$	4.4
$5.4E+07$	3.3
$2.0E+08$	5

Table 3
Sheet resistance of P–N junction diodes before and after exposure by X-ray.

	Front metal ($m\Omega/\square$)	Boron doped region (Ω/\square)	Silicon bulk (Ω/\square)	Back contact ($m\Omega/\square$)
Before	59	12.15	2232	55
After	58	12.11	2187	53

From $dV/d\ln(I)$ vs I plots, the series resistance is shown in Table 2. Therefore, using this model, the results show a dramatic reduction in the overall parasitic series resistance from several $k\Omega$ to a few Ω when the diode has been irradiated by X-rays. The series resistance of P–N junction diodes can possibly be divided into 4 parts which they are front metal contact, boron doped region, silicon bulk, and back contact. The individual sheet resistivity measurement has also been performed using the 4-point probe technique on each part.

The sheet resistances of the 4 parts, before and after exposure by X-rays are shown in Table 3, where the front metal, boron doped region, silicon bulk and back contact were separately fabricated. There are no significant changes in the sheet resistance of metal contact and boron dope region. This implies that there is permanent modification of the base materials by the X-ray irradiation. Therefore, this confirms that the X-ray irradiation has mainly influenced the silicon bulk condition. The sheet resistance of metal or aluminum contact data before and after soft X-ray irradiation is given in Table 3, where the sheet resistance of metal is a little changed after irradiation. Results show that soft X-ray irradiation is not an effect of the metal contacts. In the case of surface/interface oxide this can be explained by the capacitance–voltage (C–V) characteristics, in which the capacitances of P–N junction diode are not changed after irradiation as shown in Fig. 5, which means that the soft X-ray irradiation is not the effect of interface oxide. Moreover, the ideality factor is calculated using the same model, the average value is 1.13, which approaches to the ideal diode performance. These results show the benefit of X-ray irradiation as the post-fabrication soft annealing process to cure high parasitic resistance of our low grade P–N junction diodes with the minimum cost and effort. In addition, the optimized condition of the X-ray irradiation may still be improved, where the evidence or mechanism of silicon bulk modification by the X-ray is required to study in details.

4. Conclusion

The X-ray irradiation effects on the current–voltage characteristics of TMEC P–N junction diodes have been investigated and discussed. In the reverse bias regime, leakage currents of 40 and 55 keV were slightly increased, while, the leakage current was found to decrease with 70 keV of exposure. In the forward bias regime, the forward current was increased about 3 orders of magnitude because of a dramatic reduction in the series resistance calculated by the standard model (from several $k\Omega$ to a few

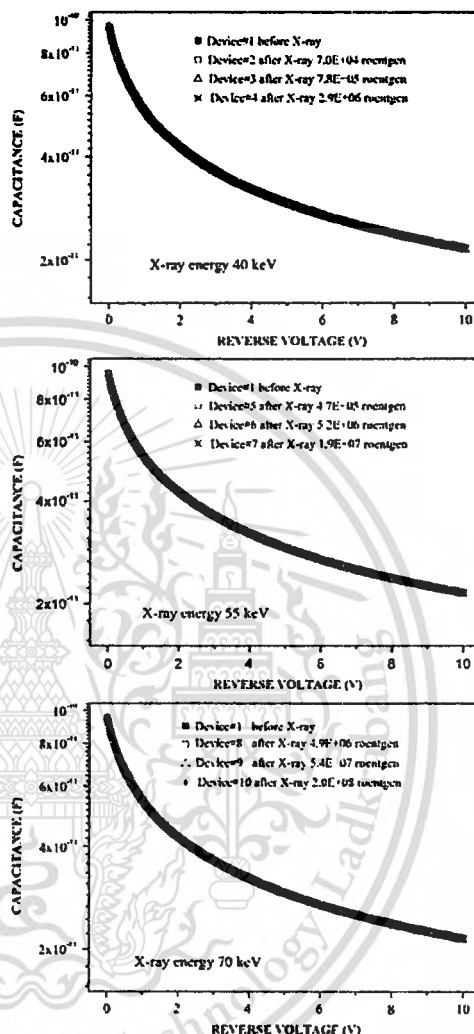


Fig. 5. Capacitance–voltage characteristics of P–N junction diode before and after X-ray irradiation.

Ω). The ideality factor of the after exposed diode can be calculated and has a value around 1.13, which confirms that these diodes approached the ideal diode performance. These results show that this is a promising method for manufacturing yield improvement with a minimum added cost and effort. In this experiment, both front and back sides were irradiated, in which the same electrical characteristics is obtained. Using the X-ray method, there is no silicon atom escaped from the lattice. On the other hand, this energy is sufficient to destroy the defect complexes in a semiconductor, in which the impurity atoms in these complexes can become electrically active.

Acknowledgment

The authors would like to acknowledge King Mongkut's University of Technology North Bangkok and Thai Microelectronics Center (TMEC) for fabrication and testing facilities, National Electronics and Computer Technology Center, Thailand and Thailand Graduate Institute of Science and Technology (TGIST) under scholarship number TG-44-22-53-014D.

References

- [1] Asensio LJ, Carvajal MA, Lopez-Villanueva JA, Viches M, Lallena AM, Palma AJ. Evaluation of a low-cost commercial mosfet as radiation dosimeter. *Sensors and Actuators A* 2006;125:288–95.
- [2] Matsumoto Yoshinori, Nakazono Akimichi, Kitahara Taisuke, Kuitze Yasuhiro. High efficiency optical coupler for a small photo acceptance area photodiode used in the high speed plastic optical fiber communication. *Sensors and Actuators A: Physical* 2002;97–98:318–22.
- [3] Asaduzzaman K, Nazrul Islam M, Shajjarmal M, Hoq Mahbubul. Infrared Security Alarming System. *Asian Journal of Information Technology* 2010;9 (4):243–7.
- [4] Kulsenskov DV, Temkin H, Oslinsky A, Gaska R, Khan MA. Low-frequency noise and performance of GaN P–N junction photodetectors. *Journal of Applied Physics* 1997;97:759–62.
- [5] Budianu E, Purica M, Iacomi F, Baban C, Prepelita P, Manea E. Silicon metal-semiconductor-metal photodetector with zinc oxide transparent conducting electrodes. *Thin Solid Films* 2008;516:1629–33.
- [6] Mao RW, Tsai CS, Yu JZ, Wang QM. Narrow line-width resonant cavity enhanced photodetectors operating at 1.55 μm . *Optics Communications* 2008;281:1582–7.
- [7] Hayama K, Ohyama H, Simoen E, Claeys C, Poyai A, Miura T, Kobayashi K. Radiation defects in STI silicon diodes and their effects on device performance. *Physica B* 2001;308–310:1217–21.
- [8] Poyai A, Simoen E, Claeys C, Czerwinski A. Silicon substrate effects on the current-voltage characteristics of advanced P–N junction diodes. *Materials Science and Engineering* 2000;873:191–6.
- [9] Ohyama H, Hayama K, Takakura K, Miura T, Shigaki K, Jono T, Simoen E, Poyai A, Claeys C. Irradiation temperature dependence of radiation damage in STI Si diodes. *Microelectronic Engineering* 2003;66:517–21.
- [10] Ohyama H, Nagano T, Takakura K, Motoki M, Matsuo K, Nakamura H, Sawada M, Midorikawa, Kuboyama S, Gonzalez MB, Simoen E, Claeys C. Effects of electron and proton irradiation on embedded SiGe source/drain diodes. *Materials Science in Semiconductor Processing* 2008;11:310–3.
- [11] Ohyama H, Takakura K, Shigaki K, Kuboyama S, Matsuda S, Simoen E, Claeys C. Radiation damage of Si photodiodes by high-temperature irradiation. *Microelectronic Engineering* 2003;66:536–41.
- [12] Ohyama H, Hirao T, Simoen E, Claeys C, Onoda S, Takami Y, Itoh H. Impact of lattice defects on the performance degradation of Si photodiodes by high-temperature gamma and electron irradiation. *Physica B* 2001;308–310:1226–9.
- [13] Ohyama H, Simoen E, Claeys C, Takakura K, Matsuo K, Jono T, Uemura J, Kishikawa T. Radiation damage in Si photodiodes by high-temperature irradiation. *Physica E* 2003;16:533–8.
- [14] Rajanapich Poopoi, Poyai Amporn, Srithanachai Itsara, Pengpad Potapon, Hruanan Charndet, Sophitpan Suwat, Ueamarnpong Surada, Titiroongruang Worrathul, Titiroongruang Wisut. Activation energy analysis of P–N junction X-ray direct detector. *ITC-CSCC* 2010:257–60.
- [15] Keffous A, Slad M, Mamma S, Belkacem Y, Lakhdar Chasouch C, Menari H, Dahmani A, Chergui W. Effect of series resistance on the performance of high resistivity silicon Schottky diode. *Applied Surface Science* 2003;218:336–42.
- [16] Sahin B, erin HC, Ayyildiz E. The effect of series resistance on capacitance-voltage characteristics of Schottky barrier diodes. *Solid State Communications* 2005;135:490–5.
- [17] Ohyama H, Kobayashi K, Vanhellefont J, Simoen E, Claeys C, Takakura K, Hirao T, Onoda S. Induced lattice defects in InGaAs photodiodes by high-temperature electron irradiation. *Physica B* 2003;340–342:337–40.
- [18] Cheung SK, Cheung NW. Extraction of Schottky diode parameters from forward current-voltage characteristics. *Applied Physical Letters* 1986;49:85.



Advanced Materials Research Vols. 378-379 (2012) pp 606-609
 Online available since 2011/Oct/27 at www.scientific.net
 © (2012) Trans Tech Publications, Switzerland
 doi:10.4028/www.scientific.net/AMR.378-379.606

New Method for Improving the Electrical Characteristics of P-N Junction Diode

Itsara Srithanachai¹, Surada Ueamanapong¹, Amporn Poyai²,
 Surasak Niemcharoen¹

¹Department of Electronics, Faculty of Engineering, King Mongkut's Institute of Technology
 Ladkrabang, Bangkok 10520, Thailand

²Thai Microelectronics Center (TMEC), Chachoengsao24000, Thailand
 srithanachai@gmail.com

Keywords: Soft X-ray annealing, series resistance, silicon bulk

Abstract. This paper investigates the effect of soft X-ray irradiation various energy and times on P-N junction diodes. X-ray energy irradiated on P-N junction diode with 55 and 70 keV with various time in the range 5-50 sec. After irradiations were study on the current-voltage (I-V) characteristics and capacitance-voltage (C-V) characteristics. Leakages current after irradiated by X-ray are not change, while forward current are increase about 3 orders. The change of current-voltage characteristics can analyze by many parameter such as carrier lifetime and series resistance. Capacitance-voltage characteristics after irradiation are not change. The results show that soft X-ray technique can be improving performance of the P-N junction diodes. These techniques are importance to use for improving device performance in industry work.

Introduction

Nowadays, the P-N junction diodes are widely use in many works such as power device [1], electronics [2], medical [3] and telecommunication [4]. General, the characteristics of P-N diode have low leakage current and high forward current. In the present, diode is low performance (high leakage current and low forward current) because the problem in fabrication process such as high ion implantation. Ion implantation is the cause to induce defect in silicon bulk. High-energy particles may produce at least two different types of effects in semiconductor devices, i.e., ionization damage and displacement damage. Initial ionization damage creates free electron-hole pairs in the SiO₂ layer by disrupting electronic bonds, which can cause either transient or long-term ionization damage. On important transient ionization degradation mechanism is the Single Event Upset (SEU). It corresponds to a single high-energy particle striking a critical node of the device, leaving behind an ionized track passing through the well area or storage capacitor. The defects are removing by thermal annealing, while this technique have the effect to junction depth, uses a long time and high temperature. In this paper investigate new technique for remove defect in silicon bulk. Soft X-ray annealing is the new technique for improve performance of the diode. This technique is not widely use because it has a little research to study the effect of X-ray irradiation in mechanism of diode. Soft X-ray annealing are use shot time, low temperature and don't effect to junction depth. The aim of this paper is to investigate a detailed characterization of radiation defects in P-N junction diode by the irradiation with X-ray [5-7].

All rights reserved. No part of contents of this paper may be reproduced or transmitted in any form or by any means without the written permission of TTP.
www.ttp.net. (ID: 161.246.254.166-23/11/11,03:19:38)

Experimental

The process flow of shallow P-N junction diode is compatible with CMOS technology on Thai Microelectronics Center (TMEC). (iii) implantation of phosphorus at energy of 120 kV and dose of $1 \times 10^{16} \text{ cm}^{-2}$ for ohmic contact on backside wafers, (iv) implantation of boron at same energy and dose on front side wafers (the implantation been followed by a thermal annealing at 1050 °C for 60 min, resulting in a junction depth of about 1 μm) (v) Al metal-deposition, 10 μm thick, on front side and backside [8], the fabrication process shows in Fig. 1.

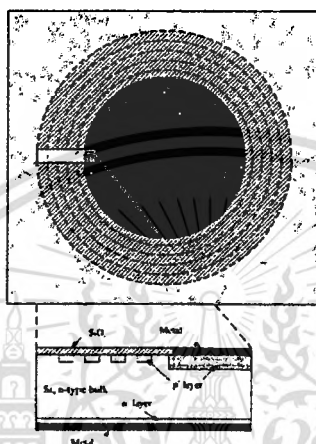


Fig. 1 Structure of P-N junction diode.

After its fabrication process, the diodes were irradiated by X-ray for energy 55 and 70 keV with various time with 5-50 sec. The semiconductor parameter analysis of model HP4156B was used to measure electrical properties of diode, before and after irradiation. The current-voltage (I-V) characteristics of the P-N diode were measured at room temperature to examine the change of the dark current (I_D) by X-ray irradiation. The current-voltage (I-V) characteristics were measured on wafer with bias step of 25 mV for both reverse (V_R) and forward (V_F) voltage, sweeping in the range of -10 to +1 V. Capacitance-voltage (C-V) measurements were performed on the same diode at a frequency of 100 kHz [9].

Results and discussion

Fig. 2 shows the experimental semi-log forward and reverse-bias characteristics of the P-N diode. The diode parameters are determined from the I-V characteristics, which is usually described by the thermionic emission theory.

$$I = I_0 \exp(qV/nkT) \quad (1)$$

Here I is the current, q is the electron charge, V the applied voltage, T the absolute temperature, k the Boltzmann constant, n the ideality factor of P-N diode, and I_0 is the saturation current. From values of V greater than nkT/q [10].

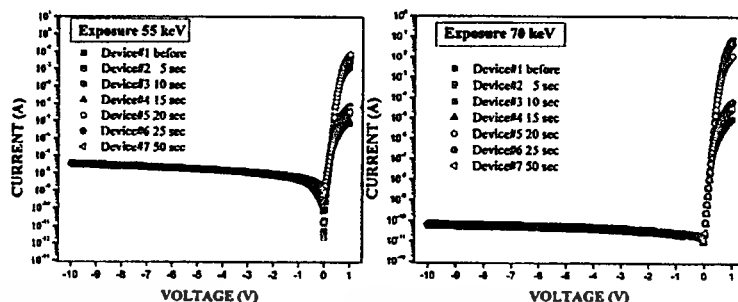


Fig. 2 I-V characteristics of diode before and after soft X-ray annealing.

From the picture leakage current compare before and after are not change, while forward current after irradiation are increase. Therefore, soft X-ray annealing technique is improving the diode performance in part of forward current.

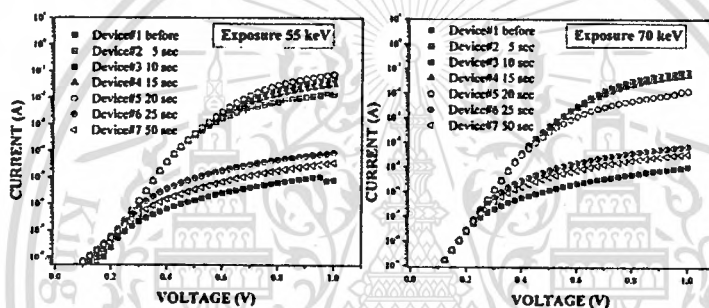


Fig. 3 Semi-log forward current of the diode irradiation by X-ray.

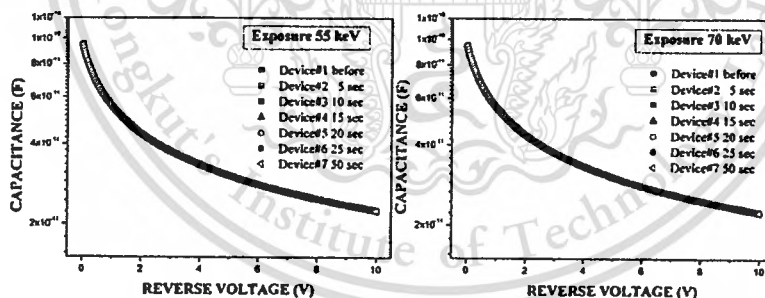


Fig. 4 Semi-log capacitance-voltage characteristics before and after X-ray irradiation.

The forward currents of diode after irradiation by X-ray are shown in Fig. 3. After irradiation with 5-20 sec for 55 and 70 keV the forward current are increases about 3 orders, while 25 and 50 sec are increases about 1 order. The change of forward current are many causes such as series resistance are decrease and X-ray remove trapping centre in silicon bulk and surface [11]. The capacitances after irradiation were not change because X-ray are not effect to junction depth of the device.

Conclusions

Soft X-ray annealing increases the diode performance. Forward current increases after irradiation with 55 and 70 keV. These results do not unambiguously point to a mechanism for the increase observed in the forward current of a silicon P-N-junction after prolonged X-ray irradiation. The identification of this mechanism requires further study. Nevertheless, the very fact that stable increases are observed in the forward currents seems noteworthy and may find application as a method for improving the characteristics of silicon diodes.

Acknowledgment

The authors would like to thank King Mongkut's University of Technology North Bangkok (KMITNB) for providing the X-ray exposure equipment for this experiment, Thai Microelectronics Center (TMEC) for fabrication P-N junction diode, National Electronics and Computer Technology Center, Thailand and Thailand Graduate Institute of Science and Technology (TGIST).

References

- [1] P. Hazdra, J. Vobeck: *Mater Sci Eng B* Vol. 124–125 (2005), p. 275–279.
- [2] Yoshinori Matsumoto, Akimichi Nakazono, Taisuke Kitahara, Yasuhiro Koike: *Sensors and Actuators A: Physical* Vol. 97-98 (2002), p. 318-322.
- [3] Bogushevich SE, Ugolev II: *Appl Radiat Isot* Vol. 52(5) (2000), p. 1217-9.
- [4] L.J. Asensio, M.A. Carvajal, J.A. Lopez-Villanueva, M. Vilches, A.M. Lallena, A.J. Palma: *Sensors and Actuators A* Vol. 125 (2006), p. 288–295.
- [5] P. Hazdra, H. Dorschner: *Nucl. Instr. and Meth. B* Vol. 201 (2003), p. 513.
- [6] M. A. Krivov, S. V. Malyanov, L. S. Smirnov: *Izv. Vuzov. Fizika*. Vol. 8 (1968), p. 1027.
- [7] M. A. Krivov, S. V. Malyanov, V. I. Gaman: *Izv. Vuzov. Fizika*. Vol. 1 (1967), p. 99.
- [8] A. Poyai and C. Claeys: *Appl. Phys. Lett.* Vol. 80 (2002), p. 1192.
- [9] A. Poyai, E. Simoen, and C. Claeys: *Appl. Phys. Lett.* Vol. 78 (2001), p. 949.
- [10] S. M. Sze: *Physics of Semiconductor Devices*, Published by John Wiley & Sons, Inc., Hoboken, New Jersey, (2007).
- [11] M.A.Krivov, S.V. Malyanov, and V.I.Gaman: *Izv. Vuzov. Fizika*. Vol. 6 (1967), p. 150.

Applied Materials and Electronics Engineering
10.4028/www.scientific.net/AMR.378-379

New Method for Improving the Electrical Characteristics of P-N Junction Diode
10.4028/www.scientific.net/AMR.378-379.606



This material is reserved for educational use only, not allowed for commercial use.

Forbidden to modify the content, and cite the document when use.

ECTI-CON 2011
KHON KAEN UNIVERSITY

8th

Electrical Engineering/ Electronics,
Computer, Telecommunications and
Information Technology (ECTI) Association,
Thailand - Conference 2011

Abstract Collections

Khon Kaen, Thailand

May 17-19, 2011

Pullman Khon Kaen Raja Orchid Hotel

ECTI
Association



**KHON KAEN
UNIVERSITY**



IEEE
THAILAND SESSION

Activation Energy Analysis of X-ray Irradiation on P-N Diode

Itsara Srithanachai and Surasak Niemcharoen

Department of Electronics, Faculty of Engineering, King Mongkut's Institute of Technology Ladkrabang,
 Charongkrung Road, Ladkrabang, Bangkok 10520, Thailand
 Phone: +66-8117-3205-0, Email: srithanachai@gmail.com

Abstract- This paper investigate characteristics of P-N diode before and after irradiated by X-ray at energy ranking about 40, 55 and 70 keV, exposure time 205 second. After irradiated leakage current at 40, 55 and 70 keV were decreased. Therefore, we explain the effect of the X-ray irradiated on diode because it can improve performance of diode. The 4 mm² P-N junctions were fabricated by boron implantation process into phosphorus doped silicon wafer. The results show that the leakage current changes after exposed to the X-ray which indicated that the types of defect have been changed. The changes of these activation energies can be higher or lower than the result before X-ray exposure, which depends on type of defects. However, the results in this paper presented that the defects that caused by X-ray irradiation are manageable.

I. INTRODUCTION

In the present, P-N diode have used in many work. However, performance degradation of diode occurs when using a long time. The degradation of the diode caused by several reasons. Analysis of cause to changes in diode is an interesting topic. When explaining the change of diode, we can fabrication the diode to use in the future are more durable. This will help in reducing the use of resources and the quality of life better. Silicon radiation detectors are used as radiation detectors for the registration and identification of fragment of nuclear reaction in physics experiments. They also fine applications in the nuclear industry when short range particles are to be detected under high gamma-ray background, due to their higher radiation selectivity. In medical works, X-ray detectors are use for scan body of human, and many applications use in security work. In the present, X-ray detectors were degradations after irradiated by X-ray. The defects are generation by X-ray irradiated [1,2]. In this study, the defect are produced by damaging the lattice using high-energy particles to from vacancies and interstitial in the Si wafer. This lattice damage consists of bounce out of S atom from the normal lattice sites or another impurity atom substituted on Si site [3].

II. EXPERIMENTAL

The process flow of shallow P-N junction diode is compatible with CMOS technology on Thai Microelectronics Center (TMEC). The diode process module consists of (i) deposition of oxide covered substrate, (ii) dry-etching of

active area, (iii) implantation of phosphorus at energy of 120 keV and dose of $1 \times 10^{16} \text{ cm}^{-2}$ for ohmic contact on backside wafers, (iv) implantation of boron at same energy and dose on front side wafers (the implantation been followed by a thermal annealing at 1050 °C for 60 min, resulting in a junction depth of about 1 μm), (v) Al metal-deposition,

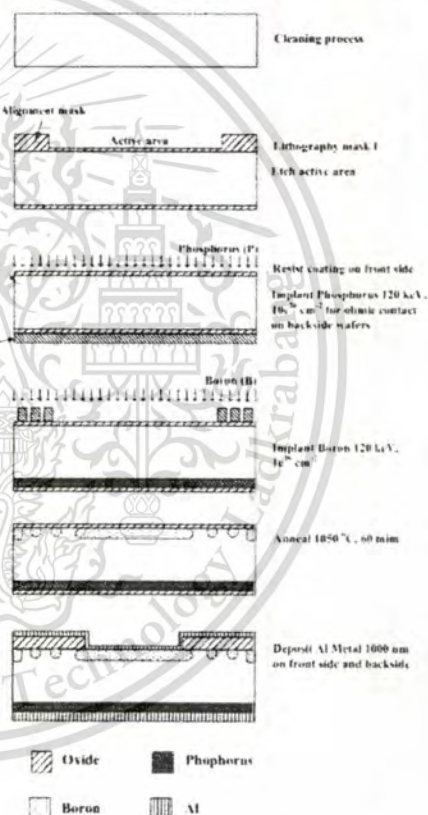


Fig. 1 Flow chart of the fabrication process for P-N diode

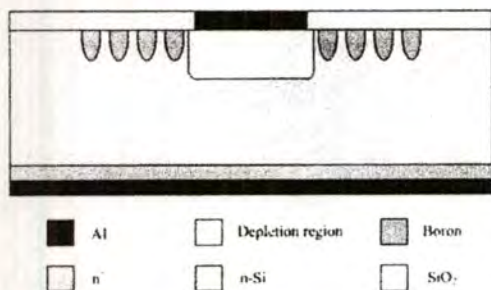


Fig. 2 Structure of the multi-ring gated diode devices used in the study

10 μm thick, on front side and backside [4], process flow show in Fig. 1. After fabrication structure of P-N diode has been showed in Fig. 2. After its fabrication process, the diodes were irradiated by X-ray at room temperature for various energy exposures such as 40, 55 and 70 keV and exposure times of 205 second. Diode was set perpendicular to the X-ray head with 15 cm distance shown in Fig. 3.

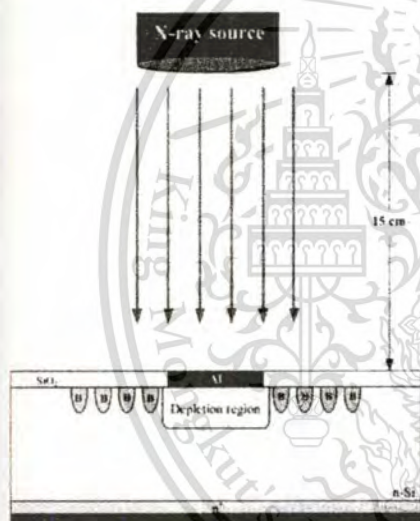


Fig. 3 Schematic diagram of the experiment setting

After its fabrication process, the diodes were irradiated by X-ray for various energy such as 40, 55 and 70 keV and exposure time of 205 second. Used HP4156B to measure electrical properties of diode. The current-voltage (I-V) characteristics were measured on wafer with bias step of 25 mV from reverse (V_r) to forward (V_f) voltage, in the range of -10 to +1 V.

III. RESULTS AND DISCUSSION

The general relation of Current-Voltage of P-N junction diode is presented in (1).

$$I = I_0 [\exp(qV/kT) - 1] \quad (1)$$

Where I_0 is the saturation current, V is the bias voltage, k is the Boltzmann's constant, q is the electronic charge constant and T is the absolute temperature. In case of reverse bias, the saturation current is presenting in (2), which is the combination of the diffusion current (I_d) and the generation current (I_g) that generate in the depletion region.

$$I_0 = I_d + Aq n_i W / \tau_g \quad (2)$$

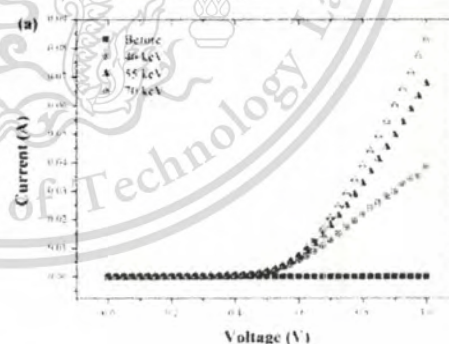
Where A is the area of P-N junction, n_i is the intrinsic carrier concentration, W is the width of depletion region and τ_g is carrier generation lifetime.

I-V characteristics of the P-N diode before and after irradiation show in Fig. 4.

Fig. 4 (a) shows forward current. The forward current slope is flatter after irradiation for a forward voltage larger than 0.5 V, which is due to the radiation-induced decrease of the p-well resistivity. This result points to the difference of irradiation on the leakage currents from the device bulk and its contact peripheral area, which dominate in the diode. The current-voltage characterization of the P-N junction diode can be explained by equation (1). [5]

Before and after irradiation, the current-voltage characteristics of the diodes were measured at room temperature to examine the change of the leakage current (I_0) by the irradiation. Fig. 4 (b) shows the typical result of I-V characteristic for X-ray irradiation at different energy.

From these figures it can be found that after irradiation the leakage current decreases.



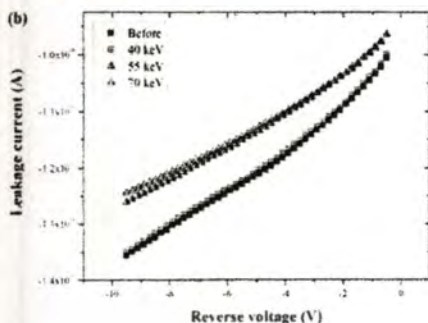


Fig. 4. I-V characteristics of P-N diode irradiated by 40, 55 and 70 keV (a) forward, (b) reward.

Leakages current were decreased because carrier generation lifetime were increased and reduced of defect.

The leakage current increases at higher reverse bias (larger depletion width higher reversed bias voltage), which can be surely explained by equation (2). The diffusion current is independent of applied bias because all of a fixed amount of the minority carriers generated by thermal energy within a diffusion length of the depletion region will essentially get swept across the junction due to the field, regardless of the applied bias and the strength of the electric field. Therefore, increasing of leakage current at higher reverse bias is mostly the result of generation current and also depends on the depletion width which can obtain from the capacitance that was shown in Fig. 5. [6]

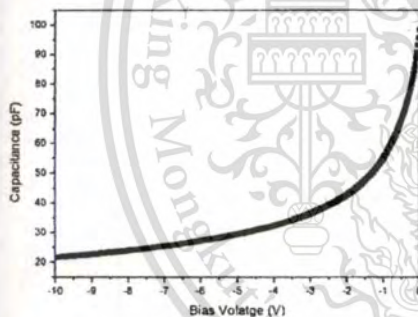


Fig. 5. The capacitance-voltage characteristics of P-N junction diode

The relation between depletion width and capacitance can explain in (3), where ϵ_{si} is permittivity of silicon. From (2), the increment of generation current is result of the increase in depletion width.

$$W = A \epsilon_{si} / C \tag{3}$$

In case of varied temperature, as shown in Fig. 6, the leakage current increases as temperature increases due to diffusion current increases with temperature. Table 1 shows the summary of the diffusion current. To derive the diffusion current, it can be calculated from the relation of leakage current and depletion width. Fig. 7 shows how to calculate the diffusion current and in this example it is 0.87 nA. From (2), the generation current was calculated after we derived the diffusion current for difference temperature.

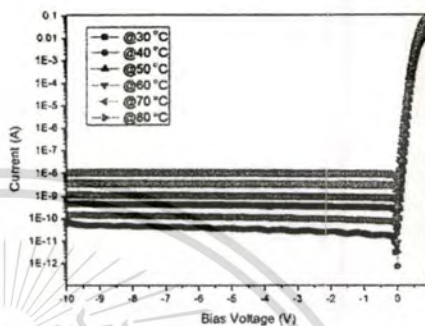


Fig. 6. The current-voltage characteristics of the silicon P-N junction diode at various temperatures

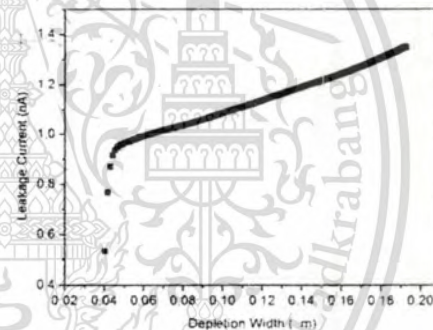


Fig. 7. The leakage current versus the depletion width of P-N junction diode

Fig. 8 shows the effect of difference temperature corrections on the activation energy from Arrhenius plot of generation current versus the temperature of the difference bias. Fig. 9 shows the activation energy. This figure shows the activation energy was changed. Before irradiated have activation energy about 0.67 eV. On the other hand, after irradiated the activation were decreased at 55 and 70 keV have activation energy about 0.65 eV.

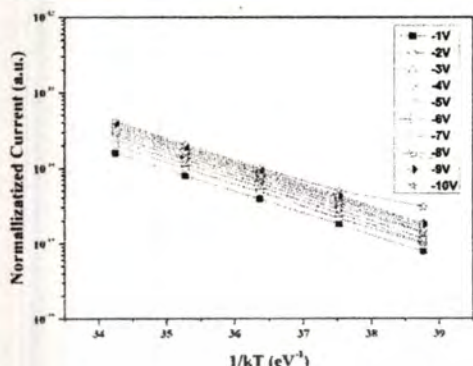


Fig 8. Arrhenius plot of generation current versus the temperature of the difference bias.

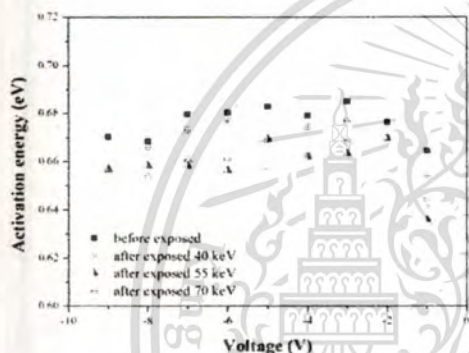


Fig 9. The value of the activation energy versus bias voltage

IV. CONCLUSION

This paper is clearly presented that in certain condition the X-ray is obviously affecting the activation energy of device after exposed to the X-ray. In the other hand, the X-ray created additional defects in device after exposed. The detail study of these defects is requiring for determine the types and amount of these defects, which will lead to the development of device defects controlling process in future.

ACKNOWLEDGMENT

The authors would like to thank King Mongkut's University of Technology North Bangkok for providing the X-ray exposure equipment for this experiment, Mr. Montre Saenlamool Thai Microelectronics Center (TMEC) for fabrication P-N junction diode, National Electronics and

Computer Technology Center, Thailand and Thailand Graduate Institute of Science and Technology (TGIST) under scholarship number TG-44-22-53-014D.

REFERENCES

- [1] A. M. Piro, L. Romano, S. Mirabella, and M. G. Grimaldi, "Room-temperature boron displacement in crystalline silicon induced by proton irradiation". *Applied physics letters* 86, pp. 081906-(1-3), 2005.
- [2] R. R. Sumathi, M. Udhayasankar, J. Kumar, P. Magudapathy, K. G. M. Nair, "Effect of proton irradiation on the characteristics of GaAs Schottky barrier diodes". *Physica B* 308-310, pp. 1209-1212, 2001.
- [3] H. Ohyama, K. Hayama, T. Miura, E. Simoen, C. Claeys, A. Poyai, M. Nakabayashi, K. Kobayashi, "Defect assessment of irradiated STI diodes". *Nuclear Instruments and Methods in Physics Research B* 186, pp. 424-428, 2002.
- [4] F. Foulon, L. Rousseau, L. Babadjian, S. Spirkovitch, A. Brambilla and P. Bergonzo, "A New Technique for the Fabrication of Thin Silicon Radiation Detectors". *IEEE transactions on nuclear science*, vol. 46, pp. 218-220, June 1999.
- [5] J. H. Kim, D. U. Lee, E. K. Kim, Y. H. Bae, "Electrical characterization of proton irradiated p+-n-n+ Si diode". *Physica B* 376-377, pp. 181-184, 2006.
- [6] Sarada, Ueamanaphong, Itsara Srithanachai, Surasak Niemcharoen "The Study and Analysis of Direct X-Ray Radiated P-N Junction Diode Characteristics". *ECON'33*, pp. 1169-1172, 2010.

Author Profile

Name-Surname Mr. Itsara Srithanachai
Birthdate 22 September 2526
Birthplace Chiang Rai
Address 568/34 Lumpinee Center C2 Rd. Happyland Klongjun Bangkokpi
 Bangkok 10520, Thailand

Education Background 2549 Department of Applied Physic, Faculty of Science, King
 Mongkut's Institute of Technology Ladkrabang.
 2553 Department of Microelectronics, Faculty of Engineering,
 King Mongkut's Institute of Technology Ladkrabang.

Expertise

- 1) Thin Film
- 2) Semiconductor device
- 3) Semiconductor Fabrication
- 4) Semiconductor measurement
- 5) Analyze the semiconductor properties

Publications

Journal Publications

- [1] I. Srithanachai, S. Ueamanapong, A. Poyai, S. Niemcharoen, "Analysis the Electrical Properties of Diode at Low Dose X-ray Irradiation", *Advance science letters*. [Accepted, IF: 1.253]
- [2] P. Rujanapich, I. Srithanachai, S. Ueamanapong, A. Poyai, S. Niemcharoen, W. Titiroongruang, "An Improvement of Forward Current of P-N Diode using Soft X-ray Method", *Advance science letters*. [Accepted, IF: 1.253]

- [3] S. Ueamanapong, I. Srithanachai, N. Klunngien, A. Poyai, S. Niemcharoen, "Enhanced Silicon Bandgap by Platinum Diffusion for UV Detector", *Advance science letters*. [Accepted, IF: 1.253]
- [4] S. Niemcharoen, S. Ueamanapong, I. Srithanachai, N. Klunngien, A. Poyai, "Removing the Transients Electron Trapping in P-N Junction Diode by Using Soft X-ray Annealing Method", *Journal of Nanoelectronics and Optoelectronics*, vol.7 (2012). [IF: 0.9][DOI:10.1166/jno.2012.1287]
- [5] J. Prabket, I. Srithanachai, S. Ueamanapong, A. Poyai, W. Titiroongruang, S. Niemcharoen, P. P Yupapin, "An improvement of electrical characteristics of P-N diode by X-ray irradiation method", *Scientific Research and Essays*, Vol. 7 (11), pp. 1230-1236 (2012). [IF: 0.475]
- [6] S. Ueamanapong, I. Srithanachai, and S. Niemcharoen, "Effect of Direct X-ray Radiation on P-N Junction Diode Characteristics", *Ladkrabang Engineer Journal*, Vol. 38, pp. 31-36 (2011).
- [7] S. Ueamanapong, I. Srithanachai, A. Poyai, S. Niemcharoen, P. P. Yupapin, "High Speed Photodetector using Accelerated Particles Controlled by Light", *JNOPM*, 21 (2), (2012). [IF: 0.667]
- [8] I. Srithanachai, S. Ueamanapong, P. Rujanapich, A. Poyai, S. Niemcharoen and W. Titiroongruang, "Effect of X-Ray Irradiation on the Current of P-N Diode", *Materials Science Forum*, Vol. 695, pp. 561-564 (2011).
- [9] I. Srithanachai, S. Ueamanapong, P. Rujanapich, N. Atiwongsangthong, S. Niemcharoen, A. Poyai, and W. Titiroongruang, "Defects study by activation energy profile for lowering leakage current in P-N junction", *Materials Science Forum*, Vol. 695, pp. 569-572 (2011).
- [10] S. Niemcharoen, I. Srithanachai, S. Ueamanapong, A. Poyai, "Improving Forward Current Characteristics of Diode by X-ray Irradiation", *Advanced Materials Research*, Vol. 433-440, pp. 6713-6716 (2012).
- [11] S. Glomglome, I. Srithanachai, C. Teeka, S. Mitatha, S. Niemcharoen, P. P Yupapin, "Optical spin generated by a soliton pulse in an add-drop filter for optoelectronic and spintronic use", *Optics and Laser Technology*, Vol. 44, pp. 1294-1297 (2012).
- [12] I. Srithanachai, S. Ueamanapong, S. Niemcharoen, P.P. Yupapin, "Novel nano-accelerator on-chip design for high solar cell device efficiency use", *Journal of nanoscience letters*, Vol. 3, pp. 1-3 (2013).

- [13] I. Srithanachai, S. Ueamanapong, S. Niemcharoen, P.P. Yupapin, "Novel Design of Solar Cell Efficiency Improvement using an Embedded Electron Accelerator on-Chip", *Optics express*, Vol. 20, pp. 12640-12648 (2012). [IF: 3.753]
- [14] I. Srithanachai, F. D. Zainol, S. Ueamanapong, S. Niemcharoen, J. Ali, P.P. Yupapin, "Photodetector Performance Enhancement using an Electron Accelerator Controlled by Light", *Applied optics*, Vol. 51 (21), pp. 5111-5118 (2012). [IF: 1.707]

Proceeding Publications

- [1] P. Rujanapich, A. Poyai, I. Srithanachai, P. Pengpad, C. Hruanan, S. Sophitpan, W. Titiroongruang, "Generation Lifetime Analysis of P-N Junction X-ray Detector", *Electrical Engineering/Electronics, Computer, Telecommunications and Information Technology Association of Thailand (ECTI-CON-2010)*, THAILAND, pp. 780-783 (2010).
- [2] S. Ueamanapong, I. Srithanachai, N. Atiwongsangthong, P. Pengpad, S. Niemcharoen, A. Poyai, and S. Supadech, "Fabrication, Characterization and Analysis of ITO/n-Si Schottky Photodetector", *Electrical Engineering/Electronics, Computer, Telecommunications and Information Technology Association of Thailand (ECTI-CON-2010)*, THAILAND, pp. 776-779 (2010).
- [3] P. Rujanapich, A. Poyai, I. Srithanachai, P. Pengpad, C. Hruanan, S. Sophitpan, S. Ueamanapong, W. Titiroongruang, W. Titiroongruang, "Saturation Current Analysis of Low Dose X-ray Irradiated P-N Junction Diodes", *Joint International Conference on Information & Communication Technology, Electronic and Electrical Engineering (JICTEE 2010)*, LAOS, pp. 231-233 (2010).
- [4] I. Srithanachai, P. Rujanapich, S. Ueamanapong, W. Titiroongruang, A. Poyai, S. Niemcharoen, and W. Titiroongruang, "Electrical Characteristics Study on the Effect of X-ray Irradiation Various Energy and Exposure Time on P-N Junction", *Joint International Conference on Information & Communication Technology, Electronic and Electrical Engineering (JICTEE 2010)*, LAOS, pp. 234-237 (2010).
- [5] S. Ueamanapong, I. Srithanachai, and S. Niemcharoen "The Study and Analysis of Direct X-Ray Radiated P-N Junction Diode Characteristics", *The 33th Electrical Engineering Conference (EECON-33) 2010*, THAILAND, pp. 1169-1172 (2010).
- [6] Y. Sundarasaradula, I. Srithanachai, P. Rujanapich, S. Ueamanaphong, P. Pengpad, M. Saenlamool, W. Titiroongruang, P. Tosranon, A. Poyai, S. Niemcharoen, and W.

- Titiroongruang, "Effect of X-ray Irradiation on the Characteristics of P-N Junction Diodes", *The 33th Electrical Engineering Conference (EECON-33)*, THAILAND, pp. 1121-1124 (2010).
- [7] K. Kidee, I. Srithanachai, S. Niemcharoen, "The Effect of Temperature to Indium Tin Oxide Thin films for Apply to Transparent Electrode of Photodetector", *The 33th Electrical Engineering Conference (EECON-33)*, THAILAND, pp. 1117-1120 (2010).
- [8] P. Rujanapich, A. Poyai, I. Srithanachai, P. Pengpad, C. Hruanan, S. Sophitpan, S. Ueamanapong, W. Titiroongruang, and W. Titiroongruang, "Activation Energy Analysis OF P-N Junction X-ray Direct Detector", *International Technical Conference on Circuits/Systems, Computers and Communications (ITC-CSCC 2010)*, THAILAND, pp. 257-260 (2010).
- [9] P. Rujanapich, A. Poyai, I. Srithanachai, P. Pengpad, C. Hruanan, S. Sophitpan, and W. Titiroongruang, "Diode analysis of X-ray Detector", *The 4th International Confernece on Sensors (Asiasense 2010)*, THAILAND (2010).
- [10] Y. Sundarasaradula, I. Srithanachai, S. Niemcharoen, W. Titiroongruang, A. Poyai, and N. Klunngien, "Study of X-ray Annealed Lowering Series Resistance of PN Junction Ppower Diode", *The 35th Electrical Engineering Conference (EECON-35)*, THAILAND, pp. 849-852 (2011).
- [11] I. Srithanachai, S. Ueamanapong, Y. Sundarasaradula, A. Poyai, and S. Niemcharoen, "X-ray Radiation Damage in P-N Junction Diode", *The 4th Annual PSU Phuket Research Conference 2011*, THAILAND (2011).
- [12] S. Niemcharoen, I. Srithanachai, S. Ueamanapong, and A. Poyai, "Improving Forward Current Characteristics of Diode by X-ray Irradiation", *The 2011 2rd International Conference on Mechanical and Aerospace Engineering (ICMAE 2011)*, THAILAND (2011).
- [13] Y. Sundarasaradula, I. Srithanchai, S. Ueamanapong, N. Atiwongsaengthong, A. Poyai, S. Niemcharoen, and W. Titiroongruan, "Electrical Characteristics of X-ray Irradiated on PN Diode", *The 5th PSU-UNS International conference on engineering and technology (ICET-2011)*, THAILAND, pp. 461-464 (2011).
- [14] I. Srithanachai, and S. Niemcharoen, "Influence of X-ray Irradiated on Junction Depth of P-N Diode", *The 5th PSU-UNS International conference on engineering and technology (ICET-2011)*, THAILAND, pp. 498-501 (2011).

- [15] P. Rujanapich, A. Poyai, I. Srithanachai, S. Ueamanapong, and W. Titiroongruang, "Defects Engineering for Silicon Power Diode by X-ray Irradiation", *26th International Conference on Defects in Semiconductors 2010 (ICDS'26)*, NEW ZEALAND (2010).
- [16] I. Srithanachai, S. Ueamanapong, N. Atiwongsangthong, A. Poyai, and S. Niemcharoen, "X-ray Radiation Damage in P-N Junction Diode", *26th International Conference on Defects in Semiconductors 2010 (ICDS'26)*, NEW ZEALAND (2010).
- [17] S. Niemcharoen, I. Srithanachai, S. Ueamanapong, N. Atiwongsangthong, and A. Poyai, "Transients Electron Trapping Phenomenon in P-N Junction Diode Fabricated in High Energy Boron Implanted", *26th International Conference on Defects in Semiconductors 2010 (ICDS'26)*, NEW ZEALAND (2010).
- [18] I. Srithanachai, S. Ueamanapong, P. Rujanapich, N. Atiwongsangthong, S. Niemcharoen, A. Poyai, and W. Titiroongruang, "Defects Study by Activation Energy Profile for Lowering Leakage Current in P-N Junction", *11th International Symposium on Eco-materials Processing and Design (ISEPD-2011)*, Thailand (2011).
- [19] I. Srithanachai, S. Ueamanapong, P. Rujanapich, A. Poyai, S. Niemcharoen and W. Titiroongruang, "Effect of X-Ray Irradiate to the Current of P-N Diode", *11th International Symposium on Eco-materials Processing and Design (ISEPD-2011)*, Thailand (2011).
- [20] I. Srithanachai, S. Ueamanapong, N. Atiwongsaengtong, A. Poyai, and S. Niemcharoen, "Enhancement of Physical Properties of ITO Films by Oxygen Annealing for the Photodetector Contact", *Proceedings of 29th Annual Conference Microscopy Society of Thailand*, THAILAND (2012).
- [21] I. Srithanachai, S. Ueamanapong, N. Atiwongsaengtong, A. Poyai, and S. Niemcharoen, "Characteristics of Indium Tin Oxide Thin Films Prepare by RF Sputtering", *Proceedings of 29th Annual Conference Microscopy Society of Thailand*, THAILAND (2012).
- [22] I. Srithanachai, S. Ueamanapong, A. Poyai, and S. Niemcharoen, "New Method for Improving the Electrical Characteristics of P-N Junction Diode", *2012nd International Conference on Applied Materials and Electronics Engineering (AMEE-2012)*, Hong Kong (2012).
- [23] I. Srithanachai, S. Ueamanapong, and S. Niemcharoen, "Electrical Characteristic of Photodetector with Transparent Contact," *Electrical Engineering/Electronics*,

Computer, Telecommunications and Information Technology Association of Thailand (ECTI-CON-2012), THAILAND (2012).



This material is reserved for educational use only, not allowed for commercial use.

Forbidden to modify the content, and cite the document when use.